

To my loving parents
and to the Society of Jesus

Acknowledgements

Filled with an immense sense of joy and gratitude, I profoundly thank Dra. Ángela Jiménez-Casas, my doctoral supervisor, for making me what I am today. When I landed in Madrid four years ago, I knew neither Spanish nor the rudiments of mathematics. It is her constant encouragement, guidance and dedication that has shaped me to step into the academic arena. Without her relentless efforts, time, help and support my research would have just remained a far fetched dream. I sincerely thank Dr Mario Castro Ponce, my second supervisor and friend, who is a great source of inspiration for me to keep always learning. His knowledge in the field and his skills in giving shape to his knowledge have positively challenged me to pursue not only in my research but also in my life to come. I would like to thank all the members of the Department of Applied Mathematics and Computations, at ICAI, for being part of me during these four years of my struggle in mathematics and engineering.

I would like to place on the record my sincere thanks to my Jesuit friends: Fr P Francis Xavier SJ, Fr Victor Arulappan SJ, Fr M Devadoss SJ, Fr Xavier Leach SJ, Fr Xavier Monserrat SJ, Fr José Ramón Busto SJ, Fr Julio Martínez SJ, Fr Juan Guerrero SJ, the Jesuit Provincial of Castilla and Fr Sebasti L. Raj SJ, the Jesuit Provincial of Madurai, all of whom are instrumental in making this doctoral research possible for me. It is my pleasure to extend my special thanks to all my Jesuit friends at Pablo Aranda, especially

viii

to Fr Agustín Alonso SJ and Fr Xavier Ilundáin SJ, who loved me immensely all these four years of my doctoral journey. Lastly, and to YOU MY BEST FRIEND, for just being with me always.

Madrid, Spain

Justine Yasappan

June, 2013

Contents

List of Tables	xvi
List of Figures	xx
Glossary	xxii
Abstract	xxv
Resumen	xxix
1 Introduction and Objectives	1
1.1 Dynamics in a closed loop thermosyphon	1
1.2 Motivation for this thesis	4
1.3 Literature survey of the physical models	5
1.3.1 Mathematical models with one component fluids	9
1.3.2 Mathematical models with binary fluids	12
1.4 Objectives of this thesis	14

2	Formulation of a novel model of viscoelastic fluids in a closed loop thermosyphon	17
2.1	Introduction	17
2.2	Conservation laws and the Maxwell constitutive equation	19
2.2.1	One component viscoelastic fluids with Newton's linear cooling law model	22
2.2.2	One component viscoelastic fluids with a prescribed heat flux model	23
2.2.3	Binary viscoelastic fluids with Soret effect model	23
3	One component viscoelastic fluids with Newton's linear cooling law	27
3.1	Introduction	27
3.2	Well-posedness and boundedness: global attractor	29
3.2.1	Existence and uniqueness of solutions	29
3.2.2	Boundedness of the solutions and global attractor	40
3.3	Asymptotic behavior: finite-dimensional systems	45
3.3.1	Inertial manifold	46
3.3.2	The reduced subsystem	55
3.4	Numerical experiments	63
3.4.1	Dynamics of the thermosyphon without diffusion ($\nu = 0$)	67
3.4.2	Dynamics of the thermosyphon with diffusion ($\nu \neq 0$)	74
3.5	Conclusions	77

4	One component viscoelastic fluids with a prescribed heat flux	81
4.1	Introduction	81
4.2	Well-posedness and boundedness: global attractor	83
4.2.1	Existence and uniqueness of solutions	83
4.2.2	Asymptotic bounds on the solutions: global attractor	87
4.3	Asymptotic behavior: finite-dimensional systems	89
4.3.1	Inertial manifold	91
4.3.2	The reduced subsystem	94
4.4	Numerical experiments	96
4.4.1	The behavior of the model for different values of $\varepsilon, \nu = 0$	101
4.4.2	The chaotic behavior of this model for $B = 50$	109
4.5	Conclusions	112
5	Binary viscoelastic fluids with Soret effect	113
5.1	Introduction	113
5.2	Well-posedness and boundedness: global attractor	115
5.2.1	Existence and uniqueness of solutions	115
5.2.2	Boundedness of the solutions and global attractor	122
5.3	Asymptotic behavior: finite-dimensional systems	126
5.3.1	Inertial manifold	129
5.3.2	The reduced subsystem	136

5.4	Numerical experiments	139
5.4.1	Experiment I: Soret coefficient $b = 0.00001$	144
5.4.2	Experiment II: Soret coefficient $b = 0.001$	147
5.4.3	Experiment III: Soret coefficient $b = 1$	150
5.4.4	Analysis of the behavior of the system using Lyapunov exponents	153
5.5	Conclusions	156
6	Conclusions and future works	159
6.1	Summary of conclusions	159
6.2	Future works	161
7	Conclusiones y trabajos futuros	163
7.1	Resumen de las conclusiones	163
7.2	Trabajos futuros	166
A	Appendix	169
A.1	Boundary layer theory	169
A.2	Sectorial Operators	170
A.2.1	Definition of sectorial operator	170
A.2.2	The interpolation scale of spaces	171
A.3	Semilinear equations: existence and uniqueness	174
A.4	Dissipative semigroups	175

A.5	L'Hopital rule	176
A.6	Inequalities	177
A.6.1	Young Inequality	177
A.6.2	Hölder's Inequality	177
A.7	Singular Gronwall lemma	177
A.8	Lyapunov exponent	177
	Bibliography	179

List of Tables

3.1	Equilibrium values of velocity for different values of ambient temperature $B, \nu = 0$	71
3.2	Behavior of the solutions without diffusion ($\nu = 0$) for different values of the viscoelastic characteristic time, ε (rows) and the ambient temperature, B (columns). We introduce the following notation to account for the obtained numerical results: ‘C’ denotes a fully chaotic behavior, ‘CS’ a transition from chaotic outburst to stable equilibria, ‘P’ a stable periodic orbit and ‘CP’ a transitional behavior from chaotic to periodic.	75
3.3	Behavior of the solutions with diffusion ($\nu \neq 0$) for different values of the viscoelastic characteristic time, ε (rows) and the ambient temperature, B (columns). We introduce the following notation to account for the obtained numerical results: ‘C’ denotes a fully chaotic behavior, ‘CS’ a transition from chaotic outburst to stable equilibria and ‘P’ a periodic orbit.	78

5.1	Qualitative summary of the overall behavior of the system for different values of the viscoelastic characteristic time, ε (columns) and the Soret coefficient b (rows). We introduce the following notation to account for the obtained numerical results: ‘S’ a stable behavior, ‘C’ denotes a fully chaotic behavior, and ‘QP’ a transitional behavior from chaotic to quasi-periodic. .	152
5.2	The maximum Lyapunov exponent of the system for different values of the viscoelastic characteristic time, ε (columns) and the Soret coefficient b (rows). We can assume that maximum Lyapunov exponents close to 0 ± 0.1 correspond to quasi-periodic behavior (as simple inspection of the time series plots confirm).	154

List of Figures

1.1	A schematic representation of a closed loop thermosyphon [29]. The section A-A represents the cross section of the pipe. Due to the incompressibility of the fluid and the large aspect ratio between the length and the diameter of the pipe, the velocity can be assumed to be uniform throughout the system, although we allow the other variables (temperature and solute concentration) to depend on the location inside the loop	2
3.1	The chaotic progress of the acceleration for $\varepsilon = 10, B = 50, \nu = 0$	66
3.2	The inconsistent behavior of velocity for $\varepsilon = 10, B = 50, \nu = 0$	67
3.3	A chaotic global attractor of real and complex temperature for $\varepsilon = 10, B = 50, \nu = 0$	68
3.4	The stabilizing progress of the acceleration for $\varepsilon = 0.1, B = 100, \nu = 0$. . .	69
3.5	Velocity stabilizes at 3.19981 for $\varepsilon = 0.1, B = 100, \nu = 0$	70
3.6	Equilibrium velocity scale for the ambient temperature $B, \nu = 0$	72
3.7	The periodic progress of the acceleration for $\varepsilon = 0.001, B = 40, \nu = 0$. . .	72

xviii LIST OF FIGURES

3.8	The periodic progress of velocity for $\varepsilon = 0.001, B = 30, \nu = 0$	73
3.9	The chaotic but periodic plot of real and complex temperature for $\varepsilon =$ $0.0001, B = 40, \nu = 0$	74
3.10	The stabilizing process of the acceleration for $\nu = 1, \varepsilon = 5, B = 1000$	76
3.11	The fast stabilization of the acceleration for $\nu = 2, \varepsilon = 5, B = 1000$	77
4.1	Acceleration for $\varepsilon = 100, B = 10, \nu = 0$	100
4.2	Temperature phase plot for $\varepsilon = 100, B = 10, \nu = 0$ (chaotic in concentric circles)	100
4.3	Acceleration for $\varepsilon = 10, B = 100, \nu = 0$	101
4.4	Temperature phase plot for $\varepsilon = 10, B = 100, \nu = 0$ (chaotic in concentric circles)	102
4.5	Acceleration for $\varepsilon = 1, B = 1, \nu = 0$	103
4.6	Temperature phase plot for $\varepsilon = 1, B = 1, \nu = 0$	104
4.7	Temperature phase plot for $\varepsilon = 0.1, B = 100, \nu = 0$	105
4.8	Temperature phase plot for $\varepsilon = 0.01, B = 50, \nu = 0$	106
4.9	Temperature phase plot for $\varepsilon = 0.0001, B = 50, \nu = 0$	108
4.10	The time evolution of the acceleration, $w(t)$ (left), and the velocity, $v(t)$ (right), with $\varepsilon = 1, A = 0, B = 50, \nu = 0.002$ and $G(v) = (v + 10^{-4})$. . .	109

4.11 Left: Phase-plane of the real and imaginary parts of Fourier transform of the temperature for $\varepsilon = 1$, $A = 0$, $B = 50$, $\nu = 0.002$ and $G(v) = (|v| + 10^{-4})$.
 Right: Same parameters as in the left panel but with $\varepsilon = 10$ 110

4.12 The time evolution of the acceleration, $w(t)$ (left), and the velocity, $v(t)$ (right), with $\varepsilon = 3$, $A = 0$, $B = 50$, $\nu = 0.002$ and $G(v) = (|v| + 10^{-4})$. . . 111

4.13 The time evolution of the acceleration, $w(t)$ (left), and the velocity, $v(t)$ (right), with $\varepsilon = 10$, $A = 0$, $B = 50$, $\nu = 0.002$ and $G(v) = (|v| + 10^{-4})$. . 112

5.1 The chaotic behavior of acceleration and velocity for $\varepsilon=0.00001$, $A=0$, $B=30$, $b=0.00001$, $\nu = 0.002$, $G(v) = (|v| + 10^{-4})$ and $l(v) = (10^{-2}|v| + 1)$. 143

5.2 The chaotic behavior of the real and imaginary parts of temperature for $\varepsilon=0.00001$, $A=0$, $B=30$, $b=0.00001$, $\nu = 0.002$, $G(v) = (|v| + 10^{-4})$ and $l(v) = (10^{-2}|v| + 1)$ 144

5.3 The chaotic behavior of the real and imaginary parts of solute concentration for $\varepsilon=0.00001$, $A=0$, $B=30$, $b=0.00001$, $\nu = 0.002$, $G(v) = (|v| + 10^{-4})$ and $l(v) = (10^{-2}|v| + 1)$ 145

5.4 The chaotic transition of the fluid acceleration and velocity for $\varepsilon=0.1$, $A=0$, $B=30$, $b=0.001$, $\nu = 0.002$, $G(v) = (|v| + 10^{-4})$ and $l(v) = (10^{-2}|v| + 1)$. . 146

5.5 The transition from chaotic to quasi-periodic behavior of the fluid acceleration and velocity for $\varepsilon=1$, $A=0$, $B=30$, $b=0.001$, $\nu = 0.002$, $G(v) = (|v| + 10^{-4})$, $l(v) = (10^{-2}|v| + 1)$ 147

5.6	The transition from chaotic to stable behavior of the fluid acceleration and velocity for $\varepsilon=10$, $A=0$, $B=30$, $b=0.001$, $\nu = 0.002$, $G(v) = (v + 10^{-4})$, $l(v) = (10^{-2} v + 1)$	149
5.7	Stable progress of the fluid acceleration and velocity for $\varepsilon=1$, $A=0$, $B=30$, $b=1$, $\nu = 0.002$, $G(v) = (v + 10^{-4})$, $l(v) = (10^{-2} v + 1)$	151
5.8	The chaotic behavior of the system determined by the Lyapunov exponents for $\varepsilon=0.00001$, $A=0$, $B=30$, $b=0.00001$, $\nu = 0.002$, $G(v) = (v + 10^{-4})$ and $l(v) = (10^{-2} v + 1)$	153
5.9	The overall behavior of the system for different values of viscoelastic and Soret coefficients (the dark area indicates chaos, shaded area indicates the stable behavior and the white area indicates the quasi-periodic behavior).	155

Glossary

Symbol	Description
t	Time
$v(t)$	Velocity of the fluid
$w(t)$	Acceleration of the fluid
x	Arc length coordinate along the loop
$T(t, x)$	Temperature of the fluid
T_a	Ambient temperature
h	Heat flux
$S(t, x)$	Solute concentration of the fluid
$a_k(t)$	Fourier coefficient of temperature
b_k	Fourier coefficient of ambient temperature or prescribed heat flux
c_k	Fourier coefficient of the geometry of the loop
$d_k(t)$	Fourier coefficient of solute concentration
ε	Viscoelastic coefficient
ν	Diffusion coefficient of temperature
A, B	Ambient temperature or heat flux parameters
b	Soret coefficient
c	Diffusion coefficient of solute concentration

Symbol	Description
$G(v)$	Friction function
$G(v) > G_0 > 0$	G_0 a positive quantity
$f(x)$	Geometry of the loop
$l(v)(T_a - T)$	Newton's linear cooling law
$l(v) > l_0 > 0$	l_0 a positive quantity
\mathcal{M}	Inertial manifold
\oint	Integration along the closed path of the circuit
$\dot{L}_{per}^p(0, 1)$	L^p Space with periodic boundary condition, zero average
$\dot{H}_{per}^m(0, 1) = H_{loc}^m(\mathbb{R}) \cap \dot{L}_{per}^p(0, 1)$	Sobolev's space

Abstract

Flow dynamics in a closed loop thermosyphon is a very complex and interesting phenomenon, as it incorporates several factors such as gravity, thermal conduction, natural convection and gradients due to a solute, all producing the emergence of complex dynamical behaviors inside the loop. The convection inside a closed loop thermosyphon is propelled and sustained by the buoyancy effect variations in the density or is caused by the diffusion of solute in dissolution due to temperature gradients. The dynamics becomes even more complex when the fluid inside the loop is viscoelastic, leading to various types of behavior such as chaotic, periodic, quasi-periodic and stable behavior.

Although these kinds of systems have been widely studied in the literature for simple (Newtonian) fluids, the behavior of viscoelastic fluids has not been explored thus far. These kinds of fluids present elastic-like behaviors and memory effects. Various viscoelastic coefficients, thermal gradients and solute gradients produce different types of complex dynamical behaviors on the system.

A theoretical study of the dynamics of Maxwell viscoelastic fluids in a closed loop thermosyphon is presented. For the first time, the mathematical derivations of the motion of a viscoelastic fluid in the interior of a closed loop thermosyphon under the effects of natural convection and a given external temperature gradient are derived. The asymptotic properties of the fluid inside the thermosyphon and the exact equations of motion in the

inertial manifold that characterize the asymptotic behavior are studied. The dynamics of the system is characterized by observing the time series plots and the phase-diagrams of acceleration, velocity, temperature and in the case of binary fluids, also solute concentration of Maxwell viscoelastic fluids. A detailed analysis of the impact of viscoelasticity and its coexistence with the Soret effect has also been extensively done in this research.

This thesis consists of the study of three related problems, all of them concerning the dynamics of viscoelastic fluids in a closed loop thermosyphon. The first model is based on one component viscoelastic fluids with Newton's linear cooling law. The second model is based on one component viscoelastic fluids with prescribed heat flux with diffusion. Finally, the third model is based on binary viscoelastic fluids with the Soret effect. In each case, we have approached the problem from a theoretical viewpoint followed by numerical experiments to unveil the behavior of the system in larger detail.

The contribution of this research is the derivation of the novel system of equations to study the behavior of a viscoelastic material inside a thermosyphon. This model can be thought as a preliminary simplification of a more complex fully spatially extended system. The main result is to prove that the original system (which involves both ordinary and partial differential equations) possesses an inertial manifold in which the dynamics can be accurately described by a low dimensional system of ODEs. By numerical integration of the reduced equations we have been able to better understand the role of viscoelasticity (as opposed to a simpler Newtonian fluid) through the parameter ε . This parameter is an adimensional version of the so-called Maxwellian viscoelastic time which accounts for the

characteristic timescale (or, alternatively, the typical timescale separating purely elastic from purely viscous behaviors).

Resumen

La dinámica del flujo en un termosifón de bucle cerrado es un fenómeno muy complejo e interesante, ya que incorpora varios factores como la gravedad, la conducción térmica, la convección natural o los gradientes debidos a un soluto, todos produciendo la aparición de comportamientos dinámicos complejos dentro del bucle. La convección en el interior de un termosifón de bucle cerrado es impulsada y sostenida por las variaciones debidas a la densidad con la temperatura o causados por la difusión de soluto en disolución debido a gradientes de temperatura. La dinámica se hace aún más compleja cuando el líquido dentro del bucle es viscoelástico, lo que conduce a diferentes tipos de comportamiento, tales como caótico, periódico, cuasi-periódico o estable.

Aunque estos tipos de sistemas se han estudiado ampliamente en la literatura para fluidos simples (Newtonianos), el comportamiento de los fluidos viscoelásticos no ha sido explorado hasta la fecha. Estos tipos de fluidos presentan comportamientos de tipo elástico y también efectos de memoria. El balance de propiedades viscoelásticas, gradientes térmicos o los gradientes de soluto producen diferentes tipos de comportamientos dinámicos complejos en el sistema.

En este trabajo se presenta, por primera vez, el estudio teórico de la dinámica de fluidos viscoelásticos de Maxwell en un termosifón de bucle cerrado. Las derivaciones matemáticas del movimiento de un fluido viscoelástico en el interior de un termosifón de bucle cerrado, bajo los efectos de la convección natural y de un gradiente de temperatura externa son pre-

sentados de manera original. Asimismo, se estudian las propiedades asintóticas del líquido en el interior del termosifón y las ecuaciones exactas del movimiento que caracteriza el comportamiento asintótico. La dinámica del sistema se caracterizó mediante la obtención de las series temporales y los diagramas de fase de aceleración, velocidad, temperatura y en el caso de fluidos binarios, también la concentración de soluto. Un análisis detallado del impacto de la viscoelasticidad y su convivencia con el efecto Soret también ha sido exhaustivamente estudiado en este trabajo.

En resumen, esta tesis consiste en el estudio de tres problemas, relacionados todos ellos, relativos a la dinámica de fluidos viscoelásticos en un termosifón de bucle cerrado. El primer modelo se basa en fluidos viscoelásticos de un componente con la ley de enfriamiento lineal de Newton. El segundo modelo se basa también en fluidos de un componente con un flujo de calor prescrito y con el efecto simultáneo de la difusión de temperatura. Finalmente, el tercer modelo considera fluidos viscoelásticos binarios con el efecto Soret. En cada caso, se ha abordado el problema desde un punto de vista teórico seguido por experimentos numéricos para poder comprender el comportamiento del sistema en mayor detalle.

La contribución de esta investigación es la derivación del nuevo sistema de ecuaciones para estudiar el comportamiento de un material viscoelástico dentro de un termosifón. Este modelo puede ser pensado como una simplificación preliminar de un sistema más complejo, espacialmente extendido. El resultado principal es demostrar que el sistema original (que implica tanto ecuaciones diferenciales en derivadas parciales y ordinarias)

posee una variedad inercial en la que la dinámica puede ser descrita con precisión por un sistema de EDOs de baja dimension. Por integración numérica de las ecuaciones reducidas hemos sido capaces de entender mejor el papel de la viscoelásticidad (a diferencia de un fluido Newtoniano simple) a través del parámetro ε . Este parámetro es una versión adimensional del tiempo viscoelástico (denominada tiempo de Maxwell) que representa la escala de tiempo característica que separa los comportamientos puramente elásticos de los comportamientos puramente viscosos.

Chapter 1

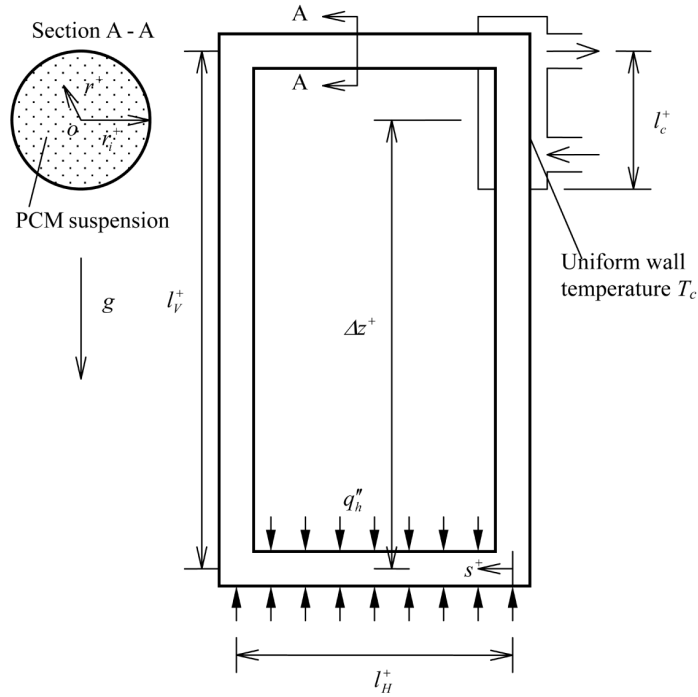
Introduction and Objectives

1.1 Dynamics in a closed loop thermosyphon

A thermosyphon is a device composed of a closed loop pipe containing a fluid [35] whose motion is driven by the action of several forces such as buoyancy induced by differences in temperature by natural convection (see Fig. 1.1). It is an energy transfer device capable of transferring heat from a source to a separate sink over a relatively long distance, without the use of active control instrumentation and any mechanically moving parts such as pumps what makes thermosyphon a common device used in different engineering scenarios.

Thermosyphons represent simplified models for the natural convection of fluids. Physically, the motion is due to the tendency of less dense fluids to move upwards, thus competing with gravity or rotational motion. The loop system enables enhancement of

2 Introduction and Objectives



Source: Ho *et al.*

Figure 1.1: A schematic representation of a closed loop thermosyphon [29]. The section A-A represents the cross section of the pipe. Due to the incompressibility of the fluid and the large aspect ratio between the length and the diameter of the pipe, the velocity can be assumed to be uniform throughout the system, although we allow the other variables (temperature and solute concentration) to depend on the location inside the loop

heat transfer and minimization of flow losses (pressure drops). Thermosyphons can be categorized [40] based on: the nature of boundaries (open or closed system for mass flow), the regime of heat transfer (convection, boiling or both), the number of type of phases present (single or two phase state) and the nature of the body force (gravitational and rotational).

The common feature of the thermosyphon model used in this dissertation is that the loop is assumed to be closed and completely full of fluid and the velocity $v(t)$ within the closed loop is a scalar quantity, depending only on time. This assumption is due to the incompressibility of the fluid and the large aspect ratio between the length and the diameter of the pipe. Thus, although we assume that the velocity of the fluid can be assumed to be uniform throughout the system, we allow other variables (temperature and solute concentration) to depend on the location inside the loop. The closed loop thermosyphon may be visualized as a long hollow pipe, bent and the ends joined to form a continuous loop, filled with working fluid and orientated in a vertical plane (see the schematic diagram of a thermosyphon in Fig. 1.1). An essentially hydrostatic pressure difference, as a result of the thermally induced temperature gradient between the hot and the cold sides, drives the fluids flow around the loop. The *buoyancy force*, as it is often termed, driving the fluid is in turn counteracted by an opposing frictional force that tends to retard the flow.

A number of experimental investigations have been conducted with the aim to parameterize the dynamics of closed loop thermosyphons. These studies allowed to identify

4 Introduction and Objectives

the following main variables affecting the thermosyphon performance:

- (i) physical variables: quantity of the working fluid (filling ratio) and the physical properties of the working fluid and tube material,
- (ii) geometric variables: length of the loop, diameter and shape of the loop,
- (iii) operational variables: open loop or closed loop operation, heating and cooling methodology (fixed *ambient* temperature vs fixed heat flux), orientation of the loop during the operation and the use of the values,
- (iv) Reynolds number and
- (v) solute concentration, in the case of binary fluids¹.

1.2 Motivation for this thesis

It is evident that there are multiple variables which simultaneously affect the operation and performance of the loop. This makes it not only more difficult to model mathematically using conventional techniques, but also represents a challenge for applied mathematicians. Hence, there has been a lot of research carried out in this field by many engineers and mathematicians such as, J.B. Keller (1966), P. Welander (1967), J.E. Hart (1985), R. Temam (1988), A. Rodríguez-Bernal (1990), K. Storey (2003), A. Jiménez-Casas (2005),

¹We will generically refer to binary fluids although in this work we constraint to systems in which a solute is dissolved in a fluid, thus neglecting phase-separation effects and focusing only on solute diffusion.

R.T. Dobson (2007) and A. Abbasi (2010) to cite a few throughout the years. However, the need for further research in the field is on the increase as thermosyphon systems are extensively used in the day-to-day chores of human life like in the case of solar water heaters, solar thermal pans, etc.

Thus far, all the works on thermosyphons analyze the behavior of Newtonian fluids inside the loop and, consequently, neglecting the elastic effects in the system coming from either the fluid itself or the elastic walls of the loop. However, many interesting fluids are known to behave slightly different from the common (Newtonian) fluids — in terms of their response to an applied stress — and are commonly referred to as viscoelastic fluids. Among them, it is worth emphasizing volcanic lavas, snow avalanches, flowing paint or biological mucosa. This fact stands as a great inspiration for this thesis in order to obtain and study different thermosyphon models with viscoelastic fluids inside.

1.3 Literature survey of the physical models

There has been consistent research carried out by many scientists and mathematicians in the field of thermosyphons. Over the years a relatively large amount of published literature is available related to thermosyphons. To limit this section, only previous works undertaken to study the mathematical models of thermosyphons are considered².

²For a general reference on thermosyphons from a practical perspective, the reader is referred to: Bhattacharyya, S., Basu, D. N., and Das, P. K. (2012). *Two-Phase Natural Circulation Loops: A Review of the Recent Advances*. Heat Transfer Engineering, **33**, 4-5, 461-482.

6 *Introduction and Objectives*

1. P. Welander [59], in his pioneering work, considered the fluid to be driven by the pressure difference and a buoyancy force, and is retarded by a frictional force. The following assumptions were made:

- The Boussinesq approximation (namely, temperature enters only through gravity terms and assuming that other density terms in the equations are constant)
- The tangential friction force on the fluid is proportional to the instantaneous flow rate.
- The temperature of the fluid is uniform over each cross-sectional area.
- The heat transfer rate between the pipe and the fluid is proportional to the difference between a prescribed wall temperature and the fluid.

Applying the above assumptions, one-dimensional (in space) equations of change are obtained for a single phase fluid.

2. J.B. Keller [39] observed that periodic oscillations can be found when a certain parameter exceeds a critical value, a periodic motion of the fluid is found in which the flow is always in the same direction but in which the speed varies. Inertia is unimportant for this oscillation, which depends upon the interplay between frictional and buoyancy forces. This periodic behavior arises when the fluid is heated at the centre of the lower horizontal segment and cooled at the centre of the upper one.

3. K. Chen [14] addressed the stability of natural convection flows in single-phase closed loop thermosyphons. Analytical and numerical solutions were presented for a range of loop aspect ratios and radii for both laminar and turbulent flows. It was found that the steady-state results for thermosyphons could be expressed in terms of a single dimensionless parameter. When the parameter is below a critical value, the flow was stable. Above that critical point, oscillatory instability exists for a narrow range of a friction parameter. The calculated neutral stability conditions showed that the flow was least stable when the aspect ratio of the loop approached unity. The frequency of the convection induced oscillation is slightly higher than the angular frequency of a fluid particle traveling along the loop.

4. J.E. Hart [26] addressed the nature of convective motions in a toroidal loop of binary fluids oriented in the vertical plane and heated from below. The boundaries of the loop were impermeable, but gradients of the solute could be set up by Soret diffusion in the direction around the loop. The existence and stability of steady solutions were discussed over the Rayleigh number-Soret coefficient parameter plane. When the Soret coefficient was negative, periodic and chaotic oscillations analogous to those of thermohaline convection were predicted. When the Soret coefficient was positive, relaxation oscillations and low Rayleigh number chaotic motions were found. Both sets of phenomena were predicted to occur for realistic thermosyphon parameters.

5. R. Grief *et al.*[23] provided a descriptive review of a number of single phase and two

phase thermosyphon loops. The single phase loop theory may be extended for the case of a two phase loop by specifying suitable equations for the friction factor, the two phase frictional multiplier, the single and two phase heat transfer coefficients and a suitable relationship for the void and mass fractions.

6. C.J. Vincent and J.B.W. Kok [58], using only ten ordinary differential equations, were able to capture the transient performance of a two phase closed loop thermosyphon. They also emphasized the value of the control volume approach as being a powerful tool to describe the overall performance of the thermosyphon with a limited number of variables.

7. Lee and Rhi [43] considered methods for computer simulation of two phase loop thermosyphons. They compared the computer simulation with five different experimental loops with maximum heat transfer rates ranging from 60 to 10^5 W. It was concluded that computer simulation alone could not give any meaningful results unless they are accompanied with empirical correlations using loop-specific experimental test results, thus emphasizing the importance of basic mathematical understanding of the solutions.

8. R.T. Dobson and J.C. Ruppertsberg [17] demonstrated how a simple explicit finite difference discretization formulation scheme is able to capture transients and the highly non-linear behavior of the loop. Dobson had applied the governing equations of mass, momentum and energy to a simplified loop consisting of a single liquid plug with dissolved vapor bubbles. The fundamental equations were applied to the model. He had also built an experimental setup for the validation of the model. The resulting second order

differential equations provided a qualitative description of the fluid oscillations inside the thermosyphon.

1.3.1 Mathematical models with one component fluids

The evolution of the variables like velocity $v(t)$ and temperature $T(t, x)$ (when the cross sectional area of the loop is kept constant and small), are derived using nonlinear and nonlocal coupled system of ordinary and partial differential equations. Mathematicians have studied the well-posedness and the asymptotic behavior of the model when time goes to infinity. The main works concerning this dissertation (both in terms of the problem considered as well as the mathematical tools used) are

- Stability analysis of a closed thermosyphon [28],
- On the dynamics of a closed thermosyphon [56],
- Attractor and inertial manifold for the dynamics of a closed thermosyphon [50],
- Complex oscillation in a closed thermosyphon [52],
- Diffusion induced chaos in a closed-loop thermosyphon [53].

1. M.A. Herrero and J.J.L. Velázquez [28], in their work, ‘Stability analysis of a closed thermosyphon’, studied the motion of a fluid in a closed loop under the effect of natural convection and a given external heat flux. More precisely, they demonstrated that

the stationary solutions of a system describing the intermediate asymptotic were structurally and linearly unstable. Those solutions are linearly unstable to arbitrarily small perturbations in the geometry or the heating applied to the circuit under consideration. An interesting open question concerns the stability of such solutions in the case where alternative assumptions are made about the heat flux.

2. J.J.L. Velázquez [56], in his work, ‘On the dynamics of a closed thermosyphon,’ focused on the motion of a fluid due to natural convection in a closed loop. Under some suitable assumptions on the physical parameters involved, the author studied the nonlocal evolution system consisting of two coupled equations for the velocity and temperature of the fluid. After obtaining the existence and uniqueness of solutions for the corresponding initial value problem, the set of stationary solutions for large Reynolds number was described. A stability analysis of those solutions was performed in such asymptotic limit. In the course of his study, it was shown that for large Reynolds number essential information about the stationary solutions and their stability was contained in the set of zeros of a suitable meromorphic function which was analyzed.

3. A. Rodríguez Bernal [50], in his work, ‘Attractors and inertial manifold for the dynamics of a closed thermosyphon’, studied the asymptotic behaviors of velocity and temperature of the system and obtained the attractors and inertial manifolds for the dynamics of a closed thermosyphon. Depending on the geometry of the loop and the ambient temperature, the author derived the existence of an inertial manifold, not necessarily of

finite dimension, i.e., an invariant exponentially attracting manifold for the flow defined by the equations. It is worth noting that the existence of the inertial manifold does not rely on the existence of big gaps in the spectrum of a linear operator. From that, it follows (non-trivially) that an explicit set of ordinary differential equations that captures all the asymptotic behaviors of the system. By properly choosing the geometry of the loop and the ambient temperature T_a any prescribed odd number of equations of the system can be obtained.

4. A. Rodríguez Bernal and E.S. Van Vleck [52], in their work, ‘Complex oscillations in a closed thermosyphon’, using an explicit construction, obtained the inertial manifold and the exact low dimensional models. The behavior of solutions was analyzed for different ranges of the relevant parameters and, for instance, the Lorenz’s model was obtained for a specific range of parameter values. This connection with Lorenz’s model is a signature of thermosyphon models as low dimensional versions of more complex buoyancy driven spatially extended flows. The relevant variables are the velocity and temperature of the fluid which are the unknowns of the problem that satisfy a system of differential equations.

5. A. Rodríguez Bernal and E.S. Van Vleck [53], in ‘Diffusion induced chaos in a closed loop thermosyphon’ studied the same model as in [52] with axial diffusion and with a prescribed heat flux. The well posedness of the model which consisted of a system of coupled ODEs and PDEs was shown for both the cases with and without temperature diffusion. Boundedness of solutions, the existence of an attractor, and an inertial manifold

were also proven, and an exact reduction to a low-dimensional model was obtained for the diffusion case. The reduced systems may have far fewer degrees of freedom than the reduction to the inertial manifold (leading, in some cases, to simple three mode ODEs). In addition, interesting numerical results were also presented for five mode models.

1.3.2 Mathematical models with binary fluids

Binary fluids were studied with the convective movements caused by inner solute fluctuations generated by the temperature gradient, known as the Soret effect. The mathematical models developed with Soret effect are considered for the following studies. In the case of well mixed binary fluids, the system has a new unknown function which describes the concentration of solute $S(t, x)$ ³.

1. A. Jiménez-Casas and A. Rodríguez Bernal [34], in their work, ‘Finite-dimensional asymptotic behavior in a thermosyphon including the Soret effect’ [34], analyzed the dynamics of a fluid transporting a soluble substance in the interior of a closed loop of arbitrary geometry and subjected to the action of gravity and natural convection. With a suitable normalization of dimensionless variables, they obtained a nonlinear and nonlocal coupled system of ordinary and partial differential equations for the velocity $v(t)$ and the distributions of the temperature $T(t, x)$ and the salinity of solute concentration $S(t, x)$ of the fluid into the loop. They considered the convective movements caused by inner solute

³As mentioned above, we neglect phase separation effects and we will use the expression *binary fluids* in a broad way to refer to this specific situation.

fluctuations generated by the Soret effect. In this work they studied the well-posedness and the asymptotic behaviour of solutions.

2. A. Jiménez-Casas and A.M. Lozano Ovejero [36], in their work, ‘Numerical analysis of a closed loop thermosyphon including the Soret effect’, studied the behavior of solutions for different ranges of the relevant parameters for the model given at the previous work [34] and also considering different heat fluxes. In this work, they obtained the nonlinear coupled system which governs the evolution of the velocity $v(t)$, the temperature $T(t, x)$ and the solute concentration $S(t, x)$ of the fluid.

3. A. Jiménez-Casas [12], in her work, ‘Well posedness and asymptotic behavior of a closed loop thermosyphon’, studied the motion of a fluid containing a soluble substance in the interior of a closed loop under the effects of natural convection and a given external heat flux. This motion is governed also by a coupled nonlinear differential system. The well posedness of the system is showed in a framework generalizing the previous works.

1.4 Objectives of this thesis

Based on the literature survey summarized in Sec. 1.3, the objectives of this research are summarized as follows:

- The primary objective of this research is to formulate a system of equations governing a closed loop thermosyphon model with a **viscoelastic** fluid, which is a generalization of the previous models [23, 35, 36, 37, 47, 50, 56, 59]. The details of the formulation of this new system are described in Chapter 2.
- The second objective is to prove the well-posedness and boundedness of solution in a suitable framework to study the asymptotic behavior of the system when time goes to infinity and to prove the existence of a global attractor and the inertial manifold. Then, describe the dynamics on the inertial manifold to obtain finite dimensional reduced subsystems. In addition, the other aim is to provide a detailed numerical analysis of the behavior of acceleration, velocity and temperature which include a thorough study of the various behaviors of the systems for different values of the Maxwell viscoelastic time. Regarding the role of temperature, we propose two alternative models: The first model deals with one component viscoelastic fluids with Newton's linear cooling law, as in [36, 37, 50, 59], i.e., $h(x, v, T) = l(v)(T_a - T)$ where $l(v)(T_a - T)$ represents the heat transfer law across the wall of the loop, with $l(v)$ a positive quantity depending on the velocity and T_a the given ambient temperature distribution which is dealt in Chapter 3.

- The third objective is to carry out analogous numerical and theoretical analysis for a second model in which one component viscoelastic fluid with a prescribed heat flux [62] is considered, instead of Newton's linear cooling law. Like the previous model, the same exercise of the derivation of the well-posedness and boundedness of solutions, global attractor, inertial manifold, finite dimensional subsystem and numerical experiments are studied and presented in Chapter 4.
- The fourth and final objective is to extend the previous results of the models with one component viscoelastic fluids to binary viscoelastic fluids, taking into account the Soret effect phenomena [26, 34, 35], which is dealt in Chapter 5. This phenomenon is an important aspect of this research, to study and compare the results obtained with already proved results, through which more insights could be drawn about the special nature of viscoelastic fluids. A study of the behavior of the viscoelastic fluids with different Soret coefficients, ranging from lower to higher Soret coefficients would further enable the understanding of the memory effects that the viscoelastic fluids hold. Lyapunov exponents calculation [60] is considered to be a standard technique to ascertain the nature of the behavior of any system. Using the Lyapunov exponents, the behaviors of the system for various ranges of parameters are presented at the end of Chapter 5.

16 *Introduction and Objectives*

Chapter 2

Formulation of a novel model of viscoelastic fluids in a closed loop thermosyphon

2.1 Introduction

Instabilities and chaos in fluids subject to temperature gradients have been a subject of intense work for its applications in engineering and in the atmospheric sciences. In this sort of systems, the fluids display non-trivial behaviors (as turbulence or the formation of convective rolls) when the fluids are subject to a heat flux that competes with buoyancy effects. A traditional approach that goes back to the pioneering work by Lorenz consists of the study of the system under some simplifications. Another approach is to study the controlled setups that capture the underlying complexity of the full system, being a thermosyphon one of those simpler cases [15].

In the engineering literature, a thermosyphon is a device composed of a closed loop *pipe* containing a fluid whose motion is driven by the action of several forces such as gravity and natural convection [35]. As mentioned in chapter 1, all the work on ther-

mosyphons analyzes the behavior of a Newtonian fluid inside the loop and, consequently, neglecting the possible elastic effects in the system coming from either the fluid itself or the elastic walls of the loop. However, many interesting fluids are known to behave slightly different from the common (Newtonian) fluids—in terms of their response to an applied stress—and are commonly referred to as viscoelastic. Among them, it is worth emphasizing volcanic lavas, snow avalanches, flowing paint and biological mucosas.

In this respect, viscoelasticity is a special property of some materials that have both viscous and elastic characteristics. Viscous materials, like water, cannot resist shear flow and deform linearly when a shear stress is applied [4]. Elastic materials, like solids, strain instantaneously when stretched and, unless the plastic limit is reached, they cannot flow. Elasticity is the result of bond stretching along crystallographic planes in an ordered solid, whereas viscosity is the result of the diffusion of atoms or molecules inside an amorphous material. Depending on the change of strain rate versus stress inside a material, the viscosity can be categorized as having a linear or non-linear response. When a material exhibits a linear response it is called, generically, a Newtonian fluid. In this case the stress is linearly proportional to the strain rate. If the material exhibits a non-linear response to the strain rate, it is called a non-Newtonian fluid [18].

Besides the linear response to stress, viscoelastic materials possess also elastic restoring forces similar to that in solids. Thus, viscoelastic materials have elements of both, viscous as well as elastic properties and, as such, exhibit time dependent strain. This combined effect of both liquids and solids can be assessed experimentally by means

of constant stress experiments (creep) or relaxation after stress removal [18].

2.2 Conservation laws and the Maxwell constitutive equation

In this research, a thermosyphon model is considered in which the confined fluid can be described as a linear viscoelastic fluid. This has some *a-priori* interesting peculiarities that could affect the dynamics with respect to the case of a Newtonian fluid. On the one hand, the dynamics has memory so its behavior depends to a certain extent on the whole past history and on the other hand, at small perturbations the fluid behaves like an elastic solid with a characteristic resonance frequency that could, eventually, be relevant (for instance, consider the behavior of jelly or toothpaste).

The simplest approach to viscoelasticity comes from the so-called Maxwell constitutive equation [46]. In this model, both Newton's law of viscosity and Hooke's law of elasticity are generalized and complemented through an evolution equation for the stress tensor, σ .

The stress tensor comes into play in the equation for the conservation of momentum:

$$\rho \left(\frac{\partial \mathbf{v}}{\partial t} + \mathbf{v} \cdot \nabla \mathbf{v} \right) = -\nabla p + \nabla \cdot \sigma \quad (2.2.1)$$

For a Maxwellian fluid, the stress tensor takes the form:

$$\frac{\mu}{E} \frac{\partial \sigma}{\partial t} + \sigma = \mu \dot{\gamma} \quad (2.2.2)$$

where μ is the fluid viscosity, E the Young's modulus and $\dot{\gamma}$ the shear strain rate

(or rate at which the fluid deforms). Under stationary flow, equation (2.2.2) reduces to Newton's law and consequently, equations (2.2.1) reduce to the celebrated Navier-Stokes equation. On the contrary, for short times where *impulsive* behavior from rest can be expected the first term dominates and the stress obeys Hooke's law of elasticity.

Memory effects can be understood from equation (2.2.2) after performing a separation of variables and integrating. Thus, the equation can be rewritten as:

$$\sigma(t) = \int_0^t e^{E/\mu(t-s)} \mu \dot{\gamma}(s) ds \quad (2.2.3)$$

where it is clear that the local state of stress, $\sigma(t)$ is calculated from the present and past values of $\dot{\gamma}(t)$ with a *memory* time scale of order μ/E , also known as Maxwell time.

In a thermosyphon, the equations of motion can be greatly simplified because of the quasi-one-dimensional geometry of the loop. Therefore, it is assumed that the section of the loop is constant and small compared with the dimensions of the physical device, so that the arc length co-ordinate along the loop (x) gives the position in the circuit. The velocity of the fluid is assumed to be independent of the position in the circuit, i.e., it is assumed to be a scalar quantity depending only on time. This approximation comes from the fact that the fluid is assumed to be incompressible, so

$$\nabla \cdot \mathbf{v} = 0, \quad (2.2.4)$$

besides the quasi-one-dimensional assumption. On the contrary, temperature is assumed to depend on time and position along the loop.

The derivation of the thermosyphon equations of motion is similar to that in [39, 59]. The simplest way to incorporate equation (2.2.2) is by differentiating equation (2.2.1) with respect to time and replacing the resulting time derivative of σ with equation (2.2.2). This way to incorporate the constitutive equation allows to reduce the number of unknowns (we remove σ from the system of equations) at the cost of increasing the order of the time derivatives to second order.

The resulting second order equation is then averaged along the loop section (as in [39]). Hence, after adimensionalizing the variables (to reduce the number of free parameters) we arrive at our main system of equations

$$\begin{cases} \varepsilon \frac{d^2v}{dt^2} + \frac{dv}{dt} + G(v)v &= \oint Tf, & v(0) = v_0, \frac{dv}{dt}(0) = w_0 \\ \frac{\partial T}{\partial t} + v \frac{\partial T}{\partial x} &= h(x, v, T) + \nu \frac{\partial^2 T}{\partial x^2}, & T(0, x) = T_0(x) \end{cases} \quad (2.2.5)$$

The parameter ε in equation (2.2.5) is the adimensional version of μ/E which has dimensions of time. Roughly speaking, it gives the (adimensional) time scale in which the transition from elastic to fluid-like occurs in the fluid.

The model taken into consideration, forms an ODE/PDE system for the velocity $v(t)$, which is assumed to be uniform along the cross section of the path of the loop, depending only on time t , the distribution of the temperature $T(t, x)$ of the fluid into the loop, $h(x, v, T)$ represents the heat transfer law along the loop, with $\nu \geq 0$. Besides, $\oint = \int_0^1 dx$ denotes integration along the closed path of the circuit. The function f describes the geometry of the loop and the distribution of gravitational forces [39, 59]. Hereafter, it is considered that all the functions involved in these models are periodic with respect

to the spacial variable x . It is noted that $\oint f = 0$.

The system of equations (2.2.5) is not a trivial extension of the Newtonian model in Ref.[52] due to the first term in the differential equation for the velocity. Specifically, the addition of a term proportional to the second derivative of v is *singular*, in the sense that it changes qualitatively the character of the equations. The implications of this singular perturbation cannot be ascertained using a standard boundary layer analysis (see the Appendix A.1 for details). So a complementary theoretical and numerical approach is mandatory.

It is assumed that $G(v)$ which specifies the friction law at the inner wall of the loop, is positive and bounded away from zero. This function has been usually taken to be $G(v) = G$, a positive constant for the linear friction case [39] (Stokes flow), or $G(v) = |v|$ for the quadratic (highly turbulent) law [28, 44] or even a rather general function given by $G(v) = \tilde{g}(Re)|v|$ where Re is the Reynolds number i.e., $Re = \rho v L / \mu$. It is considered that the general function of the velocity is assumed to be large [53, 56]. The functions G , f and h incorporate relevant physical constants of the model such as the cross sectional area D , the length of the loop L , the Prandtl, Rayleigh or Reynolds number, etc., see [56].

2.2.1 One component viscoelastic fluids with Newton's linear cooling law model

The first model proposed here consists of one component viscoelastic fluids with Newton's linear cooling law. The Newton's linear cooling law is given by $h(x, v, T) = l(v)(T_a - T)$ where $l(v)(T_a - T)$ represents the heat transfer law across the wall of the

loop, with $l(v)$ a positive quantity depending on the velocity and T_a the (given) ambient temperature distribution, see [23, 36, 56, 59]. This model is given by the following equations:

$$\begin{cases} \varepsilon \frac{d^2v}{dt^2} + \frac{dv}{dt} + G(v)v = \oint Tf, & v(0) = v_0, \frac{dv}{dt}(0) = w_0 \\ \frac{\partial T}{\partial t} + v \frac{\partial T}{\partial x} = l(v)(T_a - T) + \nu \frac{\partial^2 T}{\partial x^2}, & T(0, x) = T_0(x) \end{cases}$$

2.2.2 One component viscoelastic fluids with a prescribed heat flux model

The second model is called the one component viscoelastic fluids with a prescribed heat flux $h(x)$ model. It is customary to take the prescribed heat flux case, the general heat flux $h = h(x)$ as given in [28, 44]. As the name suggests, the temperature in this model depends on a general heat flux law $h(x)$, i.e., the heat flux depending only on the position in the loop x . And it is given by the equations:

$$\begin{cases} \varepsilon \frac{d^2v}{dt^2} + \frac{dv}{dt} + G(v)v = \oint Tf, & v(0) = v_0, \frac{dv}{dt}(0) = w_0 \\ \frac{\partial T}{\partial t} + v \frac{\partial T}{\partial x} = h(x) + \nu \frac{\partial^2 T}{\partial x^2}, & T(0, x) = T_0(x) \end{cases}$$

2.2.3 Binary viscoelastic fluids with Soret effect model

In binary fluids the interaction between the temperature gradients and the solute gradients play a critical role in the dynamical behavior of any system.

Thermodiffusion is a phenomenon of temperature gradient [16], observed in a mixture of two or more types of moving particles. The Soret effect is a very important component of the study of any physical experiment that pertains to thermodiffusion. It

gives rise to interaction between the thermal and solute gradients even when the fluid is at rest [42]. The term “Soret effect” normally means thermodiffusion in liquids. Thermodiffusion is labeled “positive” when particles move from a hot to cold region and “negative” when the reverse is true [30]. Typically, the heavier or larger species in a mixture exhibits positive thermophoretic behavior while the lighter or smaller species exhibits negative behavior.

In this model, it is considered that the distribution equation of solute into the loop is as in [39]. Here, the conservation of mass for the solute is used. It has been assumed that the fluid also transports the solute and generates Soret diffusion by molecular diffusion. Thus, the Soret diffusion or Soret effect is a molecular flux of solute generated by an internal gradient. It can generate gradients of solute in the fluid even with impermeable boundaries.

In viscoelastic fluids, because of the temperature gradients, the Soret effect induces the solute concentration gradients significantly, thus initiating a natural convection inside the loop. The dynamical behavior induced by the temperature gradients and solute gradients of the viscoelastic fluid by the Soret effect is the main focus of this research. The study of the spatiotemporal phenomena in viscoelastic fluids emerges from the integrated observations of velocity, temperature and solute concentration [30].

$$\left\{ \begin{array}{l} \varepsilon \frac{d^2 v}{dt^2} + \frac{dv}{dt} + G(v)v = \oint (T - S)f, \quad v(0) = v_0, \frac{dv}{dt}(0) = w_0 \\ \frac{\partial T}{\partial t} + v \frac{\partial T}{\partial x} = l(v)(T_a - T) + \nu \frac{\partial^2 T}{\partial x^2}, \quad T(0, x) = T_0(x) \\ \frac{\partial S}{\partial t} + v \frac{\partial S}{\partial x} = c \frac{\partial^2 S}{\partial x^2} - b \frac{\partial^2 T}{\partial x^2}, \quad S(0, x) = S_0(x) \end{array} \right. \quad (2.2.6)$$

where $l(v)(T_a - T)$ is the Newton's linear cooling law as in [23, 34, 35, 36, 37, 56, 59], which represents the heat transfer law across the loop, $l(v)$ a positive quantity depending on the velocity and T_a the (given) ambient temperature distribution, see [23, 36, 56, 59]. In addition to that, in this model we consider the diffusion of temperature given by the term $\nu \frac{\partial^2 T}{\partial x^2}$.

This model becomes more relevant as the physical world has many such complex models to be studied. This model can be generalized in many different ways, from changing the constitutive equation (from Maxwellian to other more complex situations) or to include shear-thinning effects [46] common to many non-Newtonian materials. Shear-thinning is the manifestation of a shear-rate dependent viscosity. Hence, it is commonly observed that many fluids reduce their resistance to flow for large enough imposed stresses (in this case, temperature gradients), for instance tooth paste, paint or lava. Albeit interesting, those cases fall out of the scope of the present work.

The following chapters provide the proofs of the well-posedness of the solutions, their asymptotic behaviors, their explicit reduction to finite dimensional systems and the numerical simulation of the asymptotic equations.

Chapter 3

One component viscoelastic fluids with Newton's linear cooling law

3.1 Introduction

The first model consists of one component viscoelastic fluids with Newton's linear cooling law, given by $h(x, v, T) = l(v)(T_a - T)$. Here, $l(v)(T_a - T)$ represents the heat transfer law across the loop wall, with $l(v)$ a positive quantity depending on the velocity and T_a the (given) ambient temperature distribution, see [23, 36, 56, 59]. In addition to that, the diffusion of temperature is given by the term $\nu \frac{\partial^2 T}{\partial x^2}$, where $\nu \geq 0$. The parameter ε in this system of equations is the adimensional version of μ/E which has the dimension of time. Roughly speaking, it gives the (adimensional) time scale in which the transition from elastic to fluid-like occurs in the fluid. In summary, the first model is given by the equations:

$$\begin{cases} \varepsilon \frac{d^2 v}{dt^2} + \frac{dv}{dt} + G(v)v = \oint T f, & v(0) = v_0, \frac{dv}{dt}(0) = w_0 \\ \frac{\partial T}{\partial t} + v \frac{\partial T}{\partial x} = l(v)(T_a - T) + \nu \frac{\partial^2 T}{\partial x^2}, & T(0, x) = T_0(x) \end{cases}$$

Hence, the model is a system of ODE/PDE for the velocity $v(t)$ and the distribution of the temperature $T(t, x)$ of the fluid into the loop. In the equation, $\oint = \int_0^1 dx$ denotes the integration along the closed path of the circuit. The function f describes the geometry of the loop and the distribution of gravitational forces [39, 59]. Note that $\oint f = 0$. This geometrical condition restricts the functions to periodic functional spaces as we will discuss in some detail in the following sections.

Here, it is assumed that $G(v)$ which specifies the friction law at the inner wall of the loop, is positive and bounded away from zero. It is considered that the functions G and l are continuous functions, such that $G(v) \geq G_0 > 0$, and $l(v) \geq l_0 > 0$, for G_0 and l_0 positive constants.

The objectives of this model are:

- To present an analysis beginning with the well posedness and boundedness of the solutions. Besides, the existence of an attractor and an inertial manifold is shown and an explicit reduction to low-dimensional systems is obtained. It is noteworthy that we are able to obtain an exact finite-dimensional reduction (see equation 3.3.57) that may have a much lower number of degrees of freedom.
- To provide a detailed numerical analysis of the behavior of acceleration, velocity and temperature which includes a thorough study of the various behaviors of the system for different values of viscoelastic fluid and ambient temperature distribution.
- The numerical analysis will show that viscoelasticity induces a chaotic behavior that

is not captured by a boundary layer analysis (that would predict the same qualitative behaviors as in the original model in Ref. [52], see the Appendix for details) being the new (non-trivial) emergent behaviors induced by the viscoelasticity worth characterizing.

The structure of this chapter is as follows: The first section provides an introduction to the system, explaining briefly the dynamics of the functions and the objectives of this model. In Section 2, the proofs for the existence, uniqueness and boundedness of the solutions are given. The Section 3 provides a detailed derivation of the dynamics of the system in the inertial manifold as a reduced dimensionality version of the full system of equation (2.2.5). The Section 4 presents the numerical integration of the reduced system of equations valid in the manifold to understand the role of the main parameters of the physical system.

3.2 Well-posedness and boundedness: global attractor

3.2.1 Existence and uniqueness of solutions

In this section we prove the existence and uniqueness of solutions of the thermosyphon model (2.2.5).

First, we observe that for $\nu \geq 0$, if we integrate the equation for the temperature along the loop taking into account the periodicity of T , i.e., $\oint \frac{\partial T}{\partial x} = \oint \frac{\partial^2 T}{\partial x^2} = 0$, we have

30 *One component viscoelastic fluids with Newton's linear cooling law*

$\frac{d}{dt}(\oint T) = l(v)(\oint T_a - \oint T)$. Therefore, $\oint T \rightarrow \oint T_a$ exponentially as time goes to infinity for every $\oint T_0$.

Moreover, if we consider $\tau = T - \oint T$ then from the second equation of system (2.2.5), we obtain that τ verifies the equation:

$$\frac{\partial \tau}{\partial t} + v \frac{\partial \tau}{\partial x} = \nu \frac{\partial^2 \tau}{\partial x^2} + l(v)(\tau_a - \tau), \tau(0, x) = \tau_0(x) = T_0 - \oint T_0$$

where $\tau_a = T_a - \oint T_a$.

Finally, since $\oint f = 0$, we have $\oint T f = \oint \tau f$ and the equations for v reads

$$\varepsilon \frac{d^2 v}{dt^2} + \frac{dv}{dt} + G(v)v = \oint \tau f, v(0) = v_0, \quad \frac{dv}{dt}(0) = w_0.$$

Thus, with $w = \frac{dv}{dt}$ we get (w, v, τ) verifying the system (2.2.5) with τ_a, τ_0 replacing T_a, T_0 respectively and now $\oint \tau = \oint \tau_a = \oint \tau_0 = \oint f = 0$. Therefore, hereafter we consider the system (2.2.5) where all functions have zero average.

Also, if $\nu > 0$ the operator $\nu A = -\nu \frac{\partial^2}{\partial x^2}$, together with periodic boundary conditions, is an unbounded, self-adjoint operator with compact resolvent in $L_{per}^2(0, 1)$, that is positive when restricted to the space of zero average functions $\dot{L}_{per}^2(0, 1)$. Hence, the equation for the temperature T in (2.2.5) is of parabolic type for $\nu > 0$.

i) The case with diffusion: $\nu > 0$

We consider the acceleration $w = \frac{dv}{dt}$ and write the system (2.2.5) as the following evolution system for the acceleration, velocity and temperature:

$$\left\{ \begin{array}{l} \frac{dw}{dt} + \frac{1}{\varepsilon}w = -\frac{1}{\varepsilon}G(v)v + \frac{1}{\varepsilon} \oint Tf, \quad w(0) = w_0 \\ \frac{dv}{dt} = w, \quad v(0) = v_0 \\ \frac{\partial T}{\partial t} + v \frac{\partial T}{\partial x} - \nu \frac{\partial^2 T}{\partial x^2} = l(v)(T_a - T), \quad T(0, x) = T_0(x) \end{array} \right. \quad (3.2.1)$$

this is:

$$\frac{d}{dt} \begin{pmatrix} w \\ v \\ T \end{pmatrix} + \begin{pmatrix} \frac{1}{\varepsilon} & 0 & 0 \\ 0 & 0 & 0 \\ 0 & 0 & -\nu \frac{\partial^2}{\partial x^2} \end{pmatrix} \begin{pmatrix} w \\ v \\ T \end{pmatrix} = \begin{pmatrix} F_1(w, v, T) \\ F_2(w, v, T) \\ F_3(w, v, T) \end{pmatrix} \quad (3.2.2)$$

with $F_1(w, v, T) = -\frac{1}{\varepsilon}G(v)v + \frac{1}{\varepsilon} \oint Tf$, $F_2(w, v, T) = w$ and $F_3(w, v, T) = -v \frac{\partial T}{\partial x} + l(v)(T_a -$

$T)$ and the initial data $\begin{pmatrix} w \\ v \\ T \end{pmatrix} (0) = \begin{pmatrix} w_0 \\ v_0 \\ T_0 \end{pmatrix}$.

The operator $B = \begin{pmatrix} \frac{1}{\varepsilon} & 0 & 0 \\ 0 & 0 & 0 \\ 0 & 0 & -\nu \frac{\partial^2}{\partial x^2} \end{pmatrix}$ is a sectorial operator in $\mathcal{Y} = \mathbb{R}^2 \times \dot{H}_{per}^1(0, 1)$

with domain $D(B) = \mathbb{R}^2 \times \dot{H}_{per}^3(0, 1)$ and has compact resolvent, where

$$\dot{L}_{per}^2(0, 1) = \{u \in L_{loc}^2(\mathbb{R}), u(x+1) = u(x)a.e., \oint u = 0\}, \dot{H}_{per}^m(0, 1) = H_{loc}^m(\mathbb{R}) \cap \dot{L}_{per}^2(0, 1). \quad (3.2.3)$$

Using the results and techniques of sectorial operator of [27] we obtain Theorem 3.2.1.

Theorem 3.2.1 *We assume that $\nu > 0, H(r) = rG(r)$ and $l(v)$ are locally Lipschitz, $f \in \dot{L}^2_{per}(0, 1), T_a \in \dot{H}^1_{per}(0, 1)$ and $l(v) \geq l_0 > 0$. Then, given $(w_0, v_0, T_0) \in \mathcal{Y} = \mathbb{R}^2 \times \dot{H}^1_{per}(0, 1)$, there exists a unique solution of (2.2.5) satisfying*

$$(w, v, T) \in C([0, \infty), \mathbb{R}^2 \times \dot{H}^1_{per}(0, 1)) \cap C(0, \infty, \mathbb{R}^2 \times \dot{H}^3_{per}(0, 1)),$$

$$\left(\dot{w}, w, \frac{\partial T}{\partial t}\right) \in C(0, \infty, \mathbb{R}^2 \times \dot{H}^{3-\delta}_{per}(0, 1)),$$

where $w = \dot{v} = \frac{dv}{dt}$ and $\dot{w} = \frac{d^2v}{dt^2}$ for every $\delta > 0$. In particular, (2.2.5) defines a nonlinear semigroup, $S(t)$ in $\mathcal{Y} = \mathbb{R}^2 \times \dot{H}^1_{per}(0, 1)$, with $S(t)(w_0, v_0, T_0) = (w(t), v(t), T(t))$.

PROOF. We cover several steps.

Step (i) We prove the local existence and regularity. This follows easily from the variation of constants formula of [27]. In order to prove this we write the system as (3.2.2) and we have:

$$U_t + BU = F(U), \text{ with } U = \begin{pmatrix} w \\ v \\ T \end{pmatrix}, B = \begin{pmatrix} \frac{1}{\varepsilon} & 0 & 0 \\ 0 & 0 & 0 \\ 0 & 0 & -\nu \frac{\partial^2}{\partial x^2} \end{pmatrix} \text{ and } F = \begin{pmatrix} F_1 \\ F_2 \\ F_3 \end{pmatrix}$$

where the operator B is a sectorial operator in $\mathcal{Y} = \mathbb{R}^2 \times \dot{H}^1_{per}(0, 1)$ with domain $D(B) = \mathbb{R}^2 \times \dot{H}^3_{per}(0, 1)$ and has compact resolvent. In this context, the operator $A = -\frac{\partial^2}{\partial x^2}$ must be understood in the variational sense, i.e., for every $T, \varphi \in \dot{H}^1_{per}(0, 1)$,

$$\langle A(T), \varphi \rangle = \oint \frac{\partial T}{\partial x} \frac{\partial \varphi}{\partial x}$$

and $\dot{L}_{per}^2(0, 1)$ coincides with the fractional space of exponent $\frac{1}{2}$ [27]. Hereafter we denote by $\|\cdot\|$ the norm on the space $\dot{L}_{per}^2(0, 1)$. Now, if we prove that the nonlinearity $F : \mathcal{Y} = \mathbb{R}^2 \times \dot{H}_{per}^1(0, 1) \mapsto \mathcal{Y}^{-\frac{1}{2}} = \mathbb{R}^2 \times \dot{L}_{per}^2(0, 1)$ is well defined and is Lipschitz and bounded on bounded sets, we obtain the local existence for the initial data in $\mathcal{Y} = \mathbb{R}^2 \times \dot{H}_{per}^1(0, 1)$.

Using $H(v) = G(v)v$ and $l(v)$ are locally Lipschitz together with $f \in \dot{L}_{per}^2(0, 1)$ and $T_a \in \dot{H}_{per}^1(0, 1)$, we will prove the nonlinear terms, $F_1(w, v, T) = -\frac{1}{\varepsilon}G(v)v + \frac{1}{\varepsilon} \mathcal{F} T f$, $F_2(w, v, T) = w$ and $F_3(w, v, T) = -v \frac{\partial T}{\partial x} + l(v)(T_a - T)$ satisfy $F_1 : \mathbb{R}^2 \times \dot{H}_{per}^1(0, 1) \mapsto \mathbb{R}$, $F_2 : \mathbb{R}^2 \times \dot{H}_{per}^1(0, 1) \mapsto \mathbb{R}$ and $F_3 : \mathbb{R}^2 \times \dot{H}_{per}^1(0, 1) \mapsto \dot{L}_{per}^2(0, 1)$, this is $F : \mathcal{Y} \mapsto \mathcal{Y}^{-\frac{1}{2}}$ is well defined, Lipschitz and bounded on bounded sets. It is possible to prove this by considering $T_a \in \dot{L}_{per}^2(0, 1)$. In order to prove these properties of the nonlinearity F , let $U_i = (w_i, v_i, T_i)^t$ and we note that

$$\begin{aligned} \|F_3(U_1) - F_3(U_2)\| &\leq \left\| -v_1 \frac{\partial T_1}{\partial x} + l(v_1)(T_a - T_1) + v_2 \frac{\partial T_2}{\partial x} - l(v_2)(T_a - T_2) \right\| \leq \\ &\leq |l(v_1) - l(v_2)| \|T_a\| + (1) + (2) \end{aligned}$$

where

$$(1) \equiv \left\| -v_1 \frac{\partial T_1}{\partial x} + v_2 \frac{\partial T_2}{\partial x} \right\| \text{ and } (2) \equiv \|l(v_2)T_2 - l(v_1)T_1\|$$

and adding $\pm v_1 \frac{\partial T_2}{\partial x}$, $\mp v_2 \frac{\partial T_1}{\partial x}$ and $\mp v_1 \frac{\partial T_1}{\partial x}$ in (1), we have

$$(1) \leq (|v_1| + |v_2|) \left\| \frac{\partial T_2}{\partial x} - \frac{\partial T_1}{\partial x} \right\| + |v_2 - v_1| \left\| \frac{\partial T_1}{\partial x} \right\| + |v_1| \left\| \frac{\partial T_1}{\partial x} - \frac{\partial T_2}{\partial x} \right\|$$

and adding $\pm l(v_2)T_1$ in (2), we get

$$(2) \equiv \|l(v_2)T_2 - l(v_1)T_1\| \leq |l(v_1) - l(v_2)| \|T_1\| + |l(v_2)| \|T_2 - T_1\|$$

34 *One component viscoelastic fluids with Newton's linear cooling law*

and from the above hypothesis on function $l(v)$ there exists $M > 0$ such that $\|F_3(U_1) - F_3(U_2)\| \leq M \left(|v_1 - v_2| + \|T_1 - T_2\|_{\dot{H}_{per}^1(0,1)} \right) \leq C \|U_1 - U_2\|_{\mathbb{R}^2 \times \dot{H}_{per}^1}$ and the rest is obvious.

Therefore, using the techniques of variations of constants formula of [27], we obtain the unique local solution $(w, v, T) \in C([0, \tau], \mathcal{Y})$ of (3.2.1) which are given by

$$w(t) = w_0 e^{-\frac{1}{\varepsilon}t} - \frac{1}{\varepsilon} \int_0^t e^{-\frac{1}{\varepsilon}(t-r)} H(r) dr + \frac{1}{\varepsilon} \int_0^t e^{-\frac{1}{\varepsilon}(t-r)} (\oint T(r) f) dr \quad (3.2.4)$$

with $H(r) = H(v(r))$.

$$v(t) = v_0 + \int_0^t w(r) dr \quad (3.2.5)$$

$$T(t, x) =$$

$$e^{-\nu A t} T_0(x) + \int_0^t e^{-\nu A(t-r)} l(v(r)) [T_a(r, x) - T(r, x)] dr - \int_0^t e^{-\nu A(t-r)} v(r) \frac{\partial T(r, x)}{\partial x} dr \quad (3.2.6)$$

and using again the results of [27], we get the regularity of solutions. In fact, from the smoothing effect of the equations, we have $(w, v, T) \in C([0, \tau], \mathcal{Y} = \mathbb{R}^2 \times \dot{H}_{per}^1(0, 1)) \cap C((0, \tau), \mathbb{R}^2 \times \dot{H}_{per}^2(0, 1))$ and $(\dot{w}, w, \frac{\partial T}{\partial t}) \in C((0, \tau), \mathbb{R}^2 \times \dot{H}_{per}^{2-\delta}(0, 1))$, for some positive τ and any $\delta > 0$. Now, for $\epsilon > 0$ we have $(w(\epsilon), v(\epsilon), T(\epsilon)) \in \mathbb{R}^2 \times \dot{H}_{per}^2(0, 1)$ and since $F : \mathbb{R}^2 \times \dot{H}_{per}^2(0, 1) \mapsto \mathbb{R}^2 \times \dot{H}_{per}^1(0, 1)$ is well defined, Lipschitz and bounded on bounded sets, we have $(w, v, T) \in C([\epsilon, \tau], \mathbb{R}^2 \times \dot{H}_{per}^2(0, 1)) \cap C((\epsilon, \tau), \mathbb{R}^2 \times \dot{H}_{per}^3(0, 1))$ and $(\dot{w}, w, \frac{\partial T}{\partial t}) \in C((\epsilon, \tau), \mathbb{R}^2 \times \dot{H}_{per}^{3-\delta}(0, 1))$. Since ϵ is arbitrary, we obtain the regularity of the local solution.

Step (ii) Now, we prove the solutions of (3.2.1) for every time $t \geq 0$.

To prove the global existence, we must show that the solutions are bounded in

$\mathcal{Y} = \mathbb{R}^2 \times \dot{H}_{per}^1(0, 1)$ norm on finite time intervals. First, to obtain the norm of T is bounded in finite time, we note that multiplying the equations for the temperature by T in $\dot{L}_{per}^2(0, 1)$ and integrating by parts, we have:

$$\frac{1}{2} \frac{d}{dt} \|T\|^2 + \nu \left\| \frac{\partial T}{\partial x} \right\|^2 = \int l(v)(T_a - T)T dx$$

since $\int T \frac{\partial T}{\partial x} = \frac{1}{2} \int \frac{\partial}{\partial x}(T^2) = 0$.

Using Cauchy-Schwarz and the Young inequality and then the Poincaré inequality, since $\int T = 0$ together with π^2 is the first nonzero eigenvalue of $A = -\frac{\partial^2}{\partial x^2}$ in $\dot{L}_{per}^2(0, 1)$, we obtain

$$\frac{1}{2} \frac{d}{dt} \|T\|^2 + (\nu\pi^2 + l(v))\|T\|^2 \leq \frac{l(v)}{2} \|T_a\|^2 + \frac{l(v)}{2} \|T\|^2$$

and using $l(v) \geq l_0 > 0$ we get

$$\frac{d}{dt} \|T\|^2 + (2\nu\pi^2 + l_0)\|T\|^2 \leq l(v)\|T_a\|^2 \quad (3.2.7)$$

and we conclude the norm of T in $\dot{L}_{per}^2(0, 1)$ remains bounded in finite time.

Now, we note that differentiating the second equation of (2.2.5) with respect to x , we obtain the same equations for $\left\| \frac{\partial T}{\partial x} \right\|$ considering now $\left\| \frac{\partial T_a}{\partial x} \right\|$, we obtain

$$\frac{d}{dt} \left\| \frac{\partial T}{\partial x} \right\|^2 + (2\nu\pi^2 + l_0) \left\| \frac{\partial T}{\partial x} \right\|^2 \leq l(v) \left\| \frac{\partial T_a}{\partial x} \right\|^2. \quad (3.2.8)$$

Thus we show that the norm of T in $\dot{H}_{per}^1(0, 1)$ remains bounded in finite time.

Then, using $\|T\|$ is bounded for finite time, we prove that $|w(t)|$ and $|v(t)|$ remain bounded in finite time and we conclude. \square

ii) The case with no diffusion: $\nu = 0$

The system now reads

$$\begin{cases} \varepsilon \frac{d^2 v}{dt^2} + \frac{dv}{dt} + G(v)v = \oint T f, & v(0) = v_0, \frac{dv}{dt}(0) = w_0 \\ \frac{\partial T}{\partial t} + v \frac{\partial T}{\partial x} = h(x, v, T), & T(0, x) = T_0(x) \end{cases} \quad (3.2.9)$$

where $h(x, v, T) = l(v)(T_a - T)$ i.e., we consider Newton's linear cooling law as in Refs. [34, 35, 36, 37], and it is no longer of a parabolic type system and is also given by:

$$\begin{cases} \frac{dw}{dt} + \frac{1}{\varepsilon} w = -\frac{1}{\varepsilon} G(v)v + \frac{1}{\varepsilon} \oint T f, & w(0) = w_0 \\ \frac{dv}{dt} = w, & v(0) = v_0 \\ \frac{\partial T}{\partial t} + v \frac{\partial T}{\partial x} = l(v)(T_a - T), & T(0, x) = T_0(x) \end{cases} \quad (3.2.10)$$

To prove the system is well-posed, we use the techniques from [50] considering the same transport equation for temperature in different thermosyphon models as [34, 35, 36, 37, 50].

Note that if $v(t)$ is a given continuous function then the equation for the temperature can be integrated along characteristics to obtain

$$T^v(t, x) = T_0(x - \int_0^t v) e^{-\int_0^t l(v)} + \int_0^t [l(v(r)) e^{-\int_r^t l(v)} T_a(x - \int_r^t v)] \quad (3.2.11)$$

and plugging this into the nonlocal differential equation for the acceleration and into the equation for the velocity yields

$$w^v(t) = w_0 e^{-\frac{1}{\varepsilon}t} - \frac{1}{\varepsilon} \int_0^t e^{-\frac{1}{\varepsilon}(t-r)} G(v(r))v(r)dr + \frac{1}{\varepsilon} \int_0^t e^{-\frac{1}{\varepsilon}(t-r)} (\oint T^v(r)f)dr$$

$$v(t) = v_0 + \int_0^t w^v(r)dr.$$

We note that for $T_0, T_a \in \dot{L}_{per}^2(0, 1)$ and since in this space the translations are continuous isometries, (3.2.11) defines a continuous function of time with values in this space. Although we restrict ourselves to $\dot{L}_{per}^2(0, 1)$, many other choices of space are possible for solving problem (3.2.10). In fact any Banach space of 1-periodic functions of x having zero mean and in which translations are continuous isometries can be used as an “admissible space”, X , see [50]. In particular $W_{per}^{m,p}(0, 1), C_{per}^k(0, 1)$ are admissible spaces between others. Then we can prove Lemma 3.2.2.

Lemma 3.2.2 *Let $\tau > 0$, fix $v \in C[0, \tau]$ and assume that $T_0, T_a \in X$ where X is an “admissible space”, see [50], in particular $T_0, T_a \in \dot{H}_{per}^1(0, 1)$. Then the function given in (3.2.11), $T^v \in C([0, \tau], X)$ is an integral solution of the PDE which is satisfied only if T_0 and T_a are differentiable. In particular, if $T_0, T_a \in \dot{H}_{per}^1(0, 1)$ then T^v is continuous with values in $\dot{H}_{per}^1(0, 1)$ and satisfies the PDE as an equality in $\dot{L}_{per}^2(0, 1)$, a.e. in time. Moreover, (3.2.11) satisfies the following properties:*

(i)

$$\|T^v\|_X \leq \max\{\|T_0\|_X, \|T_a\|_X\} \text{ a.e. in time} \quad (3.2.12)$$

(ii) *If there exist positive constants $c_d, d = a$ and $d = 0$ such that T_0, T_a satisfy*

$\|T_d(\cdot + h) - T_d(\cdot)\|_X \leq c_d|k|$ for all k , then T^v satisfies

$$\|T^v(t+k) - T^v(t)\|_X \leq C|k|, \quad C = C(\|v\|_\infty, \|T_a\|_X) \quad (3.2.13)$$

positive constant independent on time.

(iii) We assume that $X \subset \dot{L}_{per}^2(0, 1)$ and there exist positive constants $c_d, d = a$ and $d = 0$ such that T_0, T_a satisfy $\|T_d(\cdot + h) - T_d(\cdot)\|_{\dot{L}_{per}^2} \leq c_d|h|$ for all h . If we also assume $v_i, i = 1, 2$ are continuous in $t \in [0, \tau]$, then

$$\sup_{r \in [0, \tau]} \|T_1^v(r) - T_2^v(r)\| \leq K\tau \|v_1 - v_2\|_\infty, \quad (3.2.14)$$

K is a positive constant and $\|v_1 - v_2\|_\infty = \sup_{r \in [0, \tau]} |v_1(r) - v_2(r)|$.

Proof: see [34, 35, 36, 37, 50]. Then, we have Theorem 3.2.3. \square

Theorem 3.2.3 Assume $\nu = 0, G(v)v$ is locally Lipschitz, $f \in \dot{L}_{per}^2(0, 1), T_0, T_a \in \dot{H}_{per}^1(0, 1)$ and $w_0, v_0 \in \mathbb{R}^2$. Then there exists a unique solution of (3.2.10) satisfying

$$(w, v, T) \in C((0, \infty), \mathbb{R}^2 \times \dot{H}_{per}^1(0, 1))$$

and T satisfies the PDE in the sense of (3.2.11).

Moreover $(\dot{w}, \dot{v}, \frac{\partial T}{\partial t}) \in C([0, \infty), \mathbb{R}^2 \times \dot{L}_{per}^2(0, 1))$.

PROOF. As noted above, we need to solve the fixed point problem

$$\begin{aligned} v(t) = \mathcal{F}(v)(t) = v_0 + \int_0^t \left(w_0 e^{-\frac{1}{\varepsilon}s} - \frac{1}{\varepsilon} \int_0^s e^{-\frac{1}{\varepsilon}(s-r)} G(v(r))v(r) dr \right) ds + \\ + \frac{1}{\varepsilon} \int_0^t \left(\int_0^s e^{-\frac{1}{\varepsilon}(s-r)} \left(\oint T^v(r) f \right) dr \right) ds \end{aligned}$$

on a space of continuous functions. More precisely, we take $W = \{v \in C[0, L], v(0) = v_0, |v(t) - v_0| \leq M\}$, endowed with the sup norm, with L and M to be chosen and prove that \mathcal{F} is a contraction on W .

From (3.2.12) in Lemma 3.2.2 for T^v we have $\|T^v\| \leq \max\{\|T_0\|, \|T_a\|\}$ and this, together with the local Lipschitz property of $G(v)v$ shows that for fixed M , $\mathcal{F}(\mathcal{M}) \subset \mathcal{M}$ if L is sufficiently small.

To show that \mathcal{F} is a contraction, it is clear that we must prove some Lipschitz dependence on $\oint T^v f$ with respect to $v \in W$.

First, we note that from $T_0, T_a \in \dot{H}_{per}^1(0, 1)$, then verify (3.2.13) i.e., $\|T_d(\cdot + h) - T_d(\cdot)\|_{\dot{L}_{per}^2} \leq c_d|h|$ for all k with $d = 0, a$ and given $v_i \in W$, again from (3.2.14) in Lemma 3.2.2, we have

$$\sup_{r \in [0, \tau]} \|T_1^v(r) - T_2^v(r)\| \leq LM \|v_1 - v_2\|_\infty.$$

We find that \mathcal{F} is Lipschitz on W with a Lipschitz constant depending on L and M that tends to zero as $L \rightarrow 0$ and then \mathcal{F} is a contraction for small enough L . Therefore, local well-posedness follows.

To prove the global existence, it is sufficient to prove that $(w(t), v(t))$ is bounded on finite time intervals, since from

$$\begin{aligned} w^v(t_1) - w^v(t_2) &= \\ w_0 e^{-\frac{1}{\varepsilon}(t_1 - t_2)} - \frac{1}{\varepsilon} \int_{t_1}^{t_2} e^{-\frac{1}{\varepsilon}(t-r)} G(v(r))v(r) dr + \frac{1}{\varepsilon} \int_{t_1}^{t_2} e^{-\frac{1}{\varepsilon}(t-r)} \left(\oint T^v(r) f \right) dr \\ v(t_1) - v(t_2) &= \\ - \int_{t_1}^{t_2} \left(w_0 e^{-\frac{s}{\varepsilon}} - \frac{1}{\varepsilon} \int_0^s e^{-\frac{1}{\varepsilon}(s-r)} G(v(r))v(r) dr + \frac{1}{\varepsilon} \int_0^s e^{-\frac{1}{\varepsilon}(s-r)} \oint T^v(r) f dr ds \right) \end{aligned}$$

we find that $(w(t), v(t))$ is of Cauchy type as $t \rightarrow t_0$ for finite t_0 . Consequently, the limit of $(w(t), v(t), T(t))$ exists in $\mathbb{R}^2 \times \dot{L}_{per}^2(0, 1)$ and the solution can be prolonged.

But again from (3.2.12) together with (3.2.4) and (3.2.5) we obtain boundedness on finite time intervals and global existence follows.

As noted above, if $T_0, T_a \in \dot{H}_{per}^1(0, 1)$ then T satisfies the PDE equation as an equality in $\dot{L}_{per}^2(0, 1)$ a.e. in time. In particular, we have $\frac{\partial T}{\partial t} \in C((0, \infty), \dot{L}_{per}^2(0, 1))$. \square

3.2.2 Boundedness of the solutions and global attractor

In order to obtain asymptotic bounds on the solutions as $t \rightarrow \infty$, we consider the friction function G satisfying the hypotheses from the previous section and we also assume that there exists a constant $h_0 \geq 0$ such that:

$$\limsup_{t \rightarrow \infty} \frac{|G'(t)|}{G(t)} = 0 \text{ and } \limsup_{t \rightarrow \infty} \frac{|tG'(t)|}{G(t)} \leq h_0. \quad (3.2.15)$$

We make use of the L'Hopital's lemma proved in [52] to prove several results in this section.

Lemma 3.2.4 *L'Hopital's lemma: assume f and g are real differentiable functions on $(a, b), b \leq \infty, g'(x) \neq 0$ on (a, b) and $\lim_{x \rightarrow b} g(x) = \infty$.*

(i) *If $\limsup_{x \rightarrow b} \frac{f'(x)}{g'(x)} = L$, then $\limsup_{x \rightarrow b} \frac{f(x)}{g(x)} \leq L$.*

(ii) *If $\liminf_{x \rightarrow b} \frac{f'(x)}{g'(x)} = L$, then $\liminf_{x \rightarrow b} \frac{f(x)}{g(x)} \geq L$.*

With this, we have Lemma 3.2.5.

Lemma 3.2.5 *If we assume $G(r)$ and $H(r) = rG(r)$ satisfy the hypothesis from Theorem 3.2.1 or Theorem 3.2.3 together with (3.2.15), then:*

$$\limsup_{t \rightarrow \infty} \frac{\left| H(t) - \frac{1}{\varepsilon} \int_0^t e^{-\frac{1}{\varepsilon}(t-r)} H(r) dr \right|}{G(t)} \leq H_0 \quad (3.2.16)$$

with $H_0 = (1 + h_0)\varepsilon$ a positive constant such that $H_0 \rightarrow 0$ if $\varepsilon \rightarrow 0$.

PROOF. Integrating by parts we have:

$$H(t) - \frac{1}{\varepsilon} \int_0^t e^{-\frac{1}{\varepsilon}(t-r)} H(r) dr = \int_0^t e^{-\frac{1}{\varepsilon}(t-r)} H'(r) dr$$

and using Lemma 3.2.4 we obtain

$$\begin{aligned} \limsup_{t \rightarrow \infty} \frac{\int_0^t e^{\frac{1}{\varepsilon}r} |H'(r)| dr}{e^{\frac{1}{\varepsilon}t} G(t)} &\leq \varepsilon \limsup_{t \rightarrow \infty} \frac{|H'(t)|}{G(t) + \varepsilon G'(t)} \leq \\ &\leq \varepsilon \limsup_{t \rightarrow \infty} \frac{|G(t) + tG'(t)|}{G(t) + \varepsilon G'(t)} \end{aligned}$$

and from (3.2.15) we conclude. \square

Remark 3.2.1 We note that the conditions (3.2.15) are satisfied for all friction functions G considered in this work, i.e., the thermosyphon models where G is constant or linear or quadratic law. Moreover, the conditions (3.2.15) are also true for $G(s) \approx A|s|^n$, as $s \rightarrow \infty$.

Now, we use the asymptotic bounded for temperature to obtain the asymptotic bounded for the velocity and the acceleration functions.

Theorem 3.2.6 Under the above notations and hypothesis of Theorem 3.2.1 or Theorem 3.2.3, if we assume also that G satisfies (3.2.16) for some constant $H_0 \geq 0$, then

Part (i) General case:

$$(i) \limsup_{t \rightarrow \infty} |v(t)| \leq \frac{1}{G_0} \limsup_{t \rightarrow \infty} \left| \oint T(t, \cdot) f(\cdot) \right| + H_0 \quad (3.2.17)$$

In particular: If $\limsup_{t \rightarrow \infty} \|T\| \in \mathbb{R}$ then

$$\limsup_{t \rightarrow \infty} |v(t)| \leq \frac{1}{G_0} \|f\| \limsup_{t \rightarrow \infty} \|T\| + H_0 \in \mathbb{R}. \quad (3.2.18)$$

(ii) If $\limsup_{t \rightarrow \infty} \|T\| \in \mathbb{R}$ and we denote by $G_0^* = \limsup_{t \rightarrow \infty} G(v(t))$, then

$$\limsup_{t \rightarrow \infty} |w(t)| \leq G_0^* H_0 + \left(1 + \frac{G_0^*}{G_0}\right) I \text{ with } I = \limsup_{t \rightarrow \infty} \left| \oint T(t, \cdot) f(\cdot) \right| \text{ and} \quad (3.2.19)$$

$$\limsup_{t \rightarrow \infty} |w(t)| \leq G_0^* H_0 + \left(1 + \frac{G_0^*}{G_0}\right) \|f\| \limsup_{t \rightarrow \infty} \|T\| \in \mathbb{R}. \quad (3.2.20)$$

Part (ii) If $\nu \neq 0$ and assume that there exists L_0 a positive constant such that $L_0 \geq l(v) \geq l_0$. Then for any solution of (2.2.5) in the space $\mathcal{Y} = \mathbb{R}^2 \times \dot{H}_{per}^1(0, 1)$ we have:

(i)

$$\limsup_{t \rightarrow \infty} \|T(t)\| \leq \left(\frac{L_0}{2\nu\pi^2 + l_0}\right)^{\frac{1}{2}} \|T_a\| \text{ and } \limsup_{t \rightarrow \infty} \left\| \frac{\partial T}{\partial x}(t) \right\| \leq \left(\frac{L_0}{2\nu\pi^2 + l_0}\right)^{\frac{1}{2}} \left\| \frac{\partial T_a}{\partial x} \right\| \quad (3.2.21)$$

(ii)

$$\limsup_{t \rightarrow \infty} |v(t)| \leq \frac{1}{G_0} \left(\frac{L_0}{2\nu\pi^2 + l_0}\right)^{\frac{1}{2}} \|T_a\| \|f\| + H_0 \quad (3.2.22)$$

(iii) If we denote by $G_0^* = \limsup_{t \rightarrow \infty} G(v(t))$

$$\limsup_{t \rightarrow \infty} |w(t)| \leq G_0^* H_0 + G_2 \frac{\|T_a\| \|f\|}{\sqrt{2\nu\pi^2 + l_0}} \text{ with } G_2 = \left(1 + \frac{G_0^*}{G_0}\right) \sqrt{L_0}. \quad (3.2.23)$$

In particular, (2.2.5) has a global compact and connected attractor, \mathcal{A} , in $\mathcal{Y} = \mathbb{R}^2 \times \dot{H}_{per}^1(0, 1)$.

PROOF. **Part (i)** General case.

(i) From (3.2.1) we have that

$$\frac{dw}{dt} + \frac{1}{\varepsilon} w = -\frac{1}{\varepsilon} G(v)v + \frac{1}{\varepsilon} \oint T \cdot f \quad (3.2.24)$$

and $w(t) = \frac{dw}{dt}$ satisfies

$$\frac{dw}{ds} = w(0)e^{-\frac{1}{\varepsilon}s} - \frac{1}{\varepsilon} \int_0^s e^{-\frac{1}{\varepsilon}(s-r)} H(r) dr + \frac{1}{\varepsilon} \int_0^s \left(\oint T(r) \cdot f \right) e^{-\frac{1}{\varepsilon}(s-r)} dr \quad (3.2.25)$$

where $H(r) = H(v(r)) = v(r)G(v(r))$. First, we rewrite (3.2.25) as

$$\frac{dv}{ds} + G(s)v = w(0)e^{-\frac{1}{\varepsilon}s} + I_1(s) + I_2(s), \quad (3.2.26)$$

with

$$I_1(s) = \frac{1}{\varepsilon} \int_0^s (\oint T(r) \cdot f) e^{-\frac{1}{\varepsilon}(s-r)} dr \text{ and } I_2(s) = H(s) - \frac{1}{\varepsilon} \int_0^s e^{-\frac{1}{\varepsilon}(s-r)} H(r). \quad (3.2.27)$$

Next, for any $\delta > 0$ there exists $t_0 > 0$ such that $\delta(s) = w(0)e^{-\frac{1}{\varepsilon}s} < \delta$ for any $s \geq t_0$ and integrating with $t \geq t_0$ we obtain

$$|v(t)| \leq |v(t_0)|e^{-\int_{t_0}^t G(s)ds} + e^{-\int_{t_0}^t G(s)ds} \int_{t_0}^t e^{\int_{t_0}^s G(r)dr} (\delta + |I_1(s)| + |I_2(s)|) \quad (3.2.28)$$

Using L'Hopital's Lemma 3.2.4 proved in [52], we get

$$\begin{aligned} & \limsup_{t \rightarrow \infty} e^{-\int_{t_0}^t G(s)ds} \int_{t_0}^t e^{\int_{t_0}^s G(r)dr} (|I_1(s)| + |I_2(s)| + \delta) = \\ & = \limsup_{t \rightarrow \infty} \frac{\int_{t_0}^t e^{\int_{t_0}^s G(r)dr} (|I_1(s)| + |I_2(s)| + \delta) ds}{e^{\int_{t_0}^t G(s)ds}} \\ & \leq \limsup_{t \rightarrow \infty} \frac{|I_1(t)| + |I_2(t)| + \delta}{G(t)} \text{ for any } \delta > 0. \end{aligned} \quad (3.2.29)$$

Moreover, using again the L'Hopital's Lemma 3.2.4 proved in [52], we get

$$\limsup_{t \rightarrow \infty} |I_1(t)| \leq \limsup_{t \rightarrow \infty} \frac{\int_0^t e^{\frac{r}{\varepsilon}} |\oint T(t) \cdot f|}{\varepsilon e^{\frac{t}{\varepsilon}}} \leq \limsup_{t \rightarrow \infty} |\oint T(t) \cdot f|$$

and from (3.2.28) together with (3.2.16) we conclude that

$$\limsup_{t \rightarrow \infty} |v(t)| \leq \limsup_{t \rightarrow \infty} \frac{\limsup_{t \rightarrow \infty} |\oint T(t) \cdot f|}{G_0} + H_0 + \delta$$

for any δ .

(ii) From (3.2.24) together with singular Gronwall lemma, we get

$$|w(t)| \leq |w(t_0)|e^{-\frac{1}{\varepsilon}t} + \frac{1}{\varepsilon} \int_{t_0}^t e^{-\frac{1}{\varepsilon}(t-r)} [G(r)|v(r)| + |\oint T(r) \cdot f|] dr \quad (3.2.30)$$

where $G(r) = G(v(r))$. Consequently, for any $\delta > 0$ there exists t_0 such that for any $t \geq t_0$

$$\begin{aligned} & \frac{1}{\varepsilon} \int_{t_0}^t e^{-\frac{1}{\varepsilon}(t-r)} [G(v(r))|v(r)| + |\oint T(r) \cdot f|] dr \leq \\ & \leq \left[\delta + \limsup_{t \rightarrow \infty} (G(v(t))|v(t)| + |\oint T(t) \cdot f|) \right] (1 - e^{-\frac{1}{\varepsilon}(t-t_0)}) \end{aligned} \quad (3.2.31)$$

this is

$$\limsup_{t \rightarrow \infty} |w(t)| \leq \limsup_{t \rightarrow \infty} (G(v(t))|v(t)| + |\oint T(t) \cdot f| + \delta), \quad (3.2.32)$$

for any $\delta > 0$ and using the above results i) we get (3.2.19).

Part (ii)

(i) From (3.2.7) together with (3.2.8) we get

$$\|T\|^2 \leq \frac{L_0}{2\nu\pi^2 + l_0} \|T_a\|^2 + \left(\|T_0\|^2 - \frac{L_0}{2\nu\pi^2 + l_0} \|T_a\|^2 \right)_+ e^{-(2\pi^2\nu + l_0)t} \text{ and} \quad (3.2.33)$$

$$\left\| \frac{\partial T}{\partial x} \right\|^2 \leq \frac{L_0}{2\nu\pi^2 + l_0} \left\| \frac{\partial T_a}{\partial x} \right\|^2 + \left(\|T_0\|^2 - \frac{L_0}{2\nu\pi^2 + l_0} \|T_a\|^2 \right)_+ e^{-(2\pi^2\nu + l_0)t} \quad (3.2.34)$$

and by elementary integration we obtain (3.2.21). Using Part I the rest ii) and iii) are obvious. Since the sectorial operator B defined in the above section 3.2.1 has compact resolvent, the rest follows from [[24], Theorem 4.2.2 and 3.4.8]. \square

Remark 3.2.2 *First, we note that the hypothesis about the function $l(v)$ in the above Theorem 3.2.6, $l(v) \leq L_0$ is satisfied when we consider Newton's linear cooling law $h = k(T_a - T)$, where k is a positive quantity i.e., $l(v) = k = L_0$ as [33]. Moreover, this*

condition is also satisfied if we consider $h = l(v)(T_a - T)$ where $l(v)$ is a positive upper bounded function.

Second, it is important to note that we prove in the next section the existence of the global compact and connected attractor and the inertial manifold for the system (3.2.1), when we consider the general Newton's linear cooling law without the additional above hypothesis on $l(v)$; but we assume that the friction function $G(v)$ always satisfies 3.2.15 for every $\nu \geq 0$.

In order to get this, we consider the Fourier expansions and observing the dynamics of each coefficient of Fourier expansions to improve the asymptotic bounded of temperature. In particular, we will prove $\limsup_{t \rightarrow \infty} \|T(t)\| \leq \|T_a\|$ for every locally Lipschitz and positive function $l(v)$ and also for every $\nu \geq 0$ (see (3.3.40) in Proposition 3.3.1) for every friction function $G(v)$ always satisfying 3.2.15 for every $\nu \geq 0$.

3.3 Asymptotic behavior: finite-dimensional systems

We take a close look at the dynamics of (2.2.5) by considering the Fourier expansions of each function and observing the dynamics of each Fourier mode. Assume that $T_a \in \dot{H}_{per}^1(0, 1)$ and $f \in \dot{L}_{per}^2(0, 1)$ are given by the following Fourier expansions

$$T_a(x) = \sum_{k \in \mathcal{Z}^*} b_k e^{2\pi k i x} \text{ and } f(x) = \sum_{k \in \mathcal{Z}^*} c_k e^{2\pi k i x} \text{ with } \mathcal{Z}^* \quad (3.3.35)$$

while the initial data $T_0 \in \dot{H}_{per}^1(0, 1)$ is given by $T_0(x) = \sum_{k \in \mathcal{Z}^*} a_{k0} e^{2\pi k i x}$.

Note the Fourier expansion for all $g \in \dot{H}_{per}^m(0, 1)$, $m \geq 0$ is given by the expression

$g(x) = \sum_{k \in \mathcal{Z}^*} a_k e^{2\pi kix}$ with $\mathcal{Z}^* = \mathcal{Z} \setminus \{0\}$ and we have

$$\|g\|_{\dot{H}_{per}^m(0,1)} = (2\pi)^m \left(\sum_{k \in \mathcal{Z}^*} k^{2m} |a_k|^2 \right)^{\frac{1}{2}}. \quad (3.3.36)$$

Assume that $T(t, x) \in \dot{H}_{per}^1(0, 1)$ is given by

$$T(t, x) = \sum_{k \in \mathcal{Z}^*} a_k(t) e^{2\pi kix}. \quad (3.3.37)$$

Then, we find that the coefficients $a_k(t)$ in (3.3.37), is a solution of:

$$\dot{a}_k(t) + (2\pi kvi + 4\nu\pi^2 k^2 + l(v))a_k(t) = l(v)b_k, \quad a_k(0) = a_{k0}, \quad k \in \mathcal{Z}^*. \quad (3.3.38)$$

Since all the functions involved are real, we have $\bar{a}_k = a_{-k}$, $\bar{b}_k = b_{-k}$, and $\bar{c}_k = c_{-k}$. Therefore, (2.2.5) is equivalent to the infinite system of ODEs consisting of (3.3.38) coupled with

$$\varepsilon \frac{d^2 v}{dt^2} + \frac{dv}{dt} + G(v)v = \sum_{k \in \mathcal{Z}^*} a_k(t) c_{-k}.$$

The system of equations (2.2.5) reflects two of the main features: (i) the coupling between the modes enter only through the velocity, while diffusion acts as a linear damping term, (ii) it is important to note in this model, we have also the non linear term given by Newton's linear cooling law. In what follows, we will exploit this explicit equation for the temperature modes to analyze the asymptotic behavior of the system and to obtain the explicit low-dimensional models.

3.3.1 Inertial manifold

We consider the general case $\nu > 0$ together with the nonlinear Newton's linear cooling law introduced by [28, 56], that is $l(v)(T_a - T)$ with $l(v) \geq l_0 > 0$ locally Lipschitz

function and use inertial manifold techniques, in the spirit of nondiffusion case of [50], to give an explicit low-dimensional system of ODEs that describes the asymptotic dynamics of (2.2.5). The existence of an inertial manifold does not rely, in this case, on the existence of large gaps in the spectrum of the elliptic operator but on the invariance of certain sets of Fourier modes.

A similar explicit construction was given by Bloch and Titi in [6] for a nonlinear beam equation where the nonlinearity occurs only through the appearance of the L^2 norm of the unknown. A related construction was given by Stuart in [54] for a nonlocal reaction-diffusion equation.

We note that the system (2.2.5) is equivalent to the system (3.2.1) for acceleration, velocity and temperature. It is equivalent to the following infinite system of ODEs (3.3.39)

$$\left\{ \begin{array}{l} \frac{dw}{dt} + \frac{1}{\varepsilon}w = -\frac{1}{\varepsilon}G(v)v + \frac{1}{\varepsilon} \sum_{k \in \mathcal{Z}^*} a_k(t)c_{-k}, \quad w(0) = w_0 \\ \frac{dv}{dt} = w, \quad v(0) = v_0 \\ \dot{a}_k(t) + (2\pi k\nu i + 4\nu\pi^2 k^2 + l(v))a_k(t) = l(v)b_k, \quad a_k(0) = a_{k0}, \quad k \in \mathcal{Z}^*. \end{array} \right. \quad (3.3.39)$$

We first improve the bounds on acceleration, velocity and temperature of the previous section for all situations, with $\nu \geq 0$ and with $l(v) \geq l_0 > 0$ general locally Lipschitz function and with $G(v)$ under the hypotheses of Lemma 3.2.5 for some $H_0 \geq 0$.

We will prove in Proposition 3.3.1 that we have always an upper bounded for the temperature in $\dot{L}^2(0, 1)$ independent of the velocity and the function $l(v)$, considered in

the Newton's linear cooling law, and also independent of the diffusion coefficient. This is

$$\limsup_{t \rightarrow \infty} \|T(t, \cdot)\| \leq \|T_a\|$$

Proposition 3.3.1 *Under the above notations, for every solution of the system (2.2.5), (w, v, T) , and for every $k \in \mathcal{Z}^*$ we have*

$$(i) \limsup_{t \rightarrow \infty} |a_k(t)| \leq |b_k|, \text{ in particular } \limsup_{t \rightarrow \infty} \|T(t, \cdot)\| \leq \|T_a\| \quad (3.3.40)$$

$$(ii) \limsup_{t \rightarrow \infty} |v(t)| \leq \frac{I_0}{G_0} + H_0, \quad \text{with } I_0 = \sum_{k \in \mathcal{Z}^*} |b_k| |c_k| \quad (3.3.41)$$

and G_0 a positive constant such that $G(v) \geq G_0$.

$$(iii) \limsup_{t \rightarrow \infty} |w(t)| \leq G_0^* H_0 + \left(1 + \frac{G_0^*}{G_0}\right) I_0, \text{ with} \quad (3.3.42)$$

$$I_0 = \sum_{k \in \mathcal{Z}^*} |b_k| |c_k| \text{ and } G_0^* = \limsup_{t \rightarrow \infty} G(v(t)).$$

In particular, we have a global compact and connected attractor $\mathcal{A} \subset [-M, M] \times [-N, N] \times \mathcal{C}$ where M, N are the upper bounds for acceleration and velocity as given in (3.3.42) and (3.3.41) and $T_0 \in \mathcal{C} = \{R(x) = \sum_{k \in \mathcal{Z}^*} r_k e^{2\pi k i x}, |r_k| \leq |b_k|\}$.

PROOF. From (3.3.38), we have

$$a_k(t) = a_{k0} e^{-4\nu\pi^2 k^2 t} e^{-\int_0^t [2\pi k v i + l(v)]} + b_k \int_0^t e^{-4\nu\pi^2 k^2 (t-s)} l(v(s)) e^{-\int_s^t [2\pi k v i + l(v)]} ds \quad (3.3.43)$$

with

$$\begin{aligned} |e^{-\int_0^t 2\pi k v i}| &= |e^{-\int_s^t 2\pi k v i}| = 1 \\ e^{-4\nu\pi^2 k^2 (t-s)} &\leq 1 \\ \int_0^t l(v(s)) e^{-\int_s^t l(v)} ds &= 1 - e^{-\int_0^t l(v)}. \end{aligned} \quad (3.3.44)$$

Thus, we obtain:

$$|a_k(t)| \leq |a_{k0}|e^{-4\nu\pi^2k^2t}e^{-\int_0^t l(v)} + |b_k|(1 - e^{-\int_0^t l(v)}) \quad (3.3.45)$$

and we get $\limsup_{t \rightarrow \infty} |a_k(t)| \leq |b_k|$.

Using Theorem 3.2.6 together with $\oint Tf = \sum_{k \in \mathcal{X}^*} a_k(t)\bar{c}_k$, we get

$$\begin{aligned} \limsup_{t \rightarrow \infty} |v(t)| &\leq \frac{1}{G_0} \limsup_{t \rightarrow \infty} \left| \oint T(t, \cdot) f(\cdot) \right| + H_0 \\ \limsup_{t \rightarrow \infty} |w(t)| &\leq G_0^* H_0 + \left(1 + \frac{G_0^*}{G_0} \right) \|f\| \limsup_{t \rightarrow \infty} \|T\| \in \mathbb{R}. \end{aligned}$$

From this upper bounded for the velocity, we also have L_0 the upper bound for the continuous positive function $l(v)$ and using Part (ii) from Theorem 3.2.6 we conclude. \square

We note from the above result, we have always the upper bound for $\|T\|$ and from Theorem 3.2.6 for the velocity. Therefore we can consider L_0 the upper bound for the continuous positive function $l(v)$, we note by $L_0 = \limsup_{t \rightarrow \infty} l(v)$ and we prove in Proposition 3.3.2 the bound of solutions to show the influence of diffusion coefficient ν .

Proposition 3.3.2 *Under the above notations, for every solution of the system (2.2.5), (w, v, T) , and for every $k \in \mathcal{X}^*$ we have*

$$\limsup_{t \rightarrow \infty} |a_k(t)| \leq L_\nu^k |b_k|, \text{ with } L_\nu^k = \frac{L_0}{4\nu\pi^2k^2 + l_0} \text{ in particular} \quad (3.3.46)$$

$$\limsup_{t \rightarrow \infty} \|T(t, \cdot)\| \leq \frac{L_0}{4\nu\pi^2 + l_0} \|T_a\|.$$

Moreover, if $\nu \neq 0$ we have that

$$\|T\|_{\dot{H}_{per}^{m+2}}^2 \leq \frac{L_0}{4\nu\pi^2} \|T_a\|_{\dot{H}_{per}^m}^2$$

$$\limsup_{t \rightarrow \infty} |v(t)| \leq \frac{I_0}{G_0} + H_0, \quad \text{with } I_0 = \frac{L_0}{4\nu\pi^2 + l_0} \sum_{k \in \mathcal{Z}^*} |b_k| |c_k| \quad (3.3.47)$$

and G_0 positive constant such that $G(v) \geq G_0$.

$$\limsup_{t \rightarrow \infty} |w(t)| \leq G_0^* H_0 + 2I_0, \quad \text{with } I_0 = \frac{L_0}{4\nu\pi^2 + l_0} \sum_{k \in \mathcal{Z}^*} |b_k| |c_k| \quad \text{and } G_0^* = \limsup_{t \rightarrow \infty} G(v(t)). \quad (3.3.48)$$

PROOF. Using again

$$a_k(t) = a_{k0} e^{-4\nu\pi^2 k^2 t} e^{-\int_0^t [2\pi k v i + l(v)]} + b_k \int_0^t e^{-4\nu\pi^2 k^2 (t-s)} l(v(s)) e^{-\int_s^t [2\pi k v i + l(v)]} ds \quad (3.3.49)$$

if we assume that $0 < l_0 \leq l(v) \leq L_0$ then we obtain

$$|a_k(t)| \leq |a_{k0}| e^{-(4\nu\pi^2 k^2 + l_0)t} + |b_k| L_0 \int_0^t e^{-4(\nu\pi^2 k^2 + l_0)(t-s)}$$

and we get

$$|a_k(t)| \leq \left(|a_{k0}| - \frac{L_0}{4\nu\pi^2 k^2 + l_0} |b_k| \right)_+ e^{-(4\nu\pi^2 k^2 + l_0)t} + \frac{L_0}{4\nu\pi^2 k^2 + l_0} |b_k| \quad (3.3.50)$$

this is if $|a_{k0}| \leq \frac{L_0}{4\nu\pi^2 k^2 + l_0} |b_k|$ then $|a_k(t)| \leq \frac{L_0}{4\nu\pi^2 k^2 + l_0} |b_k|$.

In particular $|a_k(t)| \leq \frac{L_0}{4\nu\pi^2 k^2 + l_0} |b_k| \leq \frac{L_0}{4\nu\pi^2 + l_0} |b_k|$ for every $k \in \mathcal{Z}^*$ and also $|a_k(t)| \leq \frac{L_0}{4\nu\pi^2 k^2 + l_0} |b_k| \leq \frac{L_0}{4\nu\pi^2 k^2} |b_k|$, i.e., $k^2 |a_k(t)| \leq \frac{L_0}{4\nu\pi^2} |b_k|$.

Then, we also have that

$$\|T\|_{\dot{H}_{per}^{m+2}}^2 \leq \sum_{|k|=1}^{\infty} |k|^{2m+4} |a_k(t)| \leq \frac{L_0}{4\nu\pi^2} \sum_{|k|=1}^{\infty} |k|^{2m} |b_k| \leq \frac{L_0}{4\nu\pi^2} \|T_a\|_{\dot{H}_{per}^m}^2.$$

Finally, we note that if $L_0 = \limsup_{t \rightarrow \infty} l(v(t))$ then given $\delta > 0$ there exists t_0 such that $L(v(t)) \leq L_0 + \delta$ for every $t \geq t_0$ and integrating in $t \geq t_0$ we obtain

$\limsup_{t \rightarrow \infty} |a_k(t)| \leq \frac{L_0}{4\nu\pi^2 k^2 + l_0} |b_k| + \delta$, for any $\delta > 0$ and

$$\|T\|_{\dot{H}_{per}^m}^2 \leq \|T\|_{\dot{H}_{per}^{m+2}}^2 \leq \frac{L_0}{4\nu\pi^2} \|T_a\|_{\dot{H}_{per}^m}^2.$$

Using again Theorem 3.2.6 we conclude. \square

We note if $\nu = 0$ then $|a_k| \leq |b_k| \leq \frac{L_0}{l_0} |b_k|$. If $\nu > 0$ we observe in the numerical experiments, as ν is bigger, the solution becomes stable or periodic.

As a consequence, we have the following result on the smoothness of the attractor of (2.2.5).

Corollary 3.3.3 (i) If $|a_{k0}| \leq \frac{L_0}{4\nu\pi^2 k^2 + l_0} |b_k|$, then $|a_k(t)| \leq \frac{L_0}{4\nu\pi^2 k^2 + l_0} |b_k|$ for every $t \geq 0$.

(ii) If \mathcal{A} is the global attractor in the space $\mathcal{Y} = \mathbb{R}^2 \times \dot{H}_{per}^1(0, 1)$, then for every $(w_0, v_0, T_0) \in \mathcal{A}$, with $T_0(x) = \sum_{k \in \mathcal{Z}^*} a_k e^{2\pi k i x}$ we get,

$$|a_k| \leq \frac{L_0}{4\nu\pi^2 k^2 + l_0} |b_k|, \quad k \in \mathcal{Z}^*. \quad (3.3.51)$$

In particular, if $T_a \in \dot{H}_{per}^m(0, 1)$ with $m \geq 1$, the global attractor $\mathcal{A} \hookrightarrow \mathbb{R}^2 \times \dot{H}_{per}^{m+2}(0, 1)$ and is compact in this space.

PROOF. (i) From (3.3.50) we have $|a_k(t)| \leq \frac{L_0}{4\nu\pi^2 k^2 + l_0} |b_k| + (|a_{k0}| - \frac{L_0}{4\nu\pi^2 k^2 + l_0} |b_k|)_+ e^{-\int_0^t l(v)}$

therefore, if $|a_{k0}| \leq \frac{L_0}{4\nu\pi^2 k^2 + l_0} |b_k|$ then $|a_k(t)| \leq \frac{L_0}{4\nu\pi^2 k^2 + l_0} |b_k|$ for every $t \geq 0$ and $k \in \mathcal{Z}^*$.

(ii) We note from i) if $T_a(x) = \sum_{k \in \mathcal{Z}^*} b_k e^{2\pi k i x} \in \dot{H}_{per}^m$, then

$$\sum_{k \in \mathcal{Z}^*} k^{2m} |b_k|^2 < \infty$$

and therefore

$$T_0 \in \mathcal{C} = \left\{ R(x) = \sum_{k \in \mathcal{Z}^*} r_k e^{2\pi k i x} \in \dot{H}_{per}^{m+2}, 4\nu\pi^2 k^2 |r_k| \leq |b_k| \right\}$$

This is $\mathcal{A} \subset [-M, M] \times [-N, N] \times \mathcal{C}$ where M, N are the upper bounds for acceleration and velocity as given in (3.3.48) and (3.3.47). But the set \mathcal{C} is compact in \dot{H}_{per}^{m+2} since for any sequence $\{T^n\}$ in \mathcal{C} we can extract a subsequence that we still denote $\{T^n\}$ such that it converges weakly to a function T and such that for any $k \in \mathcal{Z}^*$, the Fourier coefficients verify $a_k^n \rightarrow a_k$ as $n \rightarrow \infty$, where a_k is the k th Fourier coefficient of T . Therefore, $4\nu\pi^2 k^2 |a_k| \leq |b_k|$ and for every integer E ,

$$\|T^n - T\|_{m+2}^2 \leq \sum_{|k|=1}^E |k|^{2m+4} |a_k^n - a_k|^2 + C_0 \sum_{|k|=E+1}^{\infty} |k|^{2m+4} |k|^{2m} |b_k|^2$$

where $\|\cdot\|_{m+2}$ denote the norm in \dot{H}_{per}^{m+2} . Hence the first term goes to zero as $n \rightarrow \infty$ and the second term can be made arbitrarily small as $E \rightarrow \infty$. Consequently, $T \in \mathcal{C}$ and $T^n \rightarrow T$ in \dot{H}_{per}^{m+2} and the result follows. \square

Note that this result reveals in particular the asymptotic smoothing of (2.2.5). In the next result we will prove that the dynamical system induced by (3.2.1) in the phase space $\mathcal{Y} = \mathbb{R}^2 \times \dot{H}_{per}^m(0, 1)$, $m \geq 1$ has an inertial manifold. According to [20] we have the following definition.

Definition 3.3.1 *Let $S(t), t \geq 0$, be a nonlinear semigroup in a Banach space in \mathcal{Y} that has a global attractor \mathcal{A} . Then a smooth manifold $\mathcal{M} \subset \mathcal{Y}$ is called an inertial manifold if*

(i) \mathcal{M} is positively invariant, i.e., $S(t)\mathcal{M} \subset \mathcal{M}$ for every $t \geq 0$;

(ii) \mathcal{M} contains the attractor, i.e., $\mathcal{A} \subset \mathcal{M}$ and

(iii) \mathcal{M} is exponentially attracting in the sense that there exists a constant $\delta > 0$ such that for every bounded set $B \subset \mathcal{Y}$ there exists $C = C(B) \geq 0$ such that

$$\text{dist}(S(t)B, \mathcal{M}) \leq Ce^{-\delta t} \tag{3.3.52}$$

for every $t \geq 0$.

See, for example, [20] and [47].

Assume the ambient temperature given by

$$T_a(x) = \sum_{k \in K} b_k e^{2\pi k i x} \in \dot{H}_{per}^m(0, 1) \quad (3.3.53)$$

where $K \subset \mathbf{Z}$ i.e., with $b_k \neq 0$ for every $k \in K \subset \mathbf{Z}$ with $0 \notin K$, since $\oint T_a = 0$.

Then we denote by V_m the closed linear subspace of $\dot{H}_{per}^m(0, 1)$ spanned by $\{e^{2\pi k i x}, k \in K\}$ and consider the following spectral decomposition in $\dot{H}_{per}^m(0, 1) : T = T^1 + T^2$, where T^1 denotes the projection of T onto V and T^2 the projection onto the space generated by $\{e^{2\pi k i x}, k \notin K\}$. Note that (3.2.1) is equivalent to

$$\left\{ \begin{array}{l} \varepsilon \frac{d^2 v}{dt^2} + \frac{dv}{dt} + G(v)v = \oint (T^1 + T^2) f, \quad v(0) = v_0, \frac{dv}{dt}(0) = w_0 \\ \frac{\partial T^1}{\partial t} + v \frac{\partial T^1}{\partial x} = l(v)(T_a - T^1) + \nu \frac{\partial^2 T^1}{\partial x^2}, \quad T^1(0, x) = T_0^1(x) \\ \frac{\partial T^2}{\partial t} + v \frac{\partial T^2}{\partial x} = -l(v)T^2 + \nu \frac{\partial^2 T^2}{\partial x^2}, \quad T^2(0, x) = T_0^2(x). \end{array} \right. \quad (3.3.54)$$

Note that from (3.3.38) if $b_k = 0$ then the k th mode for the temperature is damped out exponentially and therefore the space V attracts the dynamics for the temperature. This is precisely stated in the following result.

Theorem 3.3.4 *Assume that $T_a \in \dot{H}_{per}^m(0, 1)$ and $f \in \dot{L}_{per}^2(0, 1)$. Then the set $\mathcal{M} = \mathbb{R}^2 \times V_m$ is an inertial manifold for the flow of $S(t)(w_0, v_0, T_0) = (w(t), v(t), T(t))$ in the space $\mathcal{Y} = \mathbb{R}^2 \times \dot{H}_{per}^m(0, 1)$. Moreover, if $f \in V_m$ the inertial manifold \mathcal{M} has the exponential tracking property, i.e., for every $(w_0, v_0, T_0) \in \mathbb{R}^2 \times \dot{H}_{per}^m(0, 1)$ there exists $(w_1, v_1, T_1) \in \mathcal{M}$ such that if $(w_i(t), v_i(t), T_i(t)), i = 0, 1$, are the corresponding solutions of*

(3.2.1), then $(w_0(t), v_0(t), T_0(t)) - (w_1(t), v_1(t), T_1(t)) \rightarrow 0$ in $\mathbb{R}^2 \times \dot{H}_{per}^m(0, 1)$. In particular if K is a finite set, the dimension of \mathcal{M} is $|K| + 2$, where $|K|$ is the number of elements in K .

PROOF. In order to prove that \mathcal{M} is invariant, we note if $k \notin K$ then $b_k = 0$ and therefore $a_{k0} = 0, (T_0^2 = 0)$ from (3.3.45), we get that $a_k(t) = 0$ for every t , i.e., $T(t, x) = \sum_{k \in K} a_k(t) e^{2\pi k i x} = T^1$. Thus, if $(w_0, v_0, T_0) \in \mathcal{M}$, then $(w(t), v(t), T(t)) \in \mathcal{M}$ for every t , i.e., invariant manifold.

We consider the decomposition in $\dot{H}_{per}^m, T = T^1 + T^2$, where T^1 is the projection of T on V_m and T^2 is the projection of T on the subspace generated by $\{e^{2\pi k i x}, k \in \mathcal{Z}^* \setminus K\}$ i.e., $T^1 = \sum_{k \in K} a_k e^{2\pi k i x}$ and $T^2 = \sum_{k \in \mathcal{Z}^* \setminus K} a_k e^{2\pi k i x} = T - T^1$.

From (3.3.50) taking into account that $b_k = 0$ for $k \in \mathcal{Z}^* \setminus K$, we have that $|a_k(t)| \leq |a_{k0}| e^{-(4\nu\pi^2 k^2 + l_0)t}$ for every $k \in \mathcal{Z}^*$ implies that there exist positive constants C_i , such that $\|T^2(t)\|_{\dot{H}_{per}^{2m}} \leq C_1 \|T^2(t)\|_{\dot{H}_{per}^m} \leq C_2 \|T_0^2\|_{\dot{H}_{per}^m} e^{-(4\nu\pi^2 + l_0)t}$ i.e., $T^2(t) \rightarrow 0$ in $\dot{H}_{per}^{2m}(0, 1)$ if $t \rightarrow \infty$.

Therefore, we have in particular that $\|T^2(t)\|_{\dot{H}_{per}^m} \rightarrow 0$ as $t \rightarrow \infty$ with exponential decay rate $e^{-(4\nu\pi^2 + l_0)t}$. Thus \mathcal{M} also attracts $(w(t), v(t), T(t))$ with exponential rate $e^{-4\nu\pi^2 t}$, since

$$dist_{\mathcal{Y}}((w(t), v(t), T(t)), \mathcal{M}) = dist_{\dot{H}_{per}^m}(T(t), V) = \|T^2(t)\|_{\dot{H}_{per}^m} \leq C_2 \|T_0^2\|_{\dot{H}_{per}^m} e^{-(4\nu\pi^2 + l_0)t}.$$

To prove the exponential tracking property just note that the flow inside \mathcal{M} is given by setting $T^2 = 0$ this is $\oint T(x) \cdot f = \sum_{k \in K} a_k(t) \cdot c_{-k}$ i.e.,

$$\left\{ \begin{array}{ll} \dot{w} + \frac{1}{\varepsilon}w + \frac{1}{\varepsilon}G(v)v & = \frac{1}{\varepsilon} \sum_{k \in K} a_k(t) \cdot c_{-k} \\ \dot{v} & = w \\ \dot{a}_k(t) + (2\pi kvi + 4\nu\pi^2 k^2 + l(v))a_k(t) & = l(v)b_k, \quad k \in K \\ a_k & = 0, k \notin K. \end{array} \right. \quad (3.3.55)$$

Therefore, if $f \in V$, then $\mathcal{J}Tf = \mathcal{J}T_1f$ and given $(w_0, v_0, T_0) \in \mathcal{Y}$ and $(w(t), v(t), T(t))$ the solution of (3.3.54), we decompose $T_0 = T_0^1 + T_0^2$ and $T(t) = T^1(t) + T^2(t)$. Then we consider $(w(t), v(t), T^1(t)) \in \mathcal{M}$ and it is still a solution of (3.3.55). Hence $(w(t), v(t), T(t)) - (w(t), v(t), T^1(t)) = (0, 0, T^2(t))$ and the right-hand side is of order $e^{-(4\nu\pi^2 + l_0)t}$. In particular, if the set K is finite, then the inertial manifold \mathcal{M} is of finite dimension and the flow inside is equivalent to the finite system of ODEs given by (3.3.55). Thus the theorem is proved. \square

3.3.2 The reduced subsystem

Under the hypotheses and notations of Theorem 3.3.4, we suppose that

$$f(x) = \sum_{k \in J} c_k e^{2\pi kix}, \quad (3.3.56)$$

with $c_k \neq 0$ for every $k \in J \subset \mathcal{Z}$. Then $\mathcal{J}(T \cdot f) = \sum_{k \in K \cap J} a_k(t) c_{-k}$. So, the evolution of velocity v and acceleration w depend only on the coefficients of T which belong to the set $K \cap J$. Note that in (3.3.55) the set of equations for a_k with $k \in K \cap J$ together with the equation for v and w , is a subsystem of coupled equations denoted by the reduced subsystem.

Thus, we will reduce the asymptotic behavior of the initial system (2.2.5) to the dynamics of the reduced explicit system (3.3.57) when we consider the relevant modes of temperature $a_k, k \in K \cap J$.

$$\left\{ \begin{array}{l} \frac{dw}{dt} + \frac{1}{\varepsilon}w + \frac{1}{\varepsilon}G(v)v = \frac{1}{\varepsilon} \sum_{k \in (K \cap J)} a_k(t)c_{-k}, \quad w(0) = w_0 \\ \frac{dv}{dt} = w, \quad v(0) = v_0 \\ \dot{a}_k(t) + (2\pi kvi + 4\nu\pi^2k^2 + l(v))a_k(t) = l(v)b_k, \quad a_k(0) = a_{k0}. \end{array} \right. \quad (3.3.57)$$

where $a_{-k} = \bar{a}_k$, $b_{-k} = \bar{b}_k$ and $c_{-k} = \bar{c}_k$ as we consider only the real functions. After solving this, we must solve the equations for $k \notin K \cap J$ which are linear autonomous equations.

Now, we will show the modes in $k \in K \cap J$ will play an essential role in the dynamics. With the above notations we further decompose T_1 as follows:

$$T_1 = \tau + \theta,$$

where τ is the projection onto the space generated by $\{e^{2\pi kix}, k \in K \cap J\}$ and θ is the projection onto the space generated by $\{e^{2\pi kx}, k \in K \setminus J\}$. We denote by P the projection $P(w, v, T) = (w, v, \tau)$ and $Q = I - P$. With these notations and decomposing T_a as $T_a = \tau_{T_a} + \theta_{T_a}$, (3.2.1) and (3.3.54) can be decomposed as a system of the form

$$\left\{ \begin{array}{l} \frac{dw}{dt} + \frac{1}{\varepsilon}w = -\frac{1}{\varepsilon}G(v)v + \frac{1}{\varepsilon} \oint (\tau + T_2)f, \quad w(0) = w_0 \\ \frac{dv}{dt} = w, \quad v(0) = v_0 \\ \frac{\partial \tau}{\partial t} + v \frac{\partial \tau}{\partial x} = l(v)(\tau_{T_a} - \tau) + \nu \frac{\partial^2 \tau}{\partial x^2}, \quad \tau(0, x) = (T_0)_\tau(x) \\ \frac{\partial \theta}{\partial t} + v \frac{\partial \theta}{\partial x} = l(v)(\theta_{T_a} - \theta) + \nu \frac{\partial^2 \theta}{\partial x^2}, \quad \theta(0, x) = (T_0)_\theta(x) \\ \frac{\partial T^2}{\partial t} + v \frac{\partial T^2}{\partial x} = -l(v)T^2 + \nu \frac{\partial^2 T^2}{\partial x^2}, \quad T^2(0, x) = T_0^2(x). \end{array} \right. \quad (3.3.58)$$

Since $\oint \theta f = 0$ and setting $T_2 = 0$, the first four equations give the flow inside the inertial manifold \mathcal{M} , i.e., they are equivalent to (3.3.54) while the first three are the only nonlinearity coupled equations. Therefore, once this subsystem is solved, the other unknowns are determined through linear nonhomogeneous equations.

To make this idea more precise in terms of semigroup and attractors, we proceed as in [53]. We denote by $S(t)$ the semigroup generated by (3.2.1) on $\mathcal{Y} := \mathbb{R}^2 \times \dot{H}_{per}^1(0, 1)$ and by $S_M(t)$ its restriction to the inertial manifold \mathcal{M} , i.e., the semigroup generated by (3.3.59).

$$\left\{ \begin{array}{l} \frac{dw}{dt} + \frac{1}{\varepsilon}w = -\frac{1}{\varepsilon}G(v)v + \frac{1}{\varepsilon} \oint T^1 f, \quad w(0) = w_0 \\ \frac{dv}{dt} = w, \quad v(0) = v_0 \\ \frac{\partial T^1}{\partial t} + v \frac{\partial T^1}{\partial x} = l(v)(T_a - T^1) + \nu \frac{\partial^2 T^1}{\partial x^2}, \quad T^1(0, x) = T_0^1(x) \\ \frac{\partial T^2}{\partial t} + v \frac{\partial T^2}{\partial x} = -l(v)T^2 + \nu \frac{\partial^2 T^2}{\partial x^2}, \quad T^2(0, x) = T_0^2(x) \\ T^2 = 0. \end{array} \right. \quad (3.3.59)$$

We will find a reduced semigroup on the reduced space $\mathcal{Y}_{\mathcal{R}} := P(\mathcal{Y})$, denoted $S_R(t)$, that, in a sense, determines the asymptotic behavior of $S_M(t)$ and therefore that of $S(t)$.

Note that $S(t)$ and $S_M(t)$ have the same attractor, while the dimension of the space $\mathcal{Y}_{\mathcal{R}}$ might be much smaller than that of \mathcal{M} . The next result states, in particular, that the attractor of the full system can be reconstructed from the attractor of the reduced one.

Proposition 3.3.5 *With the notation above we have the following conditions.*

(i) *The system of equations*

$$\left\{ \begin{array}{l} \frac{dw}{dt} + \frac{1}{\varepsilon}w + \frac{1}{\varepsilon}G(v)v = \frac{1}{\varepsilon} \oint (\tau + T_2)f, \quad w(0) = w_0 \\ \frac{dv}{dt} = w, \quad v(0) = v_0 \\ \frac{\partial \tau}{\partial t} + v \frac{\partial \tau}{\partial x} = l(v)(\tau_{T_a} - \tau) + \nu \frac{\partial^2 \tau}{\partial x^2}, \quad \tau(0, x) = (T_0)_\tau(x). \end{array} \right. \quad (3.3.60)$$

defines a nonlinear semigroup, denoted $S_{\mathcal{R}}(t)$, on $\mathcal{Y}_{\mathcal{R}} := P(\mathcal{Y})$ that can be identified with $PS_M(t)P = PS_M(t)$ restricted to $\mathcal{Y}_{\mathcal{R}}$.

(ii) *If \mathcal{A} denotes the maximal attractor of (3.2.1), then $\mathcal{A}_{\mathcal{R}} = P(\mathcal{A})$ is the maximal attractor of (3.3.60). Moreover*

$$\mathcal{A} = \mathcal{G}(\mathcal{A}_{\mathcal{R}})$$

where $\mathcal{G} : \mathcal{A}_{\mathcal{R}} \mapsto \mathcal{A}$ is continuous.

(iii) *If the set $K \cap J$ is finite, (3.3.60) is equivalent to a system of complex ODEs of the form (3.3.57). Consequently, the asymptotic behavior of (3.2.1) is described by an explicit system of ODEs in \mathbb{R}^N with $N = |K \cap J| + 2$ an even number. In particular, if $K \cap J = \emptyset$, $l(v) = l_0$ and $G(v) = G_0$ for every $(w_0, v_0, T_0) \in \mathbb{R}^2 \times \dot{H}_{per}^1(0, 1)$ we have that the associated solution verifies $v(t) \rightarrow 0$ and $T(t) \rightarrow \theta_\infty$ in $\dot{H}_{per}^1(0, 1)$, where $\theta_\infty(x)$ is the unique solution in $\dot{H}_{per}^2(0, 1)$ of the equation*

$$-\nu \frac{\partial^2 \theta_\infty}{\partial x^2} + l_0 \theta_\infty = l_0 T_a. \quad (3.3.61)$$

Moreover, if $\nu = 0$, we get $v(t) \rightarrow 0$ and $T(t) \rightarrow T_a$.

PROOF. (i) Working as above, we prove the semigroups $S_M(t)$ and $S_R(t)$ are well defined and prove the existence of attractor \mathcal{A}_R . Using the techniques of [50] we can work as in [53] to prove (ii). Then (iii) we note that $0 \notin K \cap J$ and since $K = -K$ and $J = -J$ then the set $K \cap J$ is a symmetric set and has an even number of elements that we denote by $2n_0$. Therefore the number of the positive elements of $K \cap J$, $(K \cap J)_+$, is n_0 .

Note that $\oint T \cdot f = \sum_{k \in \mathbb{Z}^*} a_k(t) \bar{c}_k = \sum_{k \in K \cap J} a_k(t) \cdot c_{-k}$. Thus, the dynamics of the system depends only on the coefficients in $K \cap J$. Moreover the equations for a_{-k} are conjugates of the equations for a_k and therefore we have that

$$\sum_{k \in K \cap J} a_k(t) c_{-k} = 2Re \left(\sum_{k \in (K \cap J)_+} a_k(t) c_{-k} \right).$$

Taking real and imaginary parts of $a_k, k \in (K \cap J)_+$, i.e., employing real variables, $a_k = x_k + iy_k$, we have a system in \mathbb{R}^N with $N = 2n_0 + 2$.

If $K \cap J = \emptyset$, then from the equation for the velocity

$$\varepsilon \frac{d^2 v}{dt^2} + \frac{dv}{dt} + G_0 v = 0$$

we have

$$\lim_{t \rightarrow \infty} v(t) = 0 \tag{3.3.62}$$

Moreover from the equation for the temperature in (2.2.5) we have that the function $\theta = T - \theta_\infty$ satisfies the equation:

$$\frac{\partial \theta}{\partial t} + v \frac{\partial \theta}{\partial x} = -v \frac{\partial \theta_\infty}{\partial x} + \nu \frac{\partial^2 \theta}{\partial x^2} - l_0 \theta. \tag{3.3.63}$$

We can multiply by θ in $\dot{L}_{per}^2(0, 1)$ and taking into account that $\oint \frac{\partial \theta}{\partial x} \theta = \frac{1}{2} \oint \frac{\partial(\theta^2)}{\partial x} = 0$, since θ is periodic, we have

$$\frac{1}{2} \frac{d}{dt} \|\theta\|^2 + \nu \left\| \frac{\partial \theta}{\partial x} \right\|^2 = -v \oint \frac{\partial(\theta_\infty)}{\partial x} \theta - \oint l_0 \theta^2 \quad (3.3.64)$$

and using Cauchy-Schwarz and Young inequality with $\delta, C_\delta = \frac{1}{4\delta}$ and then Poincaré inequality, since $\oint \theta = 0$, together with $-l_0 \oint \theta^2 \leq 0$ we have that

$$\frac{1}{2} \frac{d}{dt} \|\theta\|^2 + (\nu\pi^2 + l_0) \|\theta\|^2 \leq |v| (C_\delta \left\| \frac{\partial \theta_\infty}{\partial x} \right\|^2 + \delta \|\theta\|^2) \quad (3.3.65)$$

Next, using $v(t) \rightarrow 0$ we prove that $\theta(t) \rightarrow 0$ in $\dot{L}_{per}^2(0, 1)$.

Now, we multiply the equation (3.3.63) by $-\frac{\partial^2 \theta}{\partial x^2}$ in \dot{L}_{per}^2 . Integrating by parts, applying Young inequality and taking into account again that $\oint \frac{\partial \theta}{\partial x} \frac{\partial^2 \theta}{\partial x^2} = 0$ since $\frac{\partial \theta}{\partial x}$ is periodic, together with $-l_0 \oint \theta \left(-\frac{\partial^2 \theta}{\partial x^2}\right) = -l_0 \oint \left(\frac{\partial \theta}{\partial x}\right)^2 \leq 0$, we obtain that

$$\frac{1}{2} \frac{d}{dt} \left\| \frac{\partial \theta}{\partial x} \right\|^2 + \nu \left\| \frac{\partial^2 \theta}{\partial x^2} \right\|^2 \leq |v| \left(C_\delta \left\| \frac{\partial \theta_\infty}{\partial x} \right\|^2 + \delta \left\| \frac{\partial^2 \theta}{\partial x^2} \right\|^2 \right) \quad (3.3.66)$$

for every $\delta > 0$ with $C_\delta = \frac{1}{4\delta}$. Thus, working as above and taking into account that $|v(t)| \rightarrow 0$ we get $\frac{\partial \theta}{\partial x}(t) \rightarrow 0$ in $\dot{L}_{per}^2(0, 1)$, i.e., $\theta \rightarrow 0 \in \dot{H}_{per}^1(0, 1)$. \square

Next, we pay attention to the other modes for the temperature a_k where $k \notin (K \cap J)$. Also, note that these modes are determined as solution of the linear nonhomogeneous equations

$$\dot{a}_k(t) + (2\pi k \nu i + 4\nu\pi^2 k^2 + l(v)) a_k(t) = l(v) b_k, \quad k \notin (K \cap J) \quad (3.3.67)$$

with initial data $a_k(0) \in C$. Therefore we call these the slave modes.

We will show in the next Proposition 3.3.6 that the dynamics of these modes are completely determined by the solution of (3.3.57), in the sense that the solution will have only one asymptotic behavior as time goes to infinity.

Proposition 3.3.6 *Assume $\{(w(t), v(t), a_k(t)), k \in K \cap J\}$, is a solution of (3.3.57). Then for any $k \notin (K \cap J)$ there exists a solution of (3.3.67), denoted $a_k^*(t)$, such that $|a_k^*(t)| \leq |b_k|$ for every $t \geq 0$ and for any other solution of (3.3.67),*

$$|a_k(t) - a_k^*(t)| \rightarrow 0$$

at an exponential rate independent of k , as $t \rightarrow \infty$. Moreover, if $k \notin K$, i.e., if $b_k = 0$, then $a_k^(t) = 0$, i.e., this subset of the slave mode is damped out exponentially. In particular, if $\{(w(t), v(t), a_k(t)), k \in K \cap J\}$, is a stationary or periodic (respectively, quasiperiodic, almost periodic) solution, then $a_k^*(t)$ can be chosen such that it is stationary or periodic with the same period (respectively, quasiperiodic, almost periodic with a set of frequencies contained in those of $v(t)$).*

PROOF. Define $|a_k^*(t)|$ as a solution of (3.3.67) with an initial condition satisfying $|a_k^*(t)| \leq |b_k|$. In particular, if $k \notin K$, i.e., if $b_k = 0$, then $|a_k^*(t)| = 0$. Then for any other solution of (3.3.67) $z_k = a_k(t) - a_k^*(t)$ satisfies the homogeneous equation

$$\dot{z}_k + [2\pi k i v + 4\nu\pi^2 k^2 + l(v)]z_k = 0$$

and $|z_k(t)| \leq |z_k(0)|e^{-\int_0^t [2\pi k i v + 4\nu\pi^2 k^2 + l(v)]}$ which proves the statement.

If the solution of (3.3.57) is stationary, i.e., independent of time, then we choose $a_k^*(t)$ to be the solution of $(2\pi k v i + 4\nu\pi^2 k^2 + l(v))a_k(t) = l(v)b_k$ and the result follows.

If $\{(w(t), v(t), a_k(t)), k \in K \cap J\}$ is a periodic solution of (3.3.57), then since the $a_k^*(t)$ are the solutions of linear scalar differential equations of the form $\dot{x}(t) + A(t)x(t) = f(t)$, with $A(t)$ and $f(t)$ period of the same period and the homogeneous equation is stable, the result follows from Fredholm's alternative. For the quasiperiodic or almost periodic case, the result follows from Theorem 6.6 in [19]. \square

Remark 3.3.1 Taking real and imaginary parts of a_k, b_k and c_k as

$$a_k(t) = a_1^k(t) + ia_2^k(t), b_k = b_1^k + ib_2^k, c_k = c_1^k + ic_2^k,$$

the asymptotic behavior of the system (2.2.5) is given by a reduced explicit system in \mathbb{R}^N , where $N = 2n_0 + 2$, given by

$$\left\{ \begin{array}{l} \frac{dw}{dt} + \frac{1}{\varepsilon}w + \frac{1}{\varepsilon}G(v)v(t) = \frac{1}{\varepsilon}2 \sum_{k \in (K \cap J)_+} [a_2^k(t)c_2^k - a_1^k(t)c_1^k] \\ \frac{dv}{dt} = w \\ \dot{a}_1^k(t) + [l(v) + 4\pi^2 k^2 \nu a_1^k(t) - 2\pi k v(t) a_2^k(t)] = l(v) b_1^k, \quad k \in (K \cap J)_+ \\ \dot{a}_2^k(t) + [l(v) + 2\pi k v(t) a_1^k(t) + 4\pi^2 k^2 \nu a_2^k(t)] = l(v) b_2^k, \quad k \in (K \cap J)_+ \end{array} \right. \quad (3.3.68)$$

where $a_{-k} = \bar{a}_k$, $b_{-k} = \bar{b}_k$ and $c_{-k} = \bar{c}_k$.

Observe that from the analysis above, it is possible to design the geometry of circuit and/or the external heating by properly choosing the functions f and/or the heat flux l and the ambient temperature T_a so that the resulting system has an arbitrary number of equations of the form $N = 2n + 2$.

Note that the set $K \cap J$ can be much smaller than the set K and therefore the reduced subsystem may possess far fewer degrees of freedom than the system on the inertial manifold. Also note that it may be the case that K and J are infinite sets, but their

intersection is finite. Also, for a circular circuit we have $f(x) \sim a\sin(x) + b\cos(x)$, i.e., $J = \{\pm 1\}$ and then $K \cap J$ is either $\{\pm 1\}$ or the empty set. Also, if in the original variables for (2.2.5) T_a is constant, we get $K \cap J = \emptyset$ for any choice of f .

The physical and mathematical implications of the resulting system of ODEs which describe the dynamics at the inertial manifold need to be analyzed numerically. The role of the parameter ε which contains the viscoelastic information of the fluid deserves special attention and will be the aim of the next section.

3.4 Numerical experiments

In this section we describe the results of the numerical experiments obtained using the MATHEMATICA package [61] for the resolution of the differential equations, using a fourth-order explicit Runge-Kutta method for stiff equations following the method used in previous works [23, 27]. We will solve a system of ordinary differential equations which are the projection of the partial differential equations (2.2.5) on the inertial manifold derived in the preceding sections. All the variables and equations that we deal with are adimensional. As the systems is multidimensional, we present the results in temporal graphs (a given variable vs time) and phase-space graphs (two physical variables plot against each other).

Specifically, we are integrating the system of equations (3.3.57) where we consider only the coefficients of temperature $a_k(t)$ with $k \in K \cap J$ (relevant modes). Then,

$$\left\{ \begin{array}{l} \frac{dw}{dt} + \frac{w}{\varepsilon} + \frac{G(v)v(t)}{\varepsilon} = \frac{2}{\varepsilon} \text{Real} \left(\sum_{k \in K \cap J} a_k(t) c_{-k} \right) \\ \frac{dv}{dt} = w \\ \dot{a}_k(t) + a_k(t)(2\pi k i v + \nu 4\pi^2 k^2 + l(v)) = l(v) b_k \end{array} \right.$$

where $a_{-k} = \bar{a}_k$, $b_{-k} = \bar{b}_k$ and $c_{-k} = \bar{c}_k$ since all the physical observable are real functions. In particular, we will consider a thermosyphon with a circular geometry, so $J = \{\pm 1\}$ and $K \cap J = \{\pm 1\}$. Consequently, we take $k = 1$ and omit the equation for $k = -1$. Hence,

$$\left\{ \begin{array}{l} \frac{dw}{dt} = \frac{2a_1 c_{-1}}{\varepsilon} - \frac{w}{\varepsilon} - \frac{G(v)v(t)}{\varepsilon}, \\ \frac{dv}{dt} = w, \\ \dot{a}_1(t) + a_1(t)(2\pi i v + \nu 4\pi^2 + l(v)) = l(v) b_1 \end{array} \right.$$

where the unknowns are $w(t)$ (the acceleration of the fluid), $v(t)$ (velocity of the fluid) and $a_1(t)$ (the Fourier mode of the temperature). More complex geometries will result in higher dimensional dynamics on the inertial manifold.

In order to reduce the number of parameters we make the change of variables $a_1 c_{-1} \rightarrow a_1$ and then we define the real and imaginary parts of the equations in the following way:

$$a_1(t) = a^1(t) + i a^2(t), \quad (3.4.69)$$

$$b_1 = A + i B \quad (3.4.70)$$

with $A \in \mathbb{R}, B \in \mathbb{R}$. Therefore, our central results correspond to the system of equations

$$\left\{ \begin{array}{l} \frac{dw}{dt} = \frac{2a^1}{\varepsilon} - \frac{w}{\varepsilon} - \frac{G(v)v(t)}{\varepsilon}, \\ \dot{v} = w, \\ \dot{a}^1 = l(v)A - l(v)a^1(t) - \nu 4\pi^2 a^1 + v 2\pi a^2, \\ \dot{a}^2 = l(v)B - l(v)a^2(t) - \nu 4\pi^2 a^2 - v 2\pi a^1 \end{array} \right. \quad (3.4.71)$$

Note that it is a system of four equations with four unknowns where we need to make explicit choices for the constitutive laws for both the fluid-mechanical and thermal properties. Thus, for the friction law $G(v)$ and $l(v)$ the function associated to heat flux, we will take the ones used in the references [23, 27]. For the numerical experiments, which are of a similar model of thermosyphon for a fluid with one component, they use the functions $G(v) = (|v| + 10^{-4})$ and $l(v) = (10^{-2}|v| + 1)$. The function $G(v)$ has a clear physical meaning; it interpolates between a low Reynolds number friction law (in which the overall friction $G(v)v$ is linear (Stokes friction law) and high Reynolds number (in which the friction is a quadratic law).

Besides, A and B refer in this model to the position-dependant (x) ambient temperature inside the loop and will be used as tuning parameters. Without loss of generality, we will assume $A = 0$ in order to simplify in analogy with the Lorenz's model as it is shown in references [23, 27] (changing A and B simultaneously only results in a change in the *phase* of initial temperature profile).

We have carried out two different sets of numerical experiments with regard to heat diffusion. The first numerical experiments are carried out keeping the heat diffusion to

zero as it was done in [52]. And the second numerical experiments are performed with heat diffusion. The initial conditions are fixed as $w(0) = 0, v(0) = 0, a_1(0) = 1, a_2(0) = 1$. This split would appear naive as diffusion tends to smooth the solution, however, as the order of the equations changes in the presence of diffusion (from first to second order due to the Laplacian) it is worth studying both cases separately.

Numerical analysis has been carried out keeping ε the viscoelastic coefficient as the tuning parameter ranging from 10^{-4} to 10^2 and B associated to the ambient temperature also as a tuning parameter ranging from 1 to 10^4 . The impact of ε on the system has been keenly observed for various intervals of time t , as short as 50 time units and as long as 5000 time units. We will show that in analogy with the classical Lorenz system, as ε varies, the dynamics of the model undergoes various transformations including steady asymptotic behavior, meta-stable chaos, i.e., transient irregular behavior followed by convergence to equilibria, periodic behaviors and chaotic progressions.

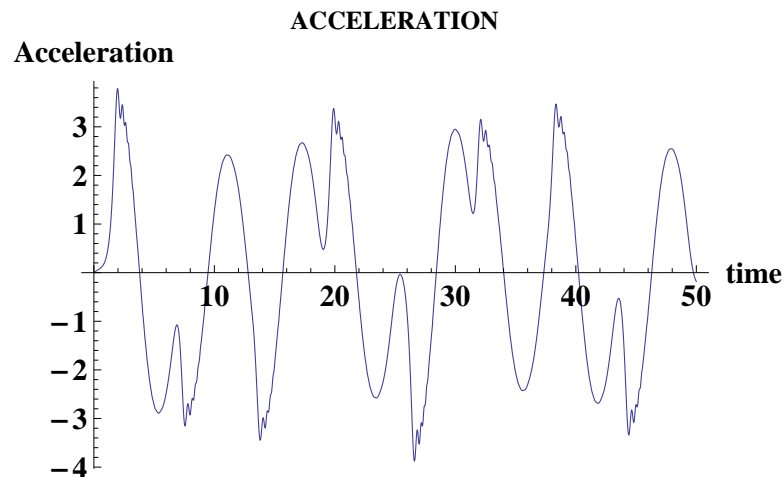


Figure 3.1: The chaotic progress of the acceleration for $\varepsilon = 10, B = 50, \nu = 0$

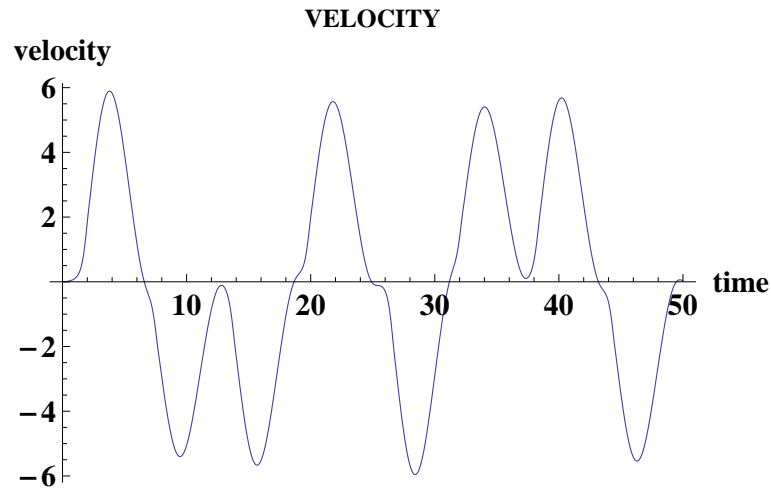


Figure 3.2: The inconsistent behavior of velocity for $\varepsilon = 10, B = 50, \nu = 0$

3.4.1 Dynamics of the thermosyphon without diffusion ($\nu = 0$)

In this section we summarize some of the outcomes of the model equations. As we have mentioned above, this behavior is highly sensitive to the choice of parameters. Thus, we present those results in different subsections accounting for the most relevant signature for each set of numerical experiments.

Chaotic behavior of the model ($\nu = 0$) for large values of ε

The simulations of the numerical experiments done for large values of ε , for instance ε ranging from 2 to 1000, show that the system exhibits chaotic behavior. For all the values of heat flux B , starting from 1 to 10^4 , this chaotic behavior is observed (see Table 3.2).

In Fig. 3.1 we show a time graph of the acceleration for a large value of the viscoelastic parameter, $\varepsilon = 10$. The acceleration ranges from -3.5 to 3.5. Since the very

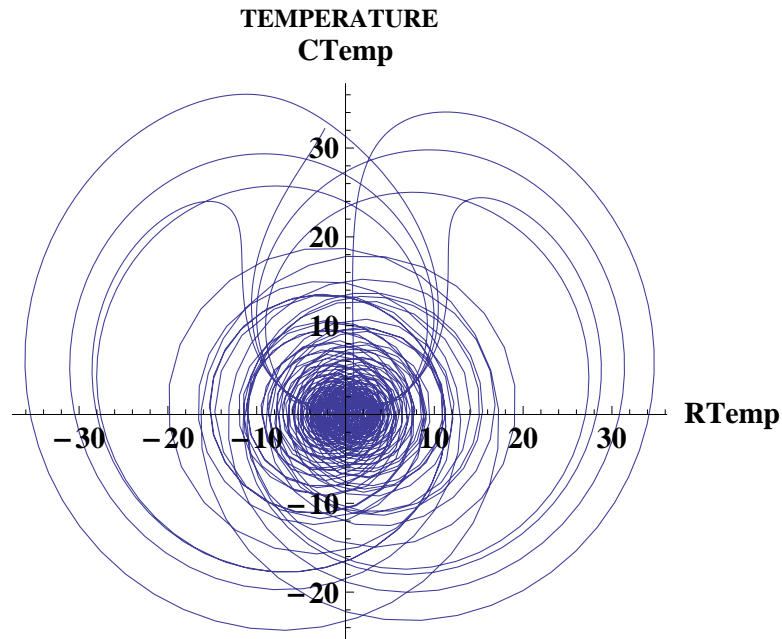


Figure 3.3: A chaotic global attractor of real and complex temperature for $\varepsilon = 10, B = 50, \nu = 0$

beginning, it displays a chaotic behavior. The curve is not very erratic although it does not show any sort of periodicity. As velocity is the time integral of acceleration, in Fig. 3.2, the curve does not present abrupt changes close to some maxima and minima, but the non-periodic features are also captured by this observable.

In Fig. 3.3 we show a phase-diagram plot for the real and imaginary parts of the temperature. As expected, it also exhibits a non-periodic pattern in which the trajectory in this phase-plane moves inwards and outwards the graph. This graph illustrates the complex underlying dynamics of the attractor (of which Fig. 3.3 is a two-dimensional projection).

This sort of behavior remains similar for other values of B as long as the viscoelastic

parameter takes values larger than unity values as summarized in Table 3.2. In other words, the elastic effects introduce a memory effect in the dynamics which avoids the system to fully stabilize but, rather, viscoelasticity sustains the chaotic pattern. This memory effect can be understood from equation (2.2.3).

To sum up this section, large values of the viscoelastic parameter, $\varepsilon = 10$, result on sustained chaotic behaviors. The dynamics becomes more complex, characterized in all the cases by periods of chaos and of violent oscillations, giving an idea of the complexity of the solutions of the system under these variables. In the detailed analysis of the evolution of the acceleration, velocity and temperature, we say that the chaotic behavior of the system reveals the chaotic nature of the viscoelastic fluids.

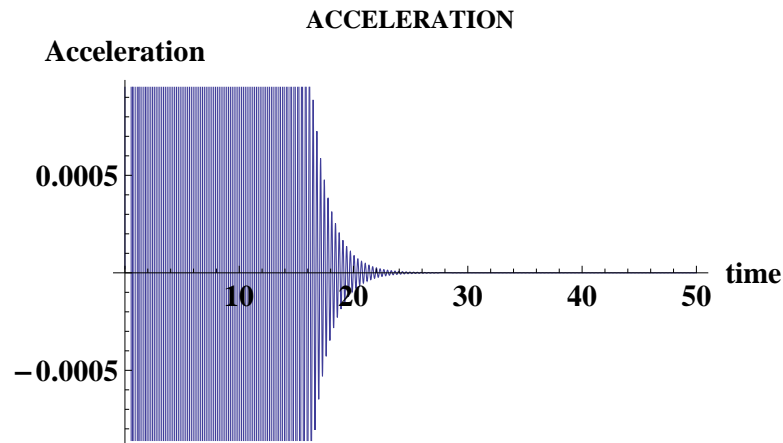


Figure 3.4: The stabilizing progress of the acceleration for $\varepsilon = 0.1$, $B = 100$, $\nu = 0$

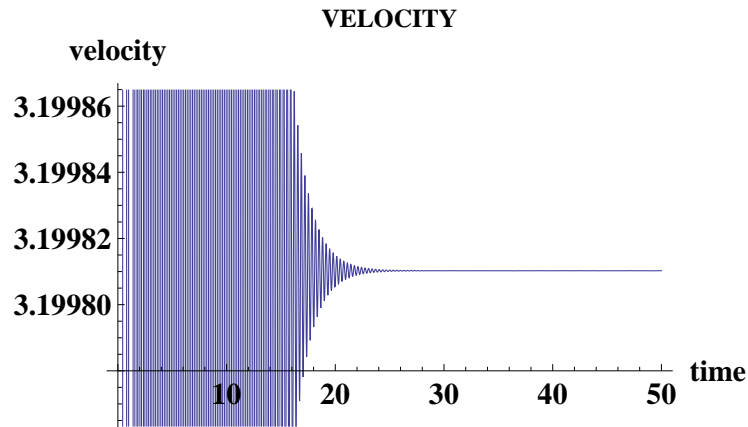


Figure 3.5: Velocity stabilizes at 3.19981 for $\varepsilon = 0.1$, $B = 100$, $\nu = 0$

Transient irregular behavior followed by stable behavior for $\varepsilon = 0.1$ to 1

For values of ε ranging from 0.1 to 1 the system tends towards a stable fixed point, although it is still chaotic in the initial stages. This transient irregular behavior followed by equilibrium is shown in Figs. 3.4-3.6.

The general behavior of the acceleration is that it has a chaotic outburst in the initial stages but, as time progresses, it tends to stabilize, attaining equilibria. The velocity too, in the initial stages, when the time period is less than 20 units, is very inconsistent and at times unpredictable. But as the time progresses, velocity converges to a stable fixed point. Interestingly, this fixed point for the velocity is not trivial ($v \neq 0$) but, on the contrary, it depends strongly on the choice of the parameters. Specifically, in Table 3.1 we summarize this asymptotic value. Physically, this means that the fluid inside the thermosyphon moves at a sustained velocity and in the same direction over time. This stage could be identified by the existence of convective rolls in a fully spatially extended system.

B	$\varepsilon = 1$	$\varepsilon = 0.1$
1	0.6718	0.6718
10	1.4723	1.4723
20	1.8601	1.8601
30	2.1325	2.1325
40	2.3495	2.3495
50	2.5329	2.5329
100	3.1998	3.1998
1000	6.9800	6.9800
10000	15.430	15.430

Table 3.1: Equilibrium values of velocity for different values of ambient temperature B , $\nu = 0$

It is worth noting in Table 3.1 that both columns have the same value for the asymptotic velocity. This is a signature that viscoelastic effects do not play any role in this case (so memory effects are damped out after the early chaotic transient).

A comment regarding Table 3.1 concerns the role of the parameter B . Roughly, B accounts for the scale of temperature gradients inside the thermosyphon. These results suggest that higher temperature gradients produce higher values of the sustained stationary velocity. Actually, as shown in Fig. 3.6, the equilibrium velocity scales with B non-trivially (as a power law with exponent $1/3$ approximately).

To sum up this section, we conclude that although the system has a chaotic initial transient, it tends to stabilize at longer times reaching a temperature gradient dependent

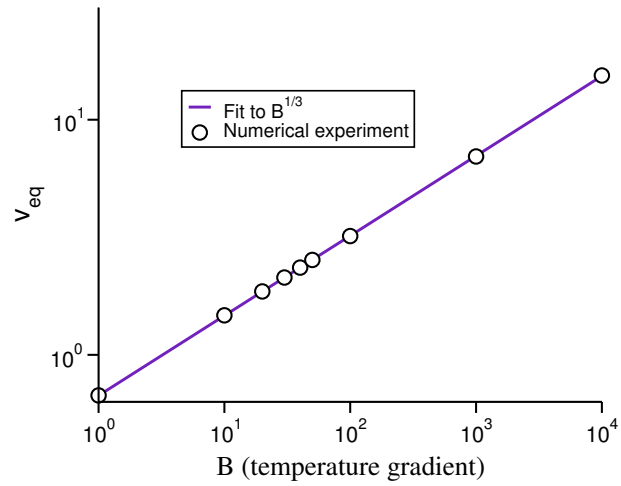


Figure 3.6: Equilibrium velocity scale for the ambient temperature $B, \nu = 0$

equilibrium velocity. Notwithstanding, this asymptotic velocity depends non-trivially on temperature as a power law, being this a signature of the underlying non-linearity of the equations.

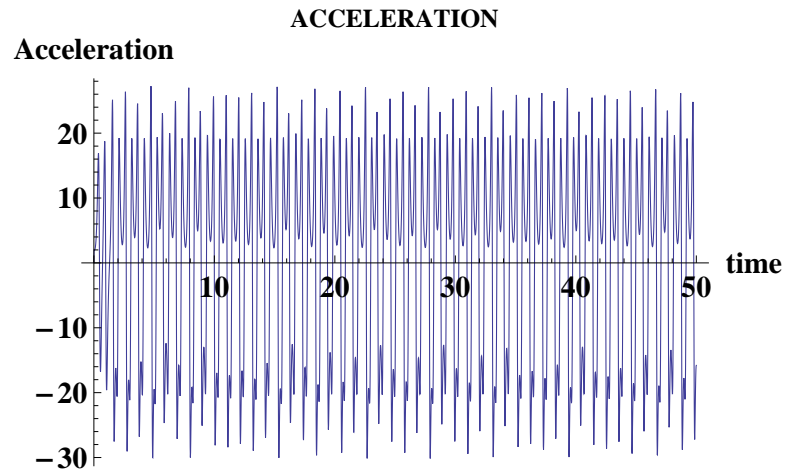


Figure 3.7: The periodic progress of the acceleration for $\varepsilon = 0.001, B = 40, \nu = 0$

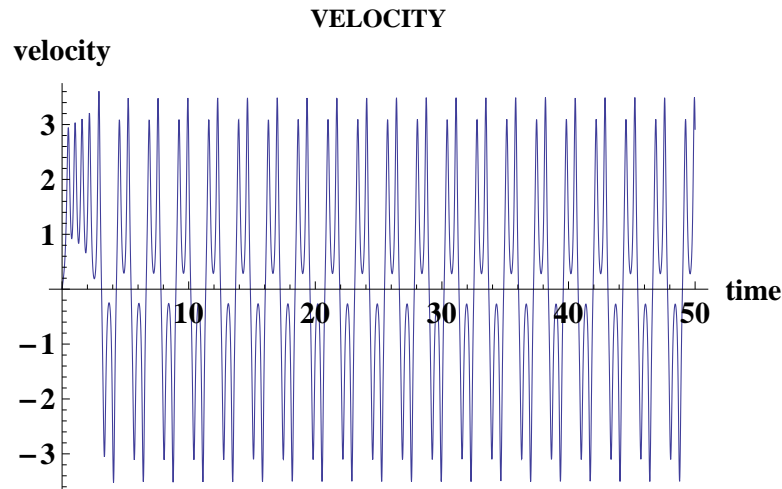


Figure 3.8: The periodic progress of velocity for $\varepsilon = 0.001$, $B = 30$, $\nu = 0$

Transition to periodic pattern of behaviors for small values of ε

When the viscoelastic effects are gradually less important (values of ε between 0.01 – 0.0001), the system exhibits different behaviors as a function of the temperature gradient (see Table 3.2 at the end of this section). For lower values of B , the system behaves in a similar fashion as for higher values of ε . On the contrary, for larger values of B , the system displays a periodic pattern (see Fig. 3.7). As in the previous case, both long-term behaviors may be preceded by an initial chaotic transient (probably caused by viscoelasticity).

To illustrate this, in Fig. 3.8 we show a periodic (non trivial) behavior for $\varepsilon = 0.001$. In some cases, the initial transient cannot be distinguished from the periodic one and we refer it simply to *periodic* type in Table 3.2.

In Fig. 3.9 we show the phase-space of the complex components of the temperature. Although at first sight it resembles a typical chaotic attractor motif, after the mentioned

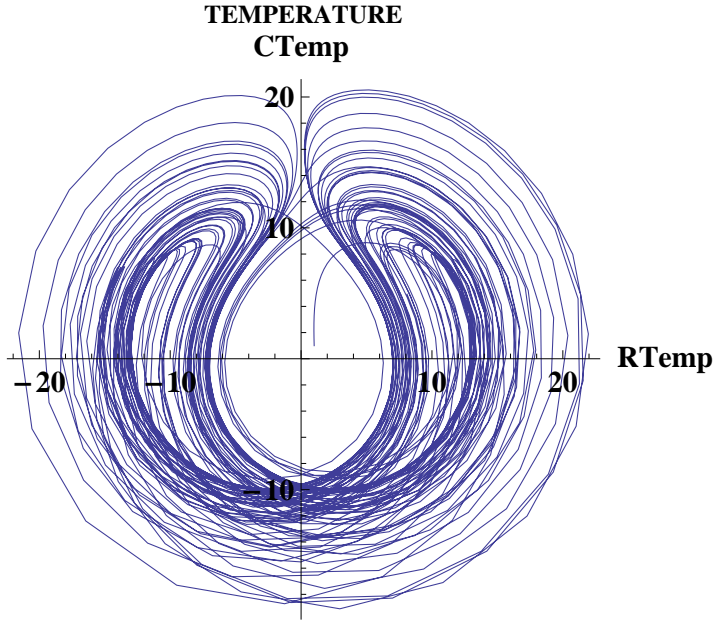


Figure 3.9: The chaotic but periodic plot of real and complex temperature for $\varepsilon = 0.0001$, $B = 40$, $\nu = 0$

initial transient, the trajectories are overlapped for longer times.

Thus, in order to summarize the information covered in the last three subsections, we collect all the outcomes of the model in Table 3.2.

3.4.2 Dynamics of the thermosyphon with diffusion ($\nu \neq 0$)

In this case, to avoid unnecessary repetitions in the text, we focus on the main differences between this case and that of the previous case.

Thus, in this second set of numerical experiments we introduce a non-zero value for the thermal diffusivity, ν . The role of diffusion is to reduce temperature gradients.

B/ε	10^{-4}	10^{-3}	10^{-2}	10^{-1}	10^0	10^1	10^2
1	CS	CS	CS	CS	CS	C	C
10	CS	CS	CS	CS	CS	C	C
20	CS	CS	CS	CS	CS	C	C
30	CP	CP	CP	CS	CS	C	C
40	CP	CP	CP	CS	CS	C	C
50	CP	CP	CP	CS	CS	C	C
100	P	P	CP	CS	CS	C	C
1000	CP	CP	CP	CS	CS	C	C
10000	CP	CP	CP	CS	CS	C	C

Table 3.2: Behavior of the solutions without diffusion ($\nu = 0$) for different values of the viscoelastic characteristic time, ε (rows) and the ambient temperature, B (columns). We introduce the following notation to account for the obtained numerical results: ‘C’ denotes a fully chaotic behavior, ‘CS’ a transition from chaotic outburst to stable equilibria, ‘P’ a stable periodic orbit and ‘CP’ a transitional behavior from chaotic to periodic.

This can be seen in a hand-waving way by realizing that

$$\partial_x^2 T \equiv -\partial_x J,$$

namely, the Laplacian can be understood as the *flux* of temperature created by a temperature *current*, $J = -\nabla T$. This current is larger in those regions where the temperature variations are also larger. Thus, the system tends to reduce those differences. As shown in Table 3.3, the variety of the behaviors is clearly less rich than in the case when $\nu = 0$.

So, here we will only illustrate the most interesting behaviors with two examples:

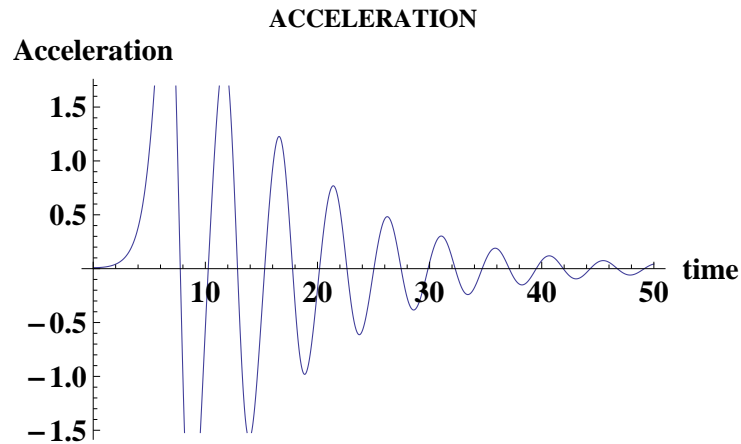


Figure 3.10: The stabilizing process of the acceleration for $\nu = 1$, $\varepsilon = 5$, $B = 1000$

The first one takes the values of heat diffusion $\nu = 1$ with $\varepsilon = 5$ and $B = 1000$. As shown in Fig. 3.10 the acceleration performs a series of *damped* oscillations that eventually stabilize.

Similarly, the second example (Fig. 3.11) takes the values $\nu = 2$, $\varepsilon = 5$ and $B = 1000$. The behavior is qualitatively equal but the period of the oscillations is enlarged. In table 3.3, we summarize the interaction between the tuning parameters.

To sum up this section, we have found that greater values of the heat diffusion, ν , smoothen the dynamics of the system which, invariably, tends to stabilize, either reaching an equilibrium steady state or stable periodic orbits. These two behaviors are governed by the value of the temperature gradient which in a similar fashion as in the previous case, tends to produce richer behaviors for large values.

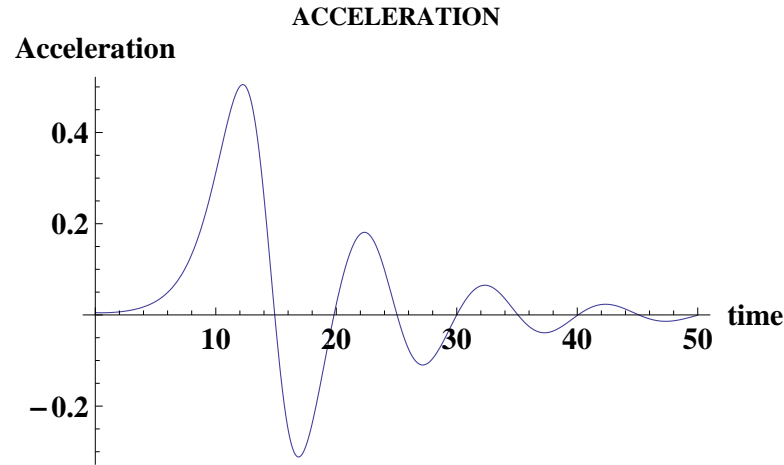


Figure 3.11: The fast stabilization of the acceleration for $\nu = 2$, $\varepsilon = 5$, $B = 1000$

3.5 Conclusions

In this model a novel system of equations to study the behavior of a viscoelastic material inside a thermosiphon is derived. This model serves as a preliminary simplification of a more complex fully spatially extend system. This model has served to find the presence/absence of complex chaotic behaviors and also to relate them with the underlying viscoelastic (memory effects).

The main result is that we are able to prove that the original system (which involves both ordinary and partial different equations) possesses an inertial manifold in which the dynamics can be accurately described by a system of ODEs. By numerical integration of the reduced equations we have been able to better understand the role of viscoelasticity (as opposed to a simpler Newtonian fluid) through the parameter ε . This parameter is an adimension version of the so-called Maxwellian viscoelastic time [46] which accounts for

B/ε	10^{-4}	10^{-3}	10^{-2}	10^{-1}	10^0	10^1	10^2
1	CS	CS	CS	CS	CS	CS	CS
10	CS	CS	CS	CS	CS	CS	CS
20	CS	CS	CS	CS	CS	CS	CS
30	CS	CS	CS	CS	CS	CS	CS
40	P	P	P	CS	CS	CS	CS
50	P	P	P	CS	CS	CS	CS
100	P	P	P	CS	CS	CS	CS
1000	P	P	P	CS	CS	CS	CS
10000	P	P	P	CS	CS	CS	CS

Table 3.3: Behavior of the solutions with diffusion ($\nu \neq 0$) for different values of the viscoelastic characteristic time, ε (rows) and the ambient temperature, B (columns). We introduce the following notation to account for the obtained numerical results: ‘C’ denotes a fully chaotic behavior, ‘CS’ a transition from chaotic outburst to stable equilibria and ‘P’ a periodic orbit.

memory effects.

The results suggest that when the value of $\varepsilon = 10$ (is large) it drives the dynamics to chaotic behaviors for all the physical observable (acceleration, velocity and temperature). As the value of ε gradually decreases, the system is no longer chaotic but stable or periodic. Notably, these results cannot be understood in terms of a boundary layer theory (see the appendix) as the attractor of the dynamics changes dramatically when the second order derivative term $\varepsilon d^2v/dt^2$ is introduced in equations 2.2.5.

Physically, this induction of chaotic behaviors is related to the memory effects inherent to viscoelastic models. Thus, in the same way as delayed equations are known to produce chaos, even in the simplest situations, viscoelasticity produces the same kind of transition (see, for instance [41]).

The other interesting results are related to the effect of heat diffusion. It is found that as the heat diffusion increases, the system tends to stabilize either to a fixed equilibrium point or to a (ν -dependent periodicity) periodic orbit.

Chapter 4

One component viscoelastic fluids with a prescribed heat flux

4.1 Introduction

As a reminder of Chapter 2, the derivation of the equations of motion of this model is similar to that in [39, 56, 59]. The simplest way to incorporate equation (2.2.2) into equation (2.2.1) is by differentiating equation (2.2.1) with respect to time and replacing the resulting time derivative of σ with equation (2.2.2). This way to incorporate the constitutive equation allows to reduce the number of unknowns (remove σ from the system of equations) at the cost of increasing the order of the time derivatives to second order. The resulting second order equation is then averaged along the loop section as in [39]. Finally, after adimensionalizing the variables (to reduce the number of free parameters) arrive at the ODE/PDE system (see section 2.2)

$$\begin{cases} \varepsilon \frac{d^2 v}{dt^2} + \frac{dv}{dt} + G(v)v &= \oint T f, & v(0) = v_0, \frac{dv}{dt}(0) = w_0 \\ \frac{\partial T}{\partial t} + v \frac{\partial T}{\partial x} &= h(x) + \nu \frac{\partial^2 T}{\partial x^2}, & T(0, x) = T_0(x) \end{cases} \quad (4.1.1)$$

where $v(t)$ is the velocity, $T(t, x)$ is the distribution of the temperature of the viscoelastic fluid in the loop, ν is the temperature diffusion coefficient, $G(v)$ is the friction law at the inner wall of the loop, the function f is the geometry of the loop and the distribution of gravitational forces, $h(x)$ is the prescribed heat flux and ε is the viscoelastic parameter, which is the dimensionless version of the viscoelastic time, $t_V = \mu/E$. Roughly speaking, it gives the time scale in which the transition from elastic to fluid-like occurs in the fluid. Consider G and h are given continuous functions, such that $G(v) \geq G_0 > 0$ and $h(x) \geq h_0 > 0$. Finally, for physical consistency, it is important to note that all the functions considered must be 1-periodic with respect to the spatial variable.

The structure of this chapter is as follows: the first section provides an introduction to the system explaining briefly the dynamics of the functions. In Section 2, the proofs for the well posedness, boundedness of the solution and the existence of a global attractor are given. The Section 3 provides the details of the derivation of an explicit reduction to finite dimensional subsystems of the behavior of viscoelastic fluids, extending the results in [53] for this kind of viscoelastic fluid, in order to get the similar results like [63] when a given heat flux is considered instead of Newton's linear cooling law. The Section 4 presents the results of the numerical experiments.

4.2 Well-posedness and boundedness: global attractor

4.2.1 Existence and uniqueness of solutions

First, we integrate the equation for the temperature along the loop, i.e., $\oint T(t) = \oint T_0 + t \oint h$. Therefore, $\oint T(t)$ is unbounded, as $t \mapsto \infty$, unless $\oint h = 0$. However, taking $\theta = T - \oint T$ and $h^* = h - \oint h$ reduces to the case $\oint T(t) = \oint T_0 = \oint h = 0$, since θ would satisfy

$$\frac{\partial \theta}{\partial t} + v \frac{\partial \theta}{\partial x} = h(x) + \nu \frac{\partial^2 \theta}{\partial x^2}$$

and $\oint T f = \oint \theta f$, since $\oint f = 0$. Therefore, hereafter we consider the system (4.1.1) where all functions have zero average. Also, the operator $\nu A = -\nu \frac{\partial^2}{\partial x^2}$, together with periodic boundary conditions, is an unbounded, self-adjoint operator with compact resolvent in $L^2_{per}(0, 1)$, that is positive when restricted to the space of zero average functions $\dot{L}^2_{per}(0, 1)$. Hence, the equation for the temperature T in (4.1.1) is of parabolic type for $\nu > 0$.

Hereafter we denote by $w = \frac{dv}{dt}$ and we write the system (4.1.1) as the following evolution system for the acceleration, velocity and temperature:

$$\left\{ \begin{array}{ll} \frac{dw}{dt} + \frac{1}{\varepsilon} w & = -\frac{1}{\varepsilon} G(v)v + \frac{1}{\varepsilon} \oint T f, & w(0) = w_0 \\ \frac{dv}{dt} & = w, & v(0) = v_0 \\ \frac{\partial T}{\partial t} + v \frac{\partial T}{\partial x} - \nu \frac{\partial^2 T}{\partial x^2} & = h(x), & T(0, x) = T_0(x) \end{array} \right. \quad (4.2.2)$$

this is:

$$\frac{d}{dt} \begin{pmatrix} w \\ v \\ T \end{pmatrix} + \begin{pmatrix} \frac{1}{\varepsilon} & 0 & 0 \\ 0 & 0 & 0 \\ 0 & 0 & -\nu \frac{\partial^2}{\partial x^2} \end{pmatrix} \begin{pmatrix} w \\ v \\ T \end{pmatrix} = \begin{pmatrix} F_1(w, v, T) \\ F_2(w, v, T) \\ F_3(w, v, T) \end{pmatrix} \quad (4.2.3)$$

with

$$F_1(w, v, T) = -\frac{1}{\varepsilon}G(v)v + \frac{1}{\varepsilon} \oint Tf, F_2(w, v, T) = w \text{ and } F_3(w, v, T) = -v \frac{\partial T}{\partial x} + h(x). \quad (4.2.4)$$

The operator $B = \begin{pmatrix} \frac{1}{\varepsilon} & 0 & 0 \\ 0 & 0 & 0 \\ 0 & 0 & -\nu \frac{\partial^2}{\partial x^2} \end{pmatrix}$ is a sectorial operator in $Y = \mathbb{R}^2 \times \dot{L}_{per}^2(0, 1)$

with domain $D(B) = \mathbb{R}^2 \times \dot{H}_{per}^2(0, 1)$ and has compact resolvent, where

$$\dot{L}_{per}^2(0, 1) = \{u \in L_{loc}^2(\mathbb{R}), u(x+1) = u(x) \text{ a.e.}, \oint u = 0\} \text{ and}$$

$$\dot{H}_{per}^m(0, 1) = H_{loc}^m(\mathbb{R}) \cap \dot{L}_{per}^2(0, 1).$$

Thus, using the result and techniques about sectorial operator of [27] we obtain the following Theorem 4.2.1

Theorem 4.2.1 *We suppose that $H(r) = rG(r)$ is locally Lipschitz, $f, h \in \dot{L}_{per}^2(0, 1)$. Then, given $(w_0, v_0, T_0) \in \mathcal{Y} = \mathbb{R}^2 \times \dot{L}_{per}^2(0, 1)$, there exists a unique solution of (4.1.1) satisfying $(w, v, T) \in C([0, \infty), \mathbb{R}^2 \times \dot{L}_{per}^2(0, 1)) \cap C(0, \infty, \mathbb{R}^2 \times \dot{H}_{per}^2(0, 1))$, $(\dot{w}, w, \frac{\partial T}{\partial t}) \in C(0, \infty, \mathbb{R}^2 \times \dot{H}_{per}^{2-\delta}(0, 1))$, where $w = \dot{v} = \frac{dv}{dt}$ and $\dot{w} = \frac{d^2v}{dt^2}$ for every $\delta > 0$. In particular, (4.1.1) defines a nonlinear semigroup, $S(t)$ in $\mathcal{Y} = \mathbb{R}^2 \times \dot{L}_{per}^2(0, 1)$, with $S(t)(w_0, v_0, T_0) = (w(t), v(t), T(t))$.*

PROOF. **Step (i)** First, we prove the local existence and regularity. This follows easily from the variation of constants formula of [27]. In order to prove this we write the system as (4.2.3) and we have:

$$U_t + BU = F(U), \text{ with } U = \begin{pmatrix} w \\ v \\ T \end{pmatrix}, B = \begin{pmatrix} \frac{1}{\varepsilon} & 0 & 0 \\ 0 & 0 & 0 \\ 0 & 0 & -\nu \frac{\partial^2}{\partial x^2} \end{pmatrix} \text{ and } F = \begin{pmatrix} F_1 \\ F_2 \\ F_3 \end{pmatrix}$$

where the operator B is a sectorial operator in $\mathcal{Y} = \mathbb{R}^2 \times \dot{H}_{per}^{-1}(0, 1)$ with domain $D(B) = \mathbb{R}^2 \times \dot{H}_{per}^1(0, 1)$ and has compact resolvent. Note that in this context the operator $A = -\frac{\partial^2}{\partial x^2}$ must be understood in the variational sense, i.e., for every $T, \varphi \in \dot{H}_{per}^1(0, 1)$, $\langle A(T), \varphi \rangle = \oint \frac{\partial T}{\partial x} \frac{\partial \varphi}{\partial x}$ and $\dot{L}_{per}^2(0, 1)$ coincides with the fractional space of exponent $\frac{1}{2}$ [27]. Hereafter we denote by $\|\cdot\|$ the norm on the space $\dot{L}_{per}^2(0, 1)$.

Under the above notations, using that $H(v) = G(v)v$ is locally Lipschitz together with $f, h \in \dot{L}_{per}^2(0, 1)$, we obtain that the nonlinearity (4.2.4) $F : \mathcal{Y} = \mathbb{R}^2 \times \dot{L}_{per}^2(0, 1) \mapsto \mathcal{Y}^{-\frac{1}{2}} = \mathbb{R}^2 \times \dot{H}_{per}^{-1}(0, 1)$ is well defined and is Lipschitz and bounded on bounded sets.

Therefore, using the techniques of variations of constants formula [27], we get the unique local solution $(w, v, T) \in C([0, \tau], \mathcal{Y} = \mathbb{R}^2 \times \dot{L}_{per}^2(0, 1))$ of (4.2.2) which are given by

$$w(t) = w_0 e^{-\frac{1}{\varepsilon}t} - \frac{1}{\varepsilon} \int_0^t e^{-\frac{1}{\varepsilon}(t-r)} H(r) dr + \frac{1}{\varepsilon} \int_0^t e^{-\frac{1}{\varepsilon}(t-r)} \left(\oint T(r) f \right) dr \quad (4.2.5)$$

with $H(r) = G(v(r))v(r)$.

$$v(t) = v_0 + \int_0^t w(r) dr \quad (4.2.6)$$

$$T(t, x) = e^{-\nu A t} T_0(x) + \int_0^t e^{-\nu A(t-r)} h(x) dr - \int_0^t e^{-\nu A(t-r)} v(r) \frac{\partial T(r, x)}{\partial x} dr \quad (4.2.7)$$

where $(w, v, T) \in C([0, \tau], Y)$ and using again the results of [27] (smoothing effect of the equations together with bootstrapping method), we get the above regularity of solutions.

Step (ii) Now, we prove that the solutions of (4.2.2) are defined for every time $t \geq 0$.

To prove the global existence, we must show that the solutions are bounded in $\mathcal{Y} = \mathbb{R}^2 \times \dot{L}_{per}^2(0, 1)$ norm on finite time intervals.

First, to obtain the norm of T is bounded in finite time, we note that multiplying the equations for the temperature by T in $\dot{L}_{per}^2(0, 1)$ and integrating by parts, we have that:

$$\frac{1}{2} \frac{d}{dt} \|T\|^2 + \nu \left\| \frac{\partial T}{\partial x} \right\|^2 = \oint h T$$

since $\oint T \frac{\partial T}{\partial x} = 0$. Using Cauchy-Schwarz and Young inequality and then Poincaré inequality for functions with zero average, since $\oint T = 0$, we obtain $\frac{1}{2} \frac{d}{dt} \|T\|^2 + \nu \pi^2 \|T\|^2 \leq C_\delta \|h\|^2 + \delta \|T\|^2$ for every $\delta > 0$ with $C_\delta = \frac{1}{4\delta}$, since π^2 is the first nonzero eigenvalue of A in $\dot{L}_{per}^2(0, 1)$. Thus, taking $\delta = \frac{\nu \pi^2}{2}$, $C_\delta = \frac{1}{2\nu \pi^2}$ we obtain

$$\frac{d}{dt} \|T\|^2 + \nu \pi^2 \|T\|^2 \leq \frac{\|h\|^2}{\nu \pi^2}. \quad (4.2.8)$$

Now, by integrating we get $\|T\|$ is bounded for finite time, and so are $|v(t)|$ and $|w(t)|$, hence we have a global solution and nonlinear semigroup in $\mathcal{Y} = \mathbb{R}^2 \times \dot{L}_{per}^2(0, 1)$. \square

4.2.2 Asymptotic bounds on the solutions: global attractor

In this section we use the results and techniques from [63] to prove the existence of the global attractor for the semigroup defined by (4.1.1) in the space $\mathcal{Y} = \mathbb{R}^2 \times \dot{L}_{per}^2(0, 1)$.

In order to obtain the asymptotic bounds on the solutions as $t \rightarrow \infty$, we consider the friction function G as in [63] i.e., satisfying the hypotheses from the previous section and we also assume that there exists a constant $g_0 \geq 0$ such that:

$$\limsup_{t \rightarrow \infty} \frac{|G'(t)|}{G(t)} = 0 \text{ and } \limsup_{t \rightarrow \infty} \frac{|tG'(t)|}{G(t)} \leq g_0. \quad (4.2.9)$$

Now, using the l'Hopital's lemma proved in [53] we have the following Lemma proved in [63].

Lemma 4.2.2 *If we assume $G(r)$ and $H(r) = rG(r)$ satisfy the hypothesis from Theorem 4.2.1 together with (4.2.9), then:*

$$\limsup_{t \rightarrow \infty} \frac{\left| H(t) - \frac{1}{\varepsilon} \int_0^t e^{-\frac{1}{\varepsilon}(t-r)} H(r) dr \right|}{G(t)} \leq H_0 \quad (4.2.10)$$

with $H_0 = (1 + g_0)\varepsilon$ a positive constant such that $H_0 \rightarrow 0$ if $\varepsilon \rightarrow 0$.

Remark 4.2.1 *We note that the conditions (4.2.9) are satisfied for all friction functions G considered in the previous works, i.e., the thermosyphon models where G is constant or linear or quadratic law. Moreover, its conditions (4.2.9) are also true for $G(s) \approx A|s|^n$, as $s \rightarrow \infty$.*

Finally, in order to obtain the asymptotic bounds on the solutions we obtain the asymptotic bounds for the temperature in this diffusion case and we will use the following

result from [63] [Theorem 2.3 Part I] to get the asymptotic bounds for the velocity and the acceleration functions.

Lemma 4.2.3 *Under the above notations and hypothesis from Theorem 4.2.1, if we assume also that G satisfies (4.2.10) for some constant $H_0 \geq 0$ and*

$$\varepsilon \frac{d^2v}{dt^2} + \frac{dv}{dt} + G(v)v = \oint T f, v(0) = v_0, \frac{dv}{dt}(0) = w_0, \text{ then}$$

$$i) \limsup_{t \rightarrow \infty} |v(t)| \leq \frac{1}{G_0} \limsup_{t \rightarrow \infty} \left| \oint T(t, \cdot) f(\cdot) \right| + H_0 \quad (4.2.11)$$

In particular: If $\limsup_{t \rightarrow \infty} \|T\| \in \mathbb{R}$ then

$$\limsup_{t \rightarrow \infty} |v(t)| \leq \frac{1}{G_0} \|f\| \limsup_{t \rightarrow \infty} \|T\| + H_0 \in \mathbb{R}. \quad (4.2.12)$$

ii) If $\limsup_{t \rightarrow \infty} \|T\| \in \mathbb{R}$ and we denote now by $G_0^ = \limsup_{t \rightarrow \infty} G(v(t))$, with $w(t) = \frac{dv}{dt}$, then*

$$\limsup_{t \rightarrow \infty} |w(t)| \leq G_0^* H_0 + \left(1 + \frac{G_0^*}{G_0}\right) I \text{ with } I = \limsup_{t \rightarrow \infty} \left| \oint T(t, \cdot) f(\cdot) \right| \text{ and} \quad (4.2.13)$$

$$\limsup_{t \rightarrow \infty} |w(t)| \leq G_0^* H_0 + \left(1 + \frac{G_0^*}{G_0}\right) \|f\| \limsup_{t \rightarrow \infty} \|T\| \in \mathbb{R}. \quad (4.2.14)$$

PROOF. First we obtain $\frac{dv}{ds} + G(s)v = w(0)e^{-\frac{1}{\varepsilon}s} + \frac{1}{\varepsilon} \int_0^s (\oint T(r) \cdot f) e^{-\frac{1}{\varepsilon}(s-r)} dr + I(s)$, with $I(s) = H(s) - \frac{1}{\varepsilon} \int_0^s e^{-\frac{1}{\varepsilon}(s-r)} H(r)$, and then from Lemma 4.2.2 together with l'Hopital's lemma we conclude (see [63] [Theorem 2.3 Part I]). \square

Proposition 4.2.4 *If $f, h \in \dot{L}_{per}^2(0, 1)$ and $H(r) = rG(r)$ is locally Lipschitz with $G(v) \geq G_0 > 0$ and satisfies (4.2.10) for some constant $H_0 \geq 0$. Then for any solution of (4.1.1) in the space $Y = \mathbb{R}^2 \times \dot{L}_{per}^2(0, 1)$ we have:*

i)

$$\limsup_{t \rightarrow \infty} \|T(t)\| \leq \frac{\|h\|}{\nu\pi^2} \text{ and } \limsup_{t \rightarrow \infty} |v(t)| \leq \frac{\|f\|\|h\|}{\nu\pi^2 G_0} + H_0 \quad (4.2.15)$$

ii) If we denote now by $G_0^* = \limsup_{t \rightarrow \infty} G(v(t))$ we get

$$\limsup_{t \rightarrow \infty} |w(t)| \leq G_0^* H_0 + G_2 \frac{\|h\|\|f\|}{\nu\pi^2} \text{ with } G_2 = \left(1 + \frac{G_0^*}{G_0}\right). \quad (4.2.16)$$

Therefore, (4.1.1) has a global compact and connected attractor, A , in $Y = \mathbb{R}^2 \times \dot{L}_{per}^2(0, 1)$.

PROOF. i) From (4.2.8) we get

$$\|T\|^2 \leq \frac{\|h\|^2}{\nu^2\pi^4} + \left(\|T_0\|^2 - \frac{\|h\|^2}{\nu^2\pi^4}\right)_+ e^{-\pi^2\nu t} \quad (4.2.17)$$

and thus we obtain the asymptotic bounded of $\|T(t)\|$. Next, from Lemma 4.2.3 we get (4.2.15) and (4.2.16). Since the sectorial operator B , defined in the above section 2.1.1., has compact resolvent; the existence of global compact and connected attractor A , follows from [[24], Theorem 4.2.2 and 3.4.8]. \square

4.3 Asymptotic behavior: finite-dimensional systems

We take a close look at the dynamics of (4.1.1) by considering the Fourier expansions of each function and observing the dynamics of each Fourier mode.

Note the Fourier expansion for all $g \in \dot{H}_{per}^m(0, 1)$, $m \geq 0$ is given by the expression $g(x) = \sum_{k \in \mathcal{Z}^*} a_k e^{2\pi k i x}$ with $\mathcal{Z}^* = \mathcal{Z} \setminus \{0\}$ and we have

$$\|g\|_{\dot{H}_{per}^m(0,1)} = (2\pi)^m \left(\sum_{k \in \mathcal{Z}^*} k^{2m} |a_k|^2 \right)^{\frac{1}{2}}. \quad (4.3.18)$$

We assume that $h, f, T_0 \in \dot{L}_{per}^2(0, 1)$ are given by the following Fourier expansions

$$h(x) = \sum_{k \in \mathbb{Z}^*} b_k e^{2\pi k i x}, f(x) = \sum_{k \in \mathbb{Z}^*} c_k e^{2\pi k i x}, T_0(x) = \sum_{k \in \mathbb{Z}^*} a_{k0} e^{2\pi k i x} \quad (4.3.19)$$

with $\mathbb{Z}^* = \mathbb{Z} \setminus \{0\}$. Assume that $T(t, x) \in \dot{L}_{per}^2(0, 1)$ is given by

$$T(t, x) = \sum_{k \in \mathbb{Z}^*} a_k(t) e^{2\pi k i x}. \quad (4.3.20)$$

Then, the coefficients $a_k(t)$ in (4.3.20), verify the equations:

$$\dot{a}_k(t) + (2\pi k \nu i + 4\nu \pi^2 k^2) a_k(t) = b_k, \quad a_k(0) = a_{k0}, \quad k \in \mathbb{Z}^* \quad (4.3.21)$$

Therefore, (4.1.1) is equivalent to the infinite system of ODEs consisting of (4.3.21) coupled with

$$\varepsilon \frac{d^2 v}{dt^2} + \frac{dv}{dt} + G(v)v = \sum_{k \in \mathbb{Z}^*} a_k(t) \bar{c}_k.$$

The two equations reflect two of the main features of (4.1.1): the coupling between modes enter only through the velocity, while diffusion acts as a linear damping term. In what follows, we will exploit this explicit equation for the temperature modes to analyze the asymptotic behavior of the system and to obtain the explicit low-dimensional models.

A similar explicit construction was given by Bloch and Titi in [6] for a nonlinear beam equation where the nonlinearity occurs only through the appearance of the L^2 norm of the unknown. A related construction was given by Stuart in [54] for a nonlocal reaction-diffusion equation.

We note that the system (4.1.1) is equivalent to the system (4.2.2) for the acceleration, velocity and temperature and this is equivalent now to the following infinite system

of ODEs (4.3.22)

$$\begin{cases} \frac{dw}{dt} + \frac{1}{\varepsilon}w = -\frac{1}{\varepsilon}G(v)v + \frac{1}{\varepsilon} \sum_{k \in \mathcal{Z}^*} a_k(t)\bar{c}_k, & w(0) = w_0 \\ \frac{dv}{dt} = w, & v(0) = v_0 \\ \dot{a}_k(t) + (2\pi kvi + 4\nu\pi^2 k^2)a_k(t) = b_k, & a_k(0) = a_{k0}, \quad k \in \mathcal{Z}^*. \end{cases} \quad (4.3.22)$$

Next, we obtain the boundedness of these coefficients that improve the boundedness of temperature of the previous section and in particular, allow us to prove the existence of the inertial manifold for the system (4.1.1).

4.3.1 Inertial manifold

Proposition 4.3.1 *For every solution of the system (4.1.1), (w, v, T) , and for every $k \in \mathcal{Z}^*$ we have*

$$\limsup_{t \rightarrow \infty} |a_k(t)| \leq \frac{|b_k|}{4\nu\pi^2 k^2}, \text{ in particular } \limsup_{t \rightarrow \infty} \|T(t, \cdot)\| \leq \frac{1}{4\nu\pi^2} \|h\| \quad (4.3.23)$$

$$\limsup_{t \rightarrow \infty} |v(t)| \leq \frac{I_0}{G_0} + H_0, \text{ with } I_0 = \sum_{k \in \mathcal{Z}^*} \frac{|b_k||c_k|}{4\nu\pi^2 k^2} \quad (4.3.24)$$

and G_0 positive constant such that $G(v) \geq G_0$.

$$\limsup_{t \rightarrow \infty} |w(t)| \leq G_0^* H_0 + \left(1 + \frac{G_0^*}{G_0}\right) I_0, \text{ with } G_0^* = \limsup_{t \rightarrow \infty} G(v(t)). \quad (4.3.25)$$

PROOF. From (4.3.21), we have that

$$a_k(t) = a_{k0} e^{-4\nu\pi^2 k^2 t} e^{-2\pi ki \int_0^t v} + e^{-4\nu\pi^2 k^2 t} b_k \int_0^t e^{4\nu\pi^2 k^2 s} e^{-2\pi ki \int_s^t v} ds$$

and taking into account that $|e^{-2\pi ki \int_0^t v}| = |e^{-2\pi ki \int_s^t v}| = 1$ we obtain:

$$|a_k(t)| \leq |a_{k0}| e^{-4\nu\pi^2 k^2 t} + \frac{|b_k|}{4\nu\pi^2 k^2} (1 - e^{-4\nu\pi^2 k^2 t}) \quad (4.3.26)$$

and we get $\limsup_{t \rightarrow \infty} |a_k(t)| \leq \frac{|b_k|}{4\nu\pi^2 k^2}$. Using Lemma 4.2.3 together with $\oint Tf = \sum_{k \in \mathbb{Z}^*} a_k(t) \bar{c}_k$, the rest is obvious. \square

Corollary 4.3.2 *i) If $|a_{k0}| \leq \frac{|b_k|}{4\nu\pi^2 k^2}$ then $|a_k(t)| \leq \frac{|b_k|}{4\nu\pi^2 k^2}$ for every $t \geq 0$.*

ii) If A is the global attractor in the space $Y = \mathbb{R}^2 \times \dot{L}_{per}^2(0,1)$, then for every $(w_0, v_0, T_0) \in A$, with $T_0(x) = \sum_{k \in \mathbb{Z}^} a_k e^{2\pi k i x}$ we get,*

$$|a_k| \leq \frac{|b_k|}{4\nu\pi^2 k^2}, \quad k \in \mathbb{Z}^*. \quad (4.3.27)$$

In particular, if $h \in \dot{H}_{per}^m$ with $m \geq 1$, the global attractor $A \hookrightarrow \mathbb{R}^2 \times \dot{H}_{per}^{m+2}$ and is compact in this space.

PROOF. i) From (4.3.26) we have $|a_k(t)| \leq \frac{|b_k|}{4\nu\pi^2 k^2} + (|a_{k0}| - \frac{|b_k|}{4\nu\pi^2 k^2})_+ e^{-4\nu\pi^2 k^2 t}$. If $|a_{k0}| \leq \frac{|b_k|}{4\nu\pi^2 k^2}$ then $|a_k(t)| \leq \frac{|b_k|}{4\nu\pi^2 k^2}$ for every $t \geq 0$ and $k \in \mathbb{Z}^*$.

ii) We take into account that from i), if $h(x) = \sum_{k \in \mathbb{Z}^*} b_k e^{2\pi k i x} \in \dot{H}_{per}^m$, then $\sum_{k \in \mathbb{Z}^*} k^{2m} |b_k|^2 < \infty$, and therefore $T_0 \in C = \{R(x) = \sum_{k \in \mathbb{Z}^*} r_k e^{2\pi k i x} \in \dot{H}_{per}^{m+2}, k^2 |r_k| \leq \frac{1}{4\pi^2 \nu} |b_k|\}$. \square

In the next result we will prove that there exists an inertial manifold M for the semigroup $S(t)$ in the phase space $Y = \mathbb{R}^2 \times \dot{H}_{per}^m$, $m \geq 1$ according to [20], i.e., a submanifold of Y such that i) $S(t)M \subset M$ for every $t \geq 0$, ii) there exists $\delta > 0$ verifying that for every bounded set $B \subset Y$, there exists $C(B) \geq 0$ such that $dist(S(t), M) \leq C(B)e^{-\delta t}$, $t \geq 0$ see, for example, [20]. Assume that $h \in \dot{H}_{per}^m$ with

$$h(x) = \sum_{k \in K} b_k e^{2\pi k i x}$$

with $b_k \neq 0$ for every $k \in K \subset \mathbb{Z}^*$ with $0 \notin K$, since $\oint h = 0$. We denote by V_m the closure of the subspace of \dot{H}_{per}^m generated by $\{e^{2\pi k i x}, k \in K\}$.

Theorem 4.3.3 Assume that $h \in \dot{H}_{per}^m$ and $f \in \dot{L}_{per}^2$. Then the set $M = \mathbb{R}^2 \times V_m$ is an inertial manifold for the flow of $S(t)(w_0, v_0, T_0) = (w(t), v(t), T(t))$ in the space $Y = \mathbb{R}^2 \times \dot{H}_{per}^m$. Moreover if K is a finite set, then the dimension of M is $|K| + 2$, where $|K|$ is the number of elements in K .

PROOF. Step (i) First, we show that M is invariant. Note that if $k \notin K$, then $b_k = 0$, and therefore if $a_{k_0} = 0$, from (4.3.26), we get that $a_k(t) = 0$ for every t , i.e., $T(t, x) = \sum_{k \in K} a_k(t) e^{2\pi k i x}$. Therefore, if $(w_0, v_0, T_0) \in M$, then $(w(t), v(t), T(t)) \in M$ for every t , i.e., M is invariant.

Step (ii) From previous assertions, $\oint T(t) \cdot f = \sum_{k \in K} a_k(t) \cdot \bar{c}_k$ and the flow on M is given by

$$\dot{w} + \frac{1}{\varepsilon} w + \frac{1}{\varepsilon} G(v)v = \frac{1}{\varepsilon} \sum_{k \in K} a_k(t) \cdot \bar{c}_k$$

$$\dot{v} = w$$

$$\dot{a}_k(t) + (2\pi k v i + 4c\pi^2 k^2) a_k(t) = b_k, \quad k \in K \quad (4.3.28)$$

$$a_k = 0, k \notin K.$$

Now, we consider the following decomposition in \dot{H}_{per}^m , $T = T^1 + T^2$, where T^1 is the projection of T on V_m and T^2 is the projection of T on the subspace generated by $\{e^{2\pi k i x}, k \in \mathbb{Z}^* \setminus K\}$ i.e., $T^1 = \sum_{k \in K} a_k e^{2\pi k i x}$ and $T^2 = \sum_{k \in \mathbb{Z}^* \setminus K} a_k e^{2\pi k i x} = T - T^1$.

Then, given $(w_0, v_0, T_0) \in Y$ we decompose $T_0 = T_0^1 + T_0^2$, and $T(t) = T^1(t) + T^2(t)$

and we consider $(w(t), v(t), T^1(t)) \in M$ and then

$$(w(t), v(t), T(t)) - (w(t), v(t), T^1(t)) = (0, 0, T^2(t)).$$

From (4.3.26) taking into account that $b_k = 0$ for $k \in \mathbb{Z}^* \setminus K$, we have that $|a_k(t)| \leq |a_{k0}|e^{-\nu\pi^2 k^2 t}$ and this together with $\nu\pi^2 k^2 t \geq \nu\pi^2 t$ for every $k \in \mathbb{Z}^*$ implies that $\|T^2(t)\|_{\dot{H}_{per}^m} \leq \|T_0^2\|_{\dot{H}_{per}^m} e^{-\nu\pi^2 t}$ i.e., $T^2(t) \rightarrow 0$ in \dot{H}_{per}^m if $t \rightarrow \infty$.

Therefore, we have that $\|T^2(t)\|_{\dot{H}_{per}^m} \rightarrow 0$ as $t \rightarrow \infty$ with exponential decay rate $e^{-\nu\pi^2 t}$. Thus M attracts $(w(t), v(t), T(t))$ with exponential rate $e^{-\nu\pi^2 t}$. \square

4.3.2 The reduced subsystem

Under the hypotheses and notations of Theorem 4.3.3, we suppose that

$$f(x) = \sum_{k \in J} c_k e^{2\pi k i x},$$

with $c_k \neq 0$ for every $k \in J \subset \mathbb{Z}$. Note that since all the functions involved are real, we have $\bar{a}_k = a_{-k}$, $\bar{b}_k = b_{-k}$ and $\bar{c}_k = c_{-k}$. Then, on the inertial manifold $\oint T(t) \cdot f = \sum_{k \in K} a_k(t) \bar{c}_k = \sum_{k \in K \cap J} a_k(t) \cdot c_{-k}$. So, the evolution of the velocity v and the acceleration w depend only on the coefficients of T which belong to the set $K \cap J$. Note that in (4.3.28) the set of equations for a_k with $k \in K \cap J$, together with the equation for v and w , are a subsystem of coupled equations. After solving this, we must solve the equations for $k \notin K \cap J$ which are linear autonomous equations. We note that $0 \notin K \cap J$ and since $K = -K$ and $J = -J$ then the set $K \cap J$ has an even number of elements, that we denote by $2n_0$.

Corollary 4.3.4 *Under the notations and hypotheses of the Theorem 4.3.3, we suppose that the set $K \cap J$ is finite and then $|K \cap J| = 2n_0$. Then the asymptotic behavior of the*

system (4.1.1), is described by a system of $N = 2n_0 + 2$ coupled equations in \mathbb{R}^N , which determine $(w, v, a_k), k \in K \cap J$, and a family of $|K \setminus (K \cap J)|$ linear non-autonomous equations. In particular, if $K \cap J = \emptyset$, and $G(v) = G_0$ then for every $(w_0, v_0, T_0) \in \mathbb{R}^2 \times \dot{L}_{per}^2(0, 1)$ we have that the associated solution verifies that $v(t) \rightarrow 0$, $w(t) \rightarrow 0$ and $T(t) \rightarrow \theta_\infty$ in $\dot{L}_{per}^2(0, 1)$, i.e., the global attractor is given by $A = \{(0, 0, \theta_\infty)\}$, where $\theta_\infty(x)$ is the unique solution in $\dot{H}_{per}^2(0, 1)$ of the equation $-\nu \frac{\partial^2 \theta_\infty}{\partial x^2} = h(x)$.

PROOF. Note that on the inertial manifold $\oint T \cdot f = \sum_{k \in K} a_k(t) \bar{c}_k = \sum_{k \in K \cap J} a_k(t) \cdot c_{-k}$.

Thus, the dynamics of the system depends only on the coefficients in $K \cap J$. Moreover the equations for a_{-k} are conjugated of the equations for a_k and therefore we have that $\sum_{k \in K \cap J} a_k(t) c_{-k} = 2Re \left(\sum_{k \in (K \cap J)_+} a_k(t) c_{-k} \right)$. From this, and taking real and imaginary parts of $a_k, (a_1^k, a_2^k), k \in (K \cap J)_+$ in (4.3.22) where $n_0 = |(K \cap J)_+|$, we conclude.

If $K \cap J = \emptyset$, and $G(v) = G_0$ then on the inertial manifold we get a homogeneous linear equation for the velocity with positive coefficients, and by this $\limsup_{t \rightarrow \infty} |v(t)| = 0$, and therefore the equation for w on the inertial manifold is $\frac{dw}{dt} + \frac{1}{\varepsilon} w = -\frac{1}{\varepsilon} G_0 v = \delta(t)$. Next, using $\delta(t) \rightarrow 0$ we get $w(t) \rightarrow 0$ as $t \rightarrow \infty$.

Moreover from the equation for the temperature in (4.1.1) we have that the function $\theta = T - \theta_\infty$ satisfies the equation: $\frac{\partial \theta}{\partial t} + v \frac{\partial \theta}{\partial x} = -\nu \frac{\partial^2 \theta}{\partial x^2} + \nu \frac{\partial^2 \theta}{\partial x^2}$.

We can multiply by θ in \dot{L}_{per}^2 and taking into account that $\oint \frac{\partial \theta}{\partial x} \theta = \frac{1}{2} \oint \frac{\partial(\theta^2)}{\partial x} = 0$ since θ is periodic, we obtain $\frac{1}{2} \frac{d}{dt} \|\theta\|^2 + \nu \|\frac{\partial \theta}{\partial x}\|^2 = -\nu \oint \frac{\partial(\theta_\infty)}{\partial x} \theta$, and using Cauchy-Schwarz and the Young inequality with $\delta = \frac{\nu \pi^2}{2}, C_\delta = \frac{1}{4\delta}$ and then the Poincaré inequality, since $\oint \theta = 0$, we have that $\frac{d}{dt} \|\theta\|^2 + \nu \pi^2 \|\theta\|^2 \leq |\nu|^2 \frac{1}{2\nu \pi^2} \|\frac{\partial \theta_\infty}{\partial x}\|^2$. Next, from singular Gronwall

lemma we get $\lim_{t \rightarrow \infty} \|\theta\|^2 \leq \lim_{t \rightarrow \infty} |v|^2 \frac{1}{2\nu^2 \pi^4} \|\frac{\partial \theta_\infty}{\partial x}\|^2$ and using $v(t) \rightarrow 0$ we prove that $\theta(t) \rightarrow 0$ in $\dot{L}_{per}^2(0, 1)$. \square

Remark 4.3.1 *Taking real and imaginary parts of coefficients $a_k(t)$ (temperature), b_k (heat flux at the wall of the loop) and c_k (geometry of circuit)*

$$a_k(t) = a_1^k(t) + ia_2^k(t), b_k = b_1^k + ib_2^k \text{ and } c_k = c_1^k + ic_2^k,$$

the asymptotic behavior of the system (4.1.1) is given by a reduced system in \mathbb{R}^N , where $N = 2n_0 + 2$ ($w(t), v(t), a_1^k(t), a_2^k(t), k \in (K \cap J)_+$) and $n_0 = |(K \cap J)_+|$.

Observe that from the above analysis, it is possible to design the geometry of circuit and/or the external heating, by properly choosing the functions f and/or the heat flux, h , so that the resulting system has an arbitrary number of equations of the form $N = 2n_0 + 2$.

Note that it may be the case that K and J are infinite sets, but their intersection is finite. Also, for a circular circuit we have $f(x) \sim a \sin(x) + b \cos(x)$, i.e., $J = \{\pm 1\}$ and then $K \cap J$ is either $\{\pm 1\}$ or the empty set. Also, if in the original variables of (4.1.1), h is constant we get $K \cap J = \emptyset$ for any choice of f . Using these results, the physical and mathematical implications of the resulting system of ODEs which describes the dynamics at the inertial manifold has been analyzed numerically in the following section.

4.4 Numerical experiments

In this section, the results of the numerical experiments obtained using the MATHEMATICA package [61] for the resolution of the differential equations is presented, using a fourth-order explicit Runge-Kutta method for stiffness equations, following the method used in previous works [23, 27]. We solve a system of ordinary differential equations which

are the projection of the partial differential equations (4.1.1) on the inertial manifold derived in the preceding sections. All the variables and equations that we deal with are adimensional. As the system is multidimensional, the results are presented in temporal graphs (a given variable vs time) and phase-space graphs (two physical variables plot against each other).

Specifically, we integrate the system of equations (4.3.22), where we consider only the coefficients of temperature $a_k(t)$ with $k \in K \cap J$ (relevant modes). Then,

$$\left\{ \begin{array}{l} \frac{dw}{dt} + \frac{w}{\varepsilon} + \frac{G(v)v(t)}{\varepsilon} = \frac{2}{\varepsilon} \text{Real} \left(\sum_{k \in K \cap J} a_k(t) c_{-k} \right) \\ \frac{dv}{dt} = w \\ \dot{a}_k(t) + a_k(t)(2\pi k i v + \nu 4\pi^2 k^2) = b_k \end{array} \right.$$

where $a_{-k} = \bar{a}_k, b_{-k} = \bar{b}_k$ and $c_{-k} = \bar{c}_k$ since all the physical observable are real functions. In particular, we will consider a thermosyphon with a circular geometry, so $J = \{\pm 1\}$ and $K \cap J = \{\pm 1\}$. Consequently, we can take $k = 1$ and omit the equation for $k = -1$. Hence,

$$\left\{ \begin{array}{l} \frac{dw}{dt} = \frac{2a_1 c_{-1}}{\varepsilon} - \frac{w}{\varepsilon} - \frac{G(v)v(t)}{\varepsilon}, \\ \frac{dv}{dt} = w, \\ \dot{a}_1(t) + a_1(t)(2\pi i v + \nu 4\pi^2) = b_1 \end{array} \right.$$

where the unknowns are $w(t)$ (the acceleration of the fluid), $v(t)$ (velocity of the fluid) and $a_1(t)$ (the Fourier mode of the temperature). More complex geometries will result in higher dimensional dynamics on the inertial manifold.

In order to reduce the number of parameters we make the change of variables

$a_1 c_{-1} \rightarrow a_1$ and we then define the real and imaginary parts of the equations in the following way:

$$a_1(t) = a^1(t) + ia^2(t), \quad (4.4.29)$$

$$b_1 = A + iB \quad (4.4.30)$$

with $A \in \mathbb{R}, B \in \mathbb{R}$. Hence, our central results correspond to the system of equations

$$\left\{ \begin{array}{l} \frac{dw}{dt} = \frac{2a^1}{\varepsilon} - \frac{w}{\varepsilon} - \frac{G(v)v(t)}{\varepsilon}, \\ \dot{v} = w, \\ \dot{a}^1 = A - \nu 4\pi^2 a^1 + v 2\pi a^2, \\ \dot{a}^2 = B - \nu 4\pi^2 a^2 - v 2\pi a^1 \end{array} \right. \quad (4.4.31)$$

Note that it is a system of four equations with four unknowns where we need to make explicit choices for the constitutive laws for both the fluid-mechanical and thermal properties. For the friction law $G(v)$ and heat flux $h(x)$ we will take the one used in the references [23, 27]. For the numerical experiments which are of a similar model of thermosyphon for a fluid with one component, they use the function $G(v) = (|v| + 10^{-4})$. The function $G(v)$ has a clear physical meaning; it interpolates between a low Reynolds number friction law (in which the overall friction $G(v)v$ is non-linear (Stokes friction law) and high Reynolds number (in which the friction is a quadratic law).

Besides, A and B , which refer in this model to the position-dependant (x) heat flux inside the loop will be used as tuning parameters. Without loss of generality, we will assume $A = 0$ in order to simplify, in analogy with the Lorenz's model, as it is shown

in references [23, 27] (changing A and B simultaneously only results in a change in the *phase* of initial temperature profile).

We have carried out two different sets of numerical experiments with regard to heat diffusion. The first set of numerical experiments are carried out keeping the heat diffusion to zero as it was done in [52]. And the second set of numerical experiments are performed with heat diffusion. The initial conditions are fixed as $w(0) = 0, v(0) = 0, a_1(0) = 1, a_2(0) = 1$. This split would appear naive as diffusion tends to smooth the solution, however, as the order of the equations changes in the presence of diffusion (from first to second order, due to the Laplacian) it is worth studying both cases separately.

Numerical analysis has been carried out keeping ε the viscoelastic coefficient as the tuning parameter ranging from 100 to 0.0001 and B the heat flux also as another tuning parameter ranging from 1 to 10000. The impact of ε on the system has been keenly observed for various intervals of time t , as short as 50 time units and as long as 5000 time units. We will show that in analogy with the classical Lorenz's system, as ε varies, the dynamics of the model undergoes various transformations including steady asymptotic behavior, meta-stable chaos, i.e., transient irregular behavior followed by convergence to equilibria, periodic behaviors and chaotic progressions.

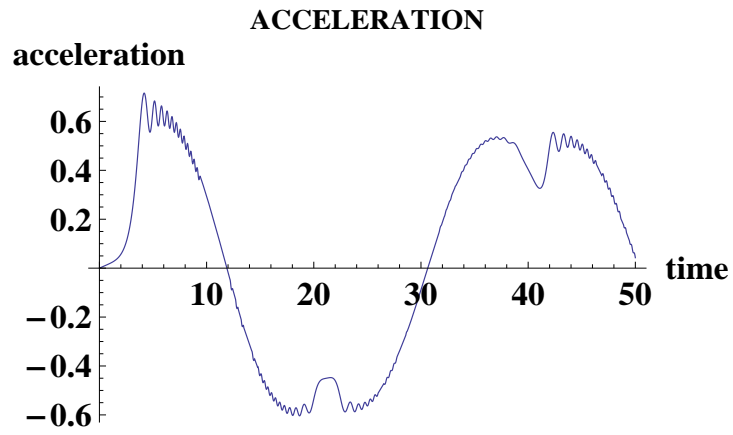


Figure 4.1: Acceleration for $\varepsilon = 100, B = 10, \nu = 0$

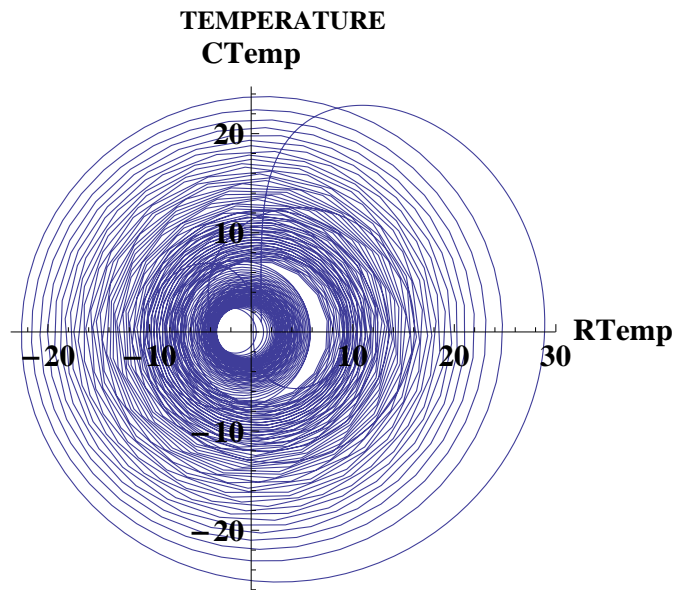


Figure 4.2: Temperature phase plot for $\varepsilon = 100, B = 10, \nu = 0$ (chaotic in concentric circles)

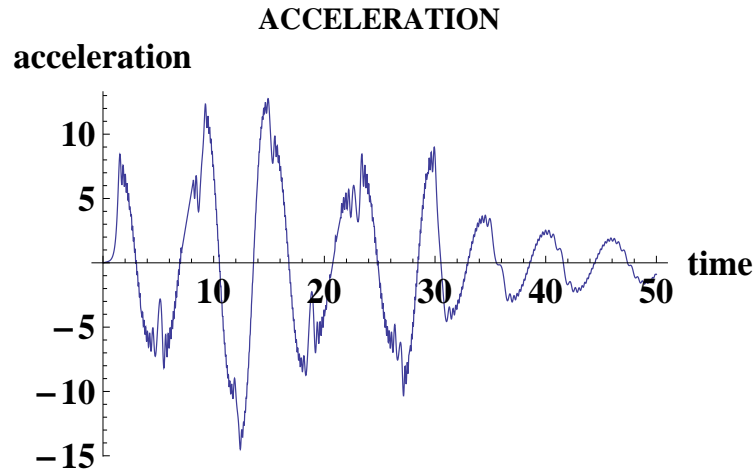


Figure 4.3: Acceleration for $\varepsilon = 10, B = 100, \nu = 0$

4.4.1 The behavior of the model for different values of $\varepsilon, \nu = 0$

$\varepsilon = 100, \nu = 0$

For $\varepsilon = 100$ a relatively large value, the acceleration ranges from -45 to 45 as the maximum deviation. Throughout the time duration it exhibits a cyclic pattern of behavior (see Fig. 4.1). The velocity ranges from -60 to 60. The real-temperature and the complex temperature range from -10000 to 10000. Throughout the time duration it exhibits a cyclic pattern of behavior of divergence and convergence (see Fig. 4.2). The real-temperature and complex-temperature together form a structure that is very chaotic. For all the values of B this chaotic cyclic behavior is observed. For large values of ε the system behaves chaotic in concentric circles.

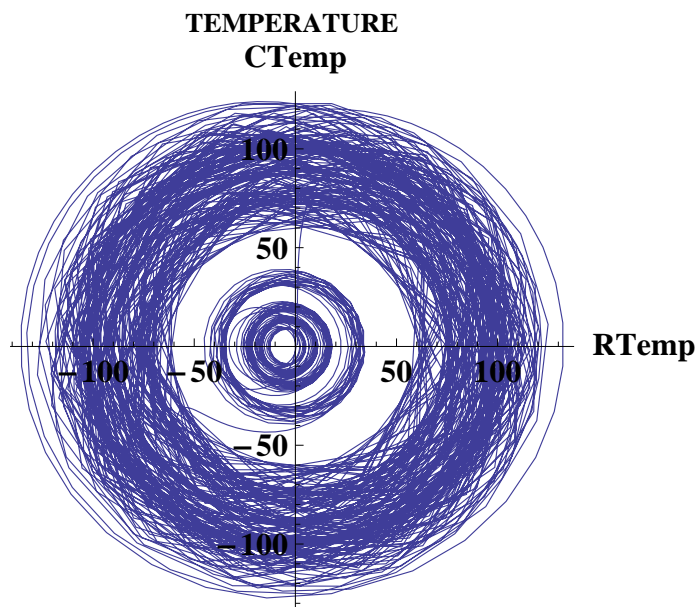


Figure 4.4: Temperature phase plot for $\varepsilon = 10, B = 100, \nu = 0$ (chaotic in concentric circles)

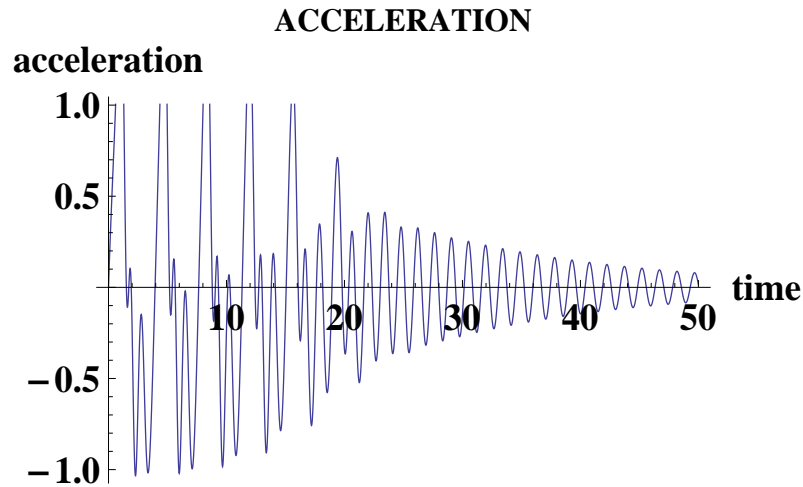


Figure 4.5: Acceleration for $\varepsilon = 1, B = 1, \nu = 0$

$\varepsilon = 10, \nu = 0$

For $\varepsilon = 10$, the acceleration ranges from -180 to 180, as the maximum deviation. Throughout the time duration it exhibits a chaotic pattern of progression (see Fig. 4.3). The velocity ranges from -80 to 80. The real-temperature and the complex temperature range from -6000 to 6000. Throughout the time duration it exhibits chaotic behavior of divergence and convergence. The real-temperature and complex-temperature together form a structure that is very chaotic. For all the values of B this chaotic behavior is observed. For $\varepsilon = 10$ the system behaves chaotic in concentric circles (see Fig. 4.4).

$\varepsilon = 1$

For $\varepsilon = 1$, the acceleration ranges from -50 to 50 as the maximum deviation. In the initial period, when the time period is less than 10 units, the plot is very inconsistent and

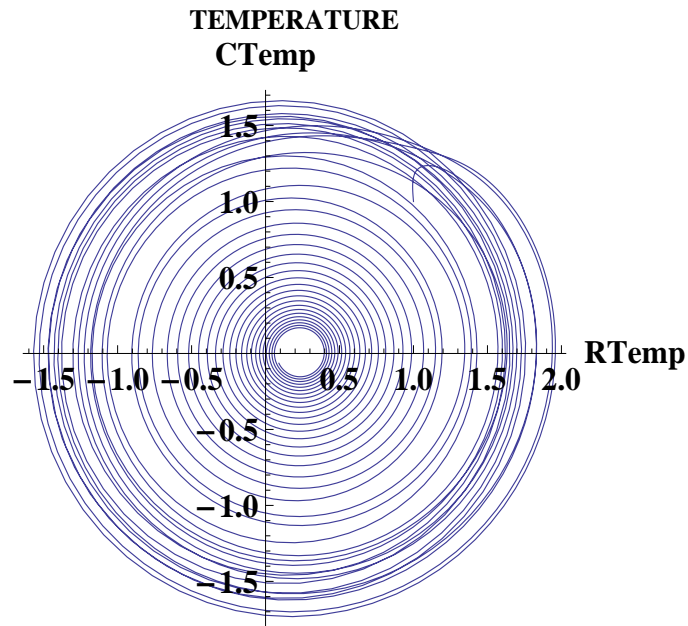


Figure 4.6: Temperature phase plot for $\varepsilon = 1, B = 1, \nu = 0$

chaotic. But as the time progresses, acceleration exhibits an oscillatory decay to a fixed stable point (see Fig. 4.5). The velocity ranges from 10 to 20. The velocity too converges to a point as the time goes further. The real-temperature and the complex temperature range from -3000 to 3000. Like acceleration and velocity, the temperature plot too shows the same convergence pattern of behavior as time moves. This is the case for all the values of B , which is a clear indication that when $\varepsilon = 1$ the system behaves chaotic in the initial times and as time moves it converges to a point, giving the system a steady state (see Fig. 4.6).

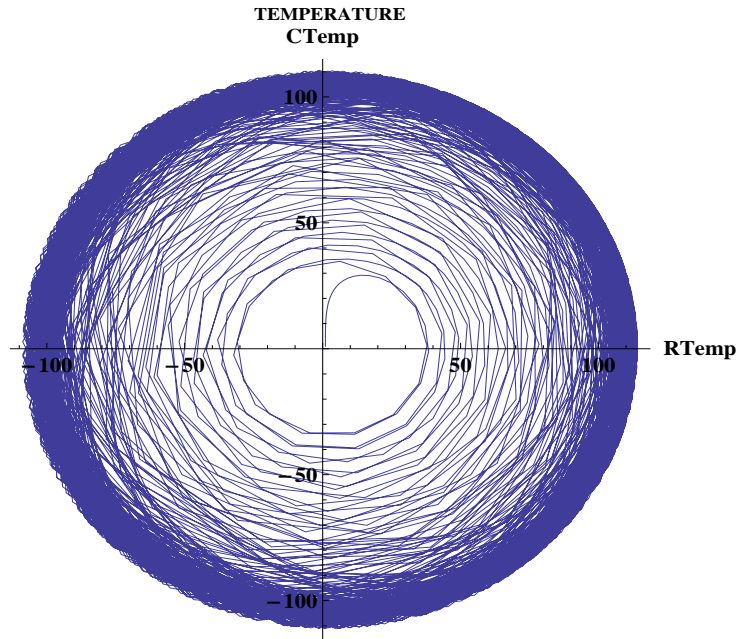


Figure 4.7: Temperature phase plot for $\varepsilon = 0.1$, $B = 100$, $\nu = 0$

$\varepsilon = 0.1$

Given the value of viscoelastic component ε is relatively less ($\varepsilon = 0.1$) the system tends towards a stable progression though it is chaotic in the initial stages. The acceleration ranges from -800 to 800. The maximum deviation is reached in the initial stages, when the time period is less than 10 units. The velocity ranges from 0 to 8.36 when ε is 0.1. In the initial stages, when the time period is less than 10 units, the plot is very inconsistent and at times unpredictable. But as the time progresses, velocity continues to progress constantly. The progress of velocity is noted to be constant as time moves. As the time increases further velocity attains constancy. The real-temperature ranges from -4000 to 4000 when ε is 0.1. In the initial stages, when the time period is less than 10 units, it

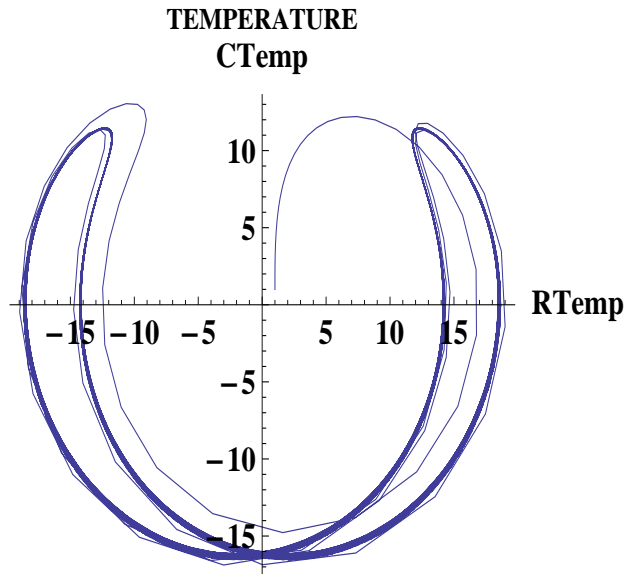


Figure 4.8: Temperature phase plot for $\varepsilon = 0.01, B = 50, \nu = 0$

has a chaotic behavior. But as the time progresses, the temperature continues to converge constantly. The progress of temperature is noted to be constant, as time moves further the deviation is found to be constant. The complex-temperature too exhibits the same pattern of behavior. The real-temperature and complex-temperature together form a structure that is chaotic and circle. It could be noted that at the origin the plot is found to be steady with rings. But as it moves away from the center it is getting chaotic (see Fig. 4.7). From the above readings we can conclude that the system tends to stabilize itself when the value of viscoelastic component is 0.1.

$$\varepsilon = 0.01$$

When the value of ε is 0.01, that is relatively less than the previous experiments, the system attains a stable progression as time moves. The acceleration ranges from -10000 to 10000 when ε is 0.01. It is a steady and constant progression for acceleration as time increases. The velocity ranges from 70 to 90. It is a chaotic progression for velocity as time increases. The real-temperature and the complex-temperature together form a circle for greater values of B. For smaller values of B, the system exhibits a transitional behavior that is not clearly chaotic nor periodic. Therefore from observing the nature of the data we can conclude that when the value of ε is less, the system behaves chaotic and tries to form a periodic pattern (see Fig. 4.8).

$$\varepsilon = 0.001$$

As the value of ε is further lessened the system behaves in a more steady state. The acceleration ranges from -1000 to 1000 when ε is 0.001. It is a steady and constant progression for acceleration as time increases. The velocity ranges from -20 to 20 when is 0.001. It is a steady and constant progression for velocity too as time increases. Throughout the progression it is consistently chaotic in nature. The real-temperature and the complex-temperature together form a periodic structure that is chaotic.

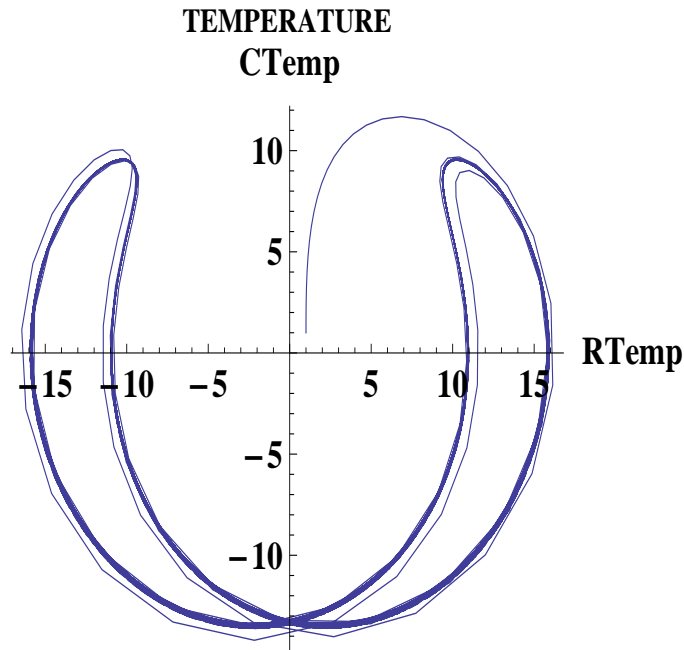


Figure 4.9: Temperature phase plot for $\varepsilon = 0.0001, B = 50, \nu = 0$

$\varepsilon = 0.0001$

As the value of ε is further decreased to 0.0001, the system behaves the same manner as in the previous cases. The acceleration ranges from -800 to 800 when ε is 0.0001. It is a steady and constant chaotic progression for acceleration as time increases. The velocity ranges from -20 to 20. Throughout the progression it is a constant chaotic progression. The real-temperature and the complex-temperature together form a chaotic periodic structure. From these observations we can conclude that as the value of viscoelastic coefficient lessens the system attains a steady and periodic behavior (see Fig. 4.9).

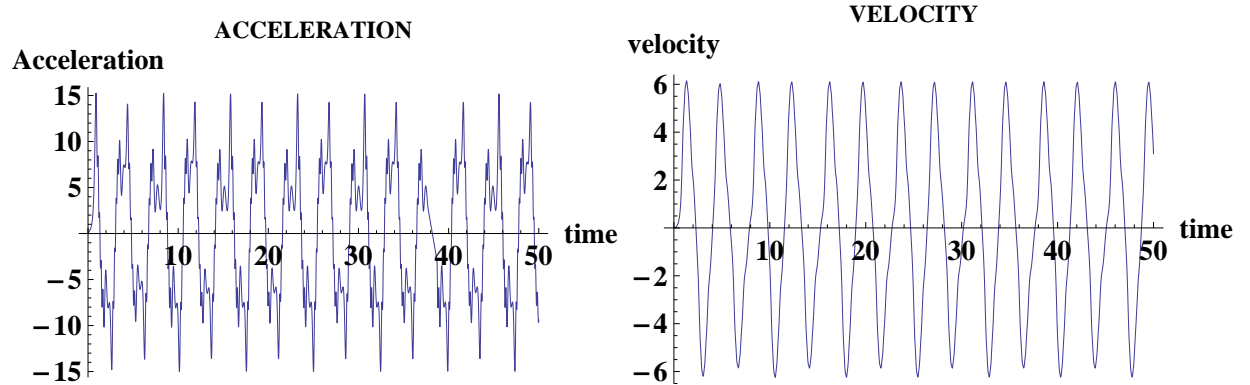


Figure 4.10: The time evolution of the acceleration, $w(t)$ (left), and the velocity, $v(t)$ (right), with $\varepsilon = 1$, $A = 0$, $B = 50$, $\nu = 0.002$ and $G(v) = (|v| + 10^{-4})$

4.4.2 The chaotic behavior of this model for $B = 50$

The impact of ε on the system has been keenly observed for various parameters, keeping the prescribed heat flux $B = 50$ especially to compare this case with the previous case. In general, as the viscoelastic component ε increases, the chaotic behavior of the system also increases. In Fig. 4.10 we show the time evolution of the acceleration, $w(t)$, and the velocity, $v(t)$, for the viscoelastic parameter $\varepsilon = 1$. The acceleration $w(t)$ ranges from -15 to 15. The plot is chaotic, although this is more apparent in the acceleration plot than in the velocity one. This is reasonable as velocity is the time integral of acceleration, namely, the velocity curve looks smoother than that of the acceleration (therefore the chaotic behavior is not so apparent).

In Fig. 4.11 we show the phase-diagram for the real $a^1(t)$ and imaginary $a^2(t)$ parts of the Fourier transform of the temperature. As expected, the trajectory in this phase-plane moves inwards and outwards. This plot illustrates the underlying complex

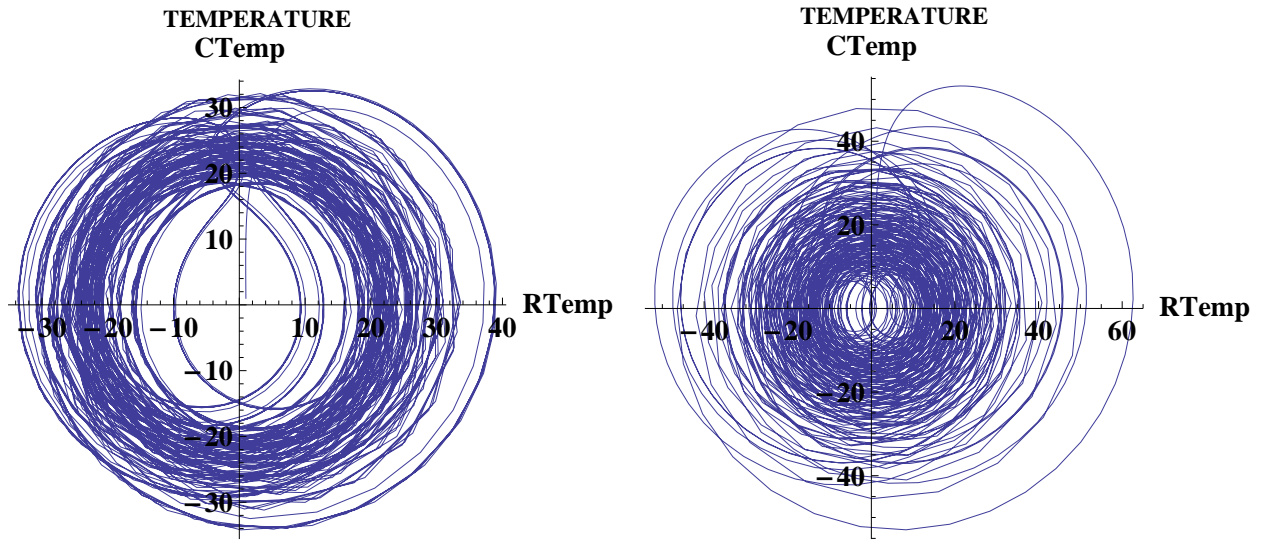


Figure 4.11: Left: Phase-plane of the real and imaginary parts of Fourier transform of the temperature for $\varepsilon = 1$, $A = 0$, $B = 50$, $\nu = 0.002$ and $G(v) = (|v| + 10^{-4})$. Right: Same parameters as in the left panel but with $\varepsilon = 10$.

dynamics of the attractor as a two dimensional projection.

In the second set of numerical experiments we increase the value of viscoelastic component to $\varepsilon = 3$. As the value of viscoelastic component ε is relatively higher than the previous experiment i.e., ($\varepsilon = 3$) the system tends to be more chaotic than the previous experiment. The acceleration $w(t)$ ranges from -10 to 10. The deviation in the progress of acceleration is maintained till the end of the progress. Apparently, the behavior is also chaotic but this chaos seems to be embedded in larger timescale oscillations. Interestingly, the number of oscillations is reduced from 15 to 9. Fig. 4.12 shows less number of peaks than the first case. This is a reflection of the memory effects associated to the viscoelastic nature of the fluid. Thus, as ε plays the role of a time scale, the larger the value the

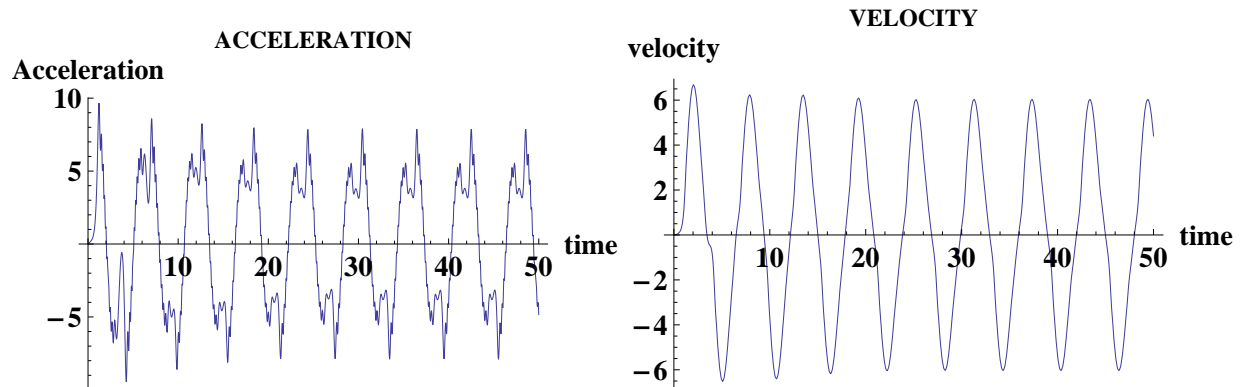


Figure 4.12: The time evolution of the acceleration, $w(t)$ (left), and the velocity, $v(t)$ (right), with $\varepsilon = 3$, $A = 0$, $B = 50$, $\nu = 0.002$ and $G(v) = (|v| + 10^{-4})$

longer is the memory effect (in our case exposed through the period of the underlying oscillations).

For $\varepsilon = 10$ (Fig. 4.13), the system still exhibits a chaotic progression, with the acceleration ranging from -4 to 4 and with even an underlying longer-period oscillations compared to the previous experiments.

Finally, in Fig. 4.11 (right panel) we show the phase-diagram for $a^1(t)$ and $a^2(t)$. Again, as expected, the trajectory in this phase-plane moves inwards and outwards. This plot illustrates the underlying complex dynamics of the attractor of a two dimensional projection.

In summary, larger values of the viscoelastic parameters ε , result in sustained chaotic behaviors overlapped with (almost) periodic behavior whose period scales with the numerical value of ε . The dynamics becomes more complex and is characterized in all the cases by periods of chaos and of violent oscillations, giving an idea of the complexity

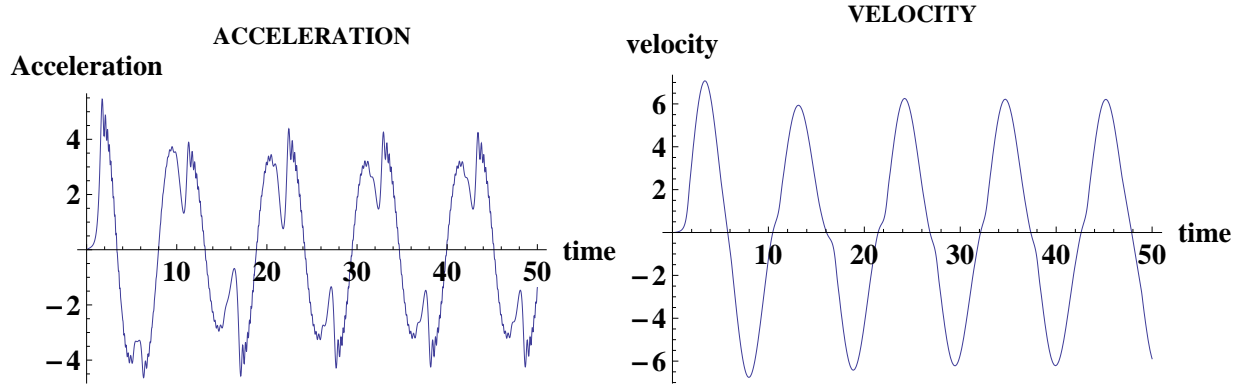


Figure 4.13: The time evolution of the acceleration, $w(t)$ (left), and the velocity, $v(t)$ (right), with $\varepsilon = 10$, $A = 0$, $B = 50$, $\nu = 0.002$ and $G(v) = (|v| + 10^{-4})$

of the solutions of the system under these variables due to memory effects.

4.5 Conclusions

The physical and mathematical implications of the resulting system of ODEs which describe the dynamics at the inertial manifold is analyzed numerically. The role of the parameter ε which contains the viscoelastic information of the fluid was treated with special attention. We studied the asymptotic behavior of the system for different values of ε the coefficient of viscoelasticity. We can conclude that for larger values of ε the system behaves more chaotic, in the same fashion as in model one, as presented in Chapter 3. Physically, this induction of chaotic behaviors is related to the memory effects inherent to viscoelastic fluids. Thus, in the same way as delayed equations are known to produce chaos, even in the simplest situations, viscoelasticity produces the same kind of transition.

Chapter 5

Binary viscoelastic fluids with Soret effect

5.1 Introduction

In this chapter, the dynamics of binary viscoelastic fluids confined in a closed loop thermosyphon and subject to the Soret effect is investigated. Various thermal gradients, viscoelastic coefficients and solute gradients produce different types of complex dynamical behaviors on the system. A study of the dynamics of the system and the competition/cooperation of these mechanisms is conducted to provide different outcomes, from chaotic to stable behavior by means of inertial manifold techniques and numerical integration of the reduced dynamics in the manifold. In particular, a study of the memory effects of viscoelastic materials through the Maxwell viscoelastic constitutive law is carried out in this model. A detailed analysis of the impact of viscoelasticity and its coexistence with the Soret effect has been exhaustively analysed in this chapter.

The Soret effect is a very important component of the study of any physical experiment that pertains to thermodiffusion. It gives rise to interaction between the thermal and

solute gradients even when the fluid is at rest [42]. Thermodiffusion is a phenomenon of temperature gradient [16] observed in a mixture of two or more types of moving particles. The term “Soret effect” normally means thermodiffusion in liquids. Thermodiffusion is labeled “positive” when particles move from a hot to cold region and “negative” when the reverse is true [30]. Typically the heavier or larger species in a mixture exhibits positive thermophoretic behavior while the lighter or smaller species exhibits negative behavior.

$$\left\{ \begin{array}{l} \varepsilon \frac{d^2v}{dt^2} + \frac{dv}{dt} + G(v)v = \oint (T - S)f, \quad v(0) = v_0, \frac{dv}{dt}(0) = w_0 \\ \frac{\partial T}{\partial t} + v \frac{\partial T}{\partial x} = l(v)(T_a - T) + \nu \frac{\partial^2 T}{\partial x^2}, \quad T(0, x) = T_0(x) \\ \frac{\partial S}{\partial t} + v \frac{\partial S}{\partial x} = c \frac{\partial^2 S}{\partial x^2} - b \frac{\partial^2 T}{\partial x^2}, \quad S(0, x) = S_0(x) \end{array} \right. \quad (5.1.1)$$

where $l(v)(T_a - T)$ is the Newton’s linear cooling law as in [23, 34, 35, 36, 37, 56, 59], which represents the heat transfer law across the loop, $l(v)$ a positive quantity depending on the velocity, T_a the (given) ambient temperature distribution, see [23, 36, 56, 59] and $S(t, x)$ the solute concentration. In addition to that, in this model, the diffusion of temperature given by the term $\nu \frac{\partial^2 T}{\partial x^2}$ is considered (see Chapter 2).

This model can be generalized in many different ways, from changing the constitutive equation (from Maxwellian to other more complex situations) or to include shear-thinning effects [46] common to many non-Newtonian materials. Shear-thinning is the manifestation of a shear-rate dependent viscosity. Thus, it is commonly observed that many fluids reduce their resistance to flow for large enough imposed stresses (in this case, temperature gradients), for instance tooth paste, paint or lava.

The contributions in this chapter are:

- To obtain a system of equations (2.2.6) governing a closed loop thermosyphon model of a viscoelastic fluid with Soret effect which, although it is a generalization of the previous models [26, 28, 34, 35, 36, 37, 50, 52, 56, 63], increasing the order of the time derivatives in velocity giving rise to routes to chaos.
- To provide a detailed numerical analysis of the behavior of acceleration, velocity, temperature and solute concentration which includes a thorough study of the various behaviors of the system for different values of viscoelastic fluid and Soret coefficient.
- To assess the impact of the viscoelastic gradient with Soret effect on the system.

5.2 Well-posedness and boundedness: global attractor

5.2.1 Existence and uniqueness of solutions

In this section, the existence and uniqueness of solutions of the thermosyphon model (5.1.1) is proved with $f \in \dot{L}_{per}^2(0, 1)$, $T_a, T_0 \in \dot{H}_{per}^1(0, 1)$ and $S_0 \in \dot{L}_{per}^2(0, 1)$, see (5.2.4). To choose the framework for $\nu > 0$, integrate the equation for the temperature along the loop, taking into account the periodicity of T , i.e., $\oint \frac{\partial T}{\partial x} = \oint \frac{\partial^2 T}{\partial x^2} = 0$, and $\frac{d}{dt}(\oint T) = l(v)(\oint T_a - \oint T)$. Therefore, $\oint T \rightarrow \oint T_a$ exponentially as time goes to infinity for every $\oint T_0$.

Consider $\tau = T - \oint T$. Then from the second equation of the system (5.1.1), τ

verifies the equation:

$$\frac{\partial \tau}{\partial t} + v \frac{\partial \tau}{\partial x} = l(v)(\tau_a - \tau) + \nu \frac{\partial^2 \tau}{\partial x^2}, \quad \tau(0, x) = \tau_0(x) = T_0 - \oint T_0$$

where $\tau_a = T_a - \oint T_a$.

Integrate the equation for the solute concentration along the loop, taking into account the periodicity of S , i.e., $\oint \frac{\partial S}{\partial x} = \oint \frac{\partial^2 S}{\partial x^2} = 0$ and $\frac{d}{dt}(\oint S) = 0$. As $\oint S$ is constant, it implies that the solute $\oint S = \oint S_0$ for all t .

Consider $\sigma = S - \oint S_0$. Then from the third equation of the system (5.1.1), σ verifies the equation:

$$\frac{\partial \sigma}{\partial t} + v \frac{\partial \sigma}{\partial x} = c \frac{\partial^2 \sigma}{\partial x^2} - b \frac{\partial^2 \tau}{\partial x^2}, \quad \sigma(0, x) = \sigma_0(x).$$

Since $\oint f = 0$, we have $\oint (T - S)f = \oint (\tau - \sigma)f$ and the equations for v is

$$\varepsilon \frac{d^2 v}{dt^2} + \frac{dv}{dt} + G(v)v = \oint (\tau - \sigma)f, \quad v(0) = v_0, \quad \frac{dv}{dt}(0) = w_0.$$

Therefore, we get (v, τ, σ) verifying the system (2.2.5) with τ_a, τ_0, σ_0 replacing T_a, T_0, S_0 respectively and $\oint f = \oint \tau_0 = \oint \tau_a = \oint \sigma_0 = 0$ and $\oint T(t) = \oint S(t) = 0$ for all $t \geq 0$. Hereafter it is considered that all the functions of the system (5.1.1) to have zero average.

Also, if $\nu, c > 0$ the operators $\nu A = -\nu \frac{\partial^2}{\partial x^2}$ and $cA = -c \frac{\partial^2}{\partial x^2}$, together with periodic boundary conditions, are unbounded, self-adjoint operators with compact resolvent in $L^2_{per}(0, 1)$, that are positive when restricted to the space of zero average functions in

$\dot{L}_{per}^2(0, 1)$. Hence, the equation for the temperature T and the equation for the solute concentration S in (5.1.1) are of parabolic type for $\nu, c > 0$.

Write the system (5.1.1) as the following evolution system for acceleration, velocity, temperature and solute concentration:

$$\left\{ \begin{array}{ll} \frac{dw}{dt} + \frac{1}{\varepsilon}w & = -\frac{1}{\varepsilon}G(v)v + \frac{1}{\varepsilon} \oint (T - S)f, & w(0) = w_0 \\ \frac{dv}{dt} & = w, & v(0) = v_0 \\ \frac{\partial T}{\partial t} + v \frac{\partial T}{\partial x} - \nu \frac{\partial^2 T}{\partial x^2} & = l(v)(T_a - T), & T(0, x) = T_0(x) \\ \frac{\partial S}{\partial t} + v \frac{\partial S}{\partial x} & = c \frac{\partial^2 S}{\partial x^2} - b \frac{\partial^2 T}{\partial x^2}, & S(0, x) = S_0(x). \end{array} \right. \quad (5.2.2)$$

That is:

$$\frac{d}{dt} \begin{pmatrix} w \\ v \\ T \\ S \end{pmatrix} + \begin{pmatrix} \frac{1}{\varepsilon} & 0 & 0 & 0 \\ 0 & 0 & 0 & 0 \\ 0 & 0 & -\nu \frac{\partial^2}{\partial x^2} & 0 \\ 0 & 0 & 0 & -c \frac{\partial^2}{\partial x^2} \end{pmatrix} \begin{pmatrix} w \\ v \\ T \\ S \end{pmatrix} = \begin{pmatrix} F_1(w, v, T, S) \\ F_2(w, v, T, S) \\ F_3(w, v, T, S) \\ F_4(w, v, T, S) \end{pmatrix} \quad (5.2.3)$$

with $F_1(w, v, T, S) = -\frac{1}{\varepsilon}G(v)v + \frac{1}{\varepsilon} \oint (T - S)f$, $F_2(w, v, T, S) = w$, $F_3(w, v, T, S) = -v \frac{\partial T}{\partial x} +$

$l(v)(T_a - T)$ and $F_4(w, v, T, S) = -v \frac{\partial S}{\partial x} - b \frac{\partial^2 T}{\partial x^2}$ and initial data $\begin{pmatrix} w \\ v \\ T \\ S \end{pmatrix} (0) = \begin{pmatrix} w_0 \\ v_0 \\ T_0 \\ S_0 \end{pmatrix}$.

The operator $B = \begin{pmatrix} \frac{1}{\varepsilon} & 0 & 0 & 0 \\ 0 & 0 & 0 & 0 \\ 0 & 0 & -\nu \frac{\partial^2}{\partial x^2} & 0 \\ 0 & 0 & 0 & -c \frac{\partial^2}{\partial x^2} \end{pmatrix}$ is a sectorial operator in $\mathcal{Y} = \mathbb{R}^2 \times \dot{H}_{per}^1(0,1) \times \dot{L}_{per}^2(0,1)$ with domain $D(B) = \mathbb{R}^2 \times \dot{H}_{per}^3(0,1) \times \dot{H}_{per}^3(0,1)$ and has compact resolvent, where

$$\dot{L}_{per}^2(0,1) = \{u \in L_{loc}^2(\mathbb{R}), u(x+1) = u(x)a.e., \oint u = 0\}, \dot{H}_{per}^m(0,1) = H_{loc}^m(\mathbb{R}) \cap \dot{L}_{per}^2(0,1). \quad (5.2.4)$$

Using the result and techniques about sectorial operator of [27] to prove the existence of solutions of the system, we have the Theorem 5.2.1.

Theorem 5.2.1 *Assume that $H(r) = rG(r)$ and $l(r)$ are locally Lipschitz, $f \in \dot{L}_{per}^2(0,1)$, $T_a \in \dot{H}_{per}^1(0,1)$, $G(v) \geq G_0 > 0$ and $l(v) \geq l_0 > 0$. Then, $(w_0, v_0, T_0, S_0) \in \mathcal{Y} = \mathbb{R}^2 \times \dot{H}_{per}^1(0,1) \times \dot{L}_{per}^2(0,1)$, then there exists a unique solution of (2.2.6) satisfying*

$$(w, v, T, S) \in C([0, \infty), \mathcal{Y}) \cap C(0, \infty, \mathbb{R}^2 \times \dot{H}_{per}^3(0,1) \times \dot{H}_{per}^2(0,1)),$$

$$\left(\frac{dw}{dt}, \frac{dv}{dt}, \frac{\partial T}{\partial t}, \frac{\partial S}{\partial t} \right) \in C(0, \infty, \mathbb{R}^2 \times \dot{H}_{per}^{3-\delta}(0,1) \times \dot{H}_{per}^{2-\delta}(0,1)),$$

for every $\delta > 0$. In particular, (5.2.2) defines a nonlinear semigroup, $S^*(t)$ in $\mathcal{Y} = \mathbb{R}^2 \times \dot{H}_{per}^1(0,1) \times \dot{L}_{per}^2(0,1)$, with $S^*(t)(w_0, v_0, T_0, S_0) = (w(t), v(t), T(t, x), S(t, x))$.

PROOF. Step (i) The first step is to prove the local existence and regularity. This follows easily from the variation of constants formula of [27]. In order to prove this, write the

system as (5.2.3), and we have:

$$U_t + BU = F(U), \text{ with } U = \begin{pmatrix} w \\ v \\ T \\ S \end{pmatrix}, B = \begin{pmatrix} \frac{1}{\varepsilon} & 0 & 0 & 0 \\ 0 & 0 & 0 & 0 \\ 0 & 0 & -\nu \frac{\partial^2}{\partial x^2} & 0 \\ 0 & 0 & 0 & -c \frac{\partial^2}{\partial x^2} \end{pmatrix}, F = \begin{pmatrix} F_1 \\ F_2 \\ F_3 \\ F_4 \end{pmatrix}$$

where the operator B is a sectorial operator in $\mathcal{Y} = \mathbb{R}^2 \times \dot{H}_{per}^1(0,1) \times \dot{L}_{per}^2(0,1)$ with domain $D(B) = \mathbb{R}^2 \times \dot{H}_{per}^3(0,1) \times \dot{H}_{per}^2(0,1)$ and has compact resolvent. In this context, the operator $A = -\frac{\partial^2}{\partial x^2}$ must be understood in the variational sense, i.e., for every $T, \varphi \in \dot{H}_{per}^1(0,1)$,

$$\langle A(T), \varphi \rangle = \oint \frac{\partial T}{\partial x} \frac{\partial \varphi}{\partial x}$$

and $\dot{L}_{per}^2(0,1)$ coincides with the fractional space of exponent $\frac{1}{2}$ as in [27]. We denote $\dot{H}_{per}^{-1}(0,1)$ as the dual space and $\|\cdot\|$ the norm on the space $\dot{L}_{per}^2(0,1)$. If we prove that the nonlinearity $F : \mathcal{Y} = \mathbb{R}^2 \times \dot{H}_{per}^1(0,1) \times \dot{L}_{per}^2(0,1) \mapsto \mathcal{Y}^{-\frac{1}{2}} = \mathbb{R}^2 \times \dot{L}_{per}^2(0,1) \times \dot{H}_{per}^{-1}(0,1)$ is well defined, Lipschitz and bounded on bounded sets, we obtain the local existence for the initial data in $\mathcal{Y} = \mathbb{R}^2 \times \dot{H}_{per}^1(0,1) \times \dot{L}_{per}^2(0,1)$.

Using $H(v) = G(v)v$ and $l(v)$ are locally Lipschitz together with $f \in \dot{L}_{per}^2(0,1)$ and $T_a \in \dot{H}_{per}^1(0,1)$, we will prove the nonlinear terms, $F_1(w, v, T, S) = -\frac{1}{\varepsilon}G(v)v + \frac{1}{\varepsilon} \oint (T-S)f$, $F_2(w, v, T, S) = w$, $F_3(w, v, T, S) = -v \frac{\partial T}{\partial x} + l(v)(T_a - T)$ and $F_4(w, v, T, S) = -v \frac{\partial S}{\partial x} - b \frac{\partial^2 T}{\partial x^2}$ satisfy $F_1 : \mathbb{R}^2 \times \dot{L}_{per}^2(0,1) \times \dot{L}_{per}^2(0,1) \mapsto \mathbb{R}$, $F_2 : \mathbb{R}^2 \times \dot{H}_{per}^1(0,1) \times \dot{L}_{per}^2(0,1) \mapsto \mathbb{R}$, $F_3 : \mathbb{R}^2 \times \dot{H}_{per}^1(0,1) \times \dot{L}_{per}^2(0,1) \mapsto \dot{L}_{per}^2(0,1)$ and $F_4 : \mathbb{R}^2 \times \dot{H}_{per}^1(0,1) \times \dot{L}_{per}^2(0,1) \mapsto \dot{H}_{per}^{-1}(0,1)$, that is $F : \mathcal{Y} \mapsto \mathcal{Y}^{-\frac{1}{2}}$ is well defined, Lipschitz and bounded on bounded sets.

Using the techniques of variation of constants formula of [27], we obtain the unique local solution $(w, v, T, S) \in C([0, \tau], \mathcal{Y})$ of (5.2.2), which are given by

$$w(t) = w_0 e^{-\frac{1}{\varepsilon}t} - \frac{1}{\varepsilon} \int_0^t e^{-\frac{1}{\varepsilon}(t-r)} H(r) dr + \frac{1}{\varepsilon} \int_0^t e^{-\frac{1}{\varepsilon}(t-r)} \oint (T - S) f(r) dr \quad (5.2.5)$$

with $H(r) = G(v(r))v(r)$.

$$v(t) = v_0 + \int_0^t w(r) dr \quad (5.2.6)$$

$$T(t, x) = e^{-\nu A t} T_0(x) + \int_0^t e^{-\nu A(t-r)} l(v(r)) [T_a(r, x) - T(r, x)] dr - \int_0^t e^{-\nu A(t-r)} v(r) \frac{\partial T(r, x)}{\partial x} dr, \quad (5.2.7)$$

$$S(t, x) = e^{-c A t} S_0(x) + \int_0^t e^{-c A(t-r)} [-v(r) \frac{\partial S}{\partial x}(r) - b \frac{\partial^2 T}{\partial x^2}(r)] dr. \quad (5.2.8)$$

where $(w, v, T, S) \in C([0, \tau], \mathcal{Y} = \mathbb{R}^2 \times \dot{H}_{per}^1(0, 1) \times \dot{L}_{per}^2(0, 1))$ and using again the results of [27], (smoothing effect of the equations together with bootstrapping method), we get the regularity of solutions.

Step (ii) To prove the global existence, we must show that the solutions are bounded in $\mathcal{Y} = \mathbb{R}^2 \times \dot{H}_{per}^1(0, 1) \times \dot{L}_{per}^2(0, 1)$ for finite time intervals and using the nonlinearity of F , maps bounded on bounded sets, we conclude.

To obtain the norm of T is bounded in finite time, we multiply the equation for the temperature by T in $\dot{L}_{per}^2(0, 1)$. Then integrating by parts, we have:

$$\frac{1}{2} \frac{d}{dt} \|T\|^2 + \nu \left\| \frac{\partial T}{\partial x} \right\|^2 = \oint l(v) (T_a - T) T dx$$

since $\oint T \frac{\partial T}{\partial x} = \frac{1}{2} \oint \frac{\partial}{\partial x}(T^2) = 0$.

Using Cauchy-Schwarz and Young inequality and then Poincaré inequality for functions of zero average, since $\oint T = 0$, together with π^2 is the first nonzero eigenvalue of $A = -\frac{\partial^2}{\partial x^2}$ in $\dot{L}_{per}^2(0, 1)$, we obtain

$$\frac{1}{2} \frac{d}{dt} \|T\|^2 + (\nu\pi^2 + l(v)) \|T\|^2 \leq \frac{l(v)}{2} \|T_a\|^2 + \frac{l(v)}{2} \|T\|^2,$$

and using $l(v) \geq l_0 > 0$ we get

$$\frac{d}{dt} \|T\|^2 + (2\nu\pi^2 + l_0) \|T\|^2 \leq l(v) \|T_a\|^2. \quad (5.2.9)$$

and we conclude that the norm of T in $\dot{L}_{per}^2(0, 1)$ remains bounded in finite time.

By differentiating the third equation of (5.2.2) with respect to x , we obtain the same equation for $\|\frac{\partial T}{\partial x}\|$ considering $\|\frac{\partial T_a}{\partial x}\|$, so we obtain

$$\frac{d}{dt} \left\| \frac{\partial T}{\partial x} \right\|^2 + (2\nu\pi^2 + l_0) \left\| \frac{\partial T}{\partial x} \right\|^2 \leq l(v) \left\| \frac{\partial T_a}{\partial x} \right\|^2 \quad (5.2.10)$$

Thus we show that the norm of T in $\dot{H}_{per}^1(0, 1)$ remains bounded in finite time.

Then, we show that the norm of S in $\dot{L}_{per}^2(0, 1)$ does not blow-up in finite time.

Multiplying the fourth equation of (5.2.2) by S , integrating by parts, applying the Young inequality and again taking into account that $\oint S \frac{\partial S}{\partial x} = \frac{1}{2} \oint \frac{\partial S^2}{\partial x} = 0$, since S is periodic, we get

$$\frac{1}{2} \frac{d}{dt} \|S\|^2 + (c - \epsilon) \left\| \frac{\partial S}{\partial x} \right\|^2 \leq b^2 C_\epsilon \left\| \frac{\partial T}{\partial x} \right\|^2 \quad (5.2.11)$$

for every $\epsilon > 0$ with $C_\epsilon = \frac{1}{4\epsilon}$. Thus, taking $\epsilon = \frac{c}{2}$, and taking into account (5.2.10) together

with the Poincaré inequality for functions with zero average, we obtain

$$\frac{d}{dt}\|S\|^2 + c\pi^2\|S\|^2 \leq \frac{b^2}{c}\left\|\frac{\partial T}{\partial x}\right\|^2 \leq k_1 \quad (5.2.12)$$

with $k_1 > 0$. Therefore $\|S(t)\|$ remains bounded in finite time. Since $\|T\|$ and $\|S\|$ are bounded in finite time, imply that $|w(t)|, |v(t)|$ remain also bounded in finite time. Hence we have a global solution in the nonlinear semigroup in $\mathcal{Y} = \mathbb{R}^2 \times \dot{H}_{per}^1(0, 1) \times \dot{L}_{per}^2(0, 1)$. \square

5.2.2 Boundedness of the solutions and global attractor

In this section, we use the results and techniques of [34, 36, 53] for a fluid with one component, to prove the existence of the global attractor for a binary fluid for the semigroup defined in the space $\mathcal{Y} = \mathbb{R}^2 \times \dot{H}_{per}^1(0, 1) \times \dot{L}_{per}^2(0, 1)$.

To obtain the asymptotic bounds on the solutions as $t \rightarrow \infty$, we consider the friction function G as in [34, 36, 53] satisfying the hypotheses of the previous section and there exists a constant $h_0 \geq 0$ such that:

$$\limsup_{t \rightarrow \infty} \frac{|G'(t)|}{G(t)} = 0 \text{ and } \limsup_{t \rightarrow \infty} \frac{|tG'(t)|}{G(t)} \leq h_0. \quad (5.2.13)$$

Using the l'Hopital's lemma proved in [52] we have the following lemma proved in [63].

Lemma 5.2.2 *If we assume $G(r)$ and $H(r) = rG(r)$ satisfy the hypothesis of Theorem 5.2.1, together with (5.2.13), then:*

$$\limsup_{t \rightarrow \infty} \frac{\left| H(t) - \frac{1}{\varepsilon} \int_0^t e^{-\frac{1}{\varepsilon}(t-r)} H(r) dr \right|}{G(t)} \leq H_0 \quad (5.2.14)$$

with $H_0 = (1 + h_0)\varepsilon$ a positive constant such that $H_0 \rightarrow 0$ if $\varepsilon \rightarrow 0$.

Remark 5.2.1 *Note that the conditions (5.2.13) are satisfied for all the friction functions G considered in the previous works, i.e., the thermosyphon models where G is constant or linear or quadratic law. Moreover, the conditions (5.2.13) are true for $G(s) \approx A|s|^n$, as $s \rightarrow \infty$.*

Theorem 5.2.3 *Under the above notations and hypothesis of Theorem 5.2.1, assume that G satisfies (5.2.14) for some constant $H_0 \geq 0$ then*

Part (i)

$$(i) \limsup_{t \rightarrow \infty} |v(t)| \leq \frac{1}{G_0} \limsup_{t \rightarrow \infty} \left| \oint (T - S)f \right| + H_0 \quad (5.2.15)$$

In particular: If $\limsup_{t \rightarrow \infty} \|(T - S)\| \in \mathbb{R}$ then

$$\limsup_{t \rightarrow \infty} |v(t)| \leq \frac{1}{G_0} \|f\| \limsup_{t \rightarrow \infty} \|(T - S)\| + H_0 \in \mathbb{R}. \quad (5.2.16)$$

(ii) If $\limsup_{t \rightarrow \infty} \|(T - S)\| \in \mathbb{R}$ and $G_0^ = \limsup_{t \rightarrow \infty} G(v(t))$ with $w(t) = \frac{dw}{dt}$, then*

$$\limsup_{t \rightarrow \infty} |w(t)| \leq G_0^* H_0 + \left(1 + \frac{G_0^*}{G_0}\right) I \quad \text{with } I = \limsup_{t \rightarrow \infty} \left| \oint (T - S)(t, \cdot) f(\cdot) \right| \quad \text{and} \quad (5.2.17)$$

$$\limsup_{t \rightarrow \infty} |w(t)| \leq G_0^* H_0 + \left(1 + \frac{G_0^*}{G_0}\right) \|f\| \limsup_{t \rightarrow \infty} \|(T - S)\| \in \mathbb{R}. \quad (5.2.18)$$

Part (ii) *If $\nu \neq 0$ and there exists L_0 a positive constant such that $L_0 \geq l(v) \geq l_0$, then for any solution of (5.1.1) in the space $\mathcal{Y} = \mathbb{R}^2 \times \dot{H}_{per}^1(0, 1) \times \dot{L}_{per}^2(0, 1)$ we have:*

(i)

$$\limsup_{t \rightarrow \infty} \|T(t)\| \leq \left(\frac{L_0}{2\nu\pi^2 + l_0}\right)^{\frac{1}{2}} \|T_a\| \quad \text{and} \quad \limsup_{t \rightarrow \infty} \left\| \frac{\partial T}{\partial x} \right\| \leq \left(\frac{L_0}{2\nu\pi^2 + l_0}\right)^{\frac{1}{2}} \left\| \frac{\partial T_a}{\partial x} \right\| \quad (5.2.19)$$

(ii)

$$\limsup_{t \rightarrow \infty} \|S(t)\| \leq \frac{1}{\pi} \left(\frac{B_l}{c}\right)^{\frac{1}{2}} \left\| \frac{\partial T_a}{\partial x} \right\| \quad \text{where } B_l = \frac{b^2}{c} \left(\frac{L_0}{2\nu\pi^2 + l_0}\right) > 0. \quad (5.2.20)$$

(iii)

$$\limsup_{t \rightarrow \infty} |v(t)| \leq \frac{\|f\|}{G_0} \left[\left(\frac{L_0}{2\nu\pi^2 + l_0}\right)^{\frac{1}{2}} \|T_a\| + \frac{1}{\pi} \left(\frac{B_l}{c}\right)^{\frac{1}{2}} \left\| \frac{\partial T_a}{\partial x} \right\| \right] + H_0 \quad (5.2.21)$$

(iv)

$$\limsup_{t \rightarrow \infty} |w(t)| \leq G_0^* H_0 + \left(1 + \frac{G_0^*}{G_0}\right) \|f\| \left[\left(\frac{L_0}{2\nu\pi^2 + l_0}\right)^{\frac{1}{2}} \|T_a\| + \frac{1}{\pi} \left(\frac{B_l}{c}\right)^{\frac{1}{2}} \left\| \frac{\partial T_a}{\partial x} \right\| \right]. \quad (5.2.22)$$

In particular, we have a global compact and connected attractor \mathcal{A} in $\mathcal{Y} = \mathbb{R}^2 \times \dot{H}_{per}^1(0, 1) \times \dot{L}_{per}^2(0, 1)$.

PROOF. **Part (i)** (i) From (5.2.2) we have

$$\frac{dw}{dt} + \frac{1}{\varepsilon}w = -\frac{1}{\varepsilon}G(v)v + \frac{1}{\varepsilon} \oint (T - S)f \quad (5.2.23)$$

and $w(t) = \frac{dv}{dt}$ satisfies

$$\frac{dv}{ds} = w(0)e^{-\frac{1}{\varepsilon}s} - \frac{1}{\varepsilon} \int_0^s e^{-\frac{1}{\varepsilon}(s-r)} H(r)dr + \frac{1}{\varepsilon} \int_0^s \left[\oint (T - S)(r) \cdot f \right] e^{-\frac{1}{\varepsilon}(s-r)} dr \quad (5.2.24)$$

where $H(r) = H(v(r)) = v(r)G(v(r))$. We rewrite (5.2.24) as

$$\frac{dv}{ds} + G(s)v = w(0)e^{-\frac{1}{\varepsilon}s} + I_1(s) + I_2(s), \quad (5.2.25)$$

with

$$I_1(s) = \frac{1}{\varepsilon} \int_0^s \left[\oint (T - S)(r) \cdot f \right] e^{-\frac{1}{\varepsilon}(s-r)} dr \text{ and } I_2(s) = H(s) - \frac{1}{\varepsilon} \int_0^s e^{-\frac{1}{\varepsilon}(s-r)} H(r)dr. \quad (5.2.26)$$

For any $\delta > 0$ there exists $t_0 > 0$ such that $\delta(s) = w(0)e^{-\frac{1}{\varepsilon}s} < \delta$ for any $s \geq t_0$ and integrating (5.2.25) with $t \geq t_0$ we obtain

$$|v(t)| \leq |v(t_0)|e^{-\int_{t_0}^t G(s)ds} + e^{-\int_{t_0}^t G(s)ds} \int_{t_0}^t e^{\int_{t_0}^s G(r)dr} (\delta + |I_1(s)| + |I_2(s)|) ds \quad (5.2.27)$$

Using L'Hopital's lemma proved in [52], we get

$$\begin{aligned} & \limsup_{t \rightarrow \infty} e^{-\int_{t_0}^t G(s)ds} \int_{t_0}^t e^{\int_{t_0}^s G(r)dr} (|I_1(s)| + |I_2(s)| + \delta) ds = \\ & = \limsup_{t \rightarrow \infty} \frac{\int_{t_0}^t e^{\int_{t_0}^s G(r)dr} (|I_1(s)| + |I_2(s)| + \delta) ds}{e^{\int_{t_0}^t G(s)ds}} \leq \\ & \leq \limsup_{t \rightarrow \infty} \frac{|I_1(t)| + |I_2(t)| + \delta}{G(t)} \text{ for any } \delta > 0. \end{aligned}$$

Using again the L'Hopital's lemma proved in [52], we get

$$\limsup_{t \rightarrow \infty} |I_1(t)| \leq \limsup_{t \rightarrow \infty} \frac{\int_0^t e^{\frac{r}{\varepsilon}} |\mathcal{F}(T-S)(t) \cdot f|}{\varepsilon e^{\frac{t}{\varepsilon}}} \leq \limsup_{t \rightarrow \infty} |\mathcal{F}(T-S)(t) \cdot f|$$

and from (5.2.27) together with (5.2.14) we conclude for any δ ,

$$\limsup_{t \rightarrow \infty} |v(t)| \leq \limsup_{t \rightarrow \infty} \frac{\limsup_{t \rightarrow \infty} |\mathcal{F}(T-S)(t) \cdot f|}{G_0} + H_0 + \delta.$$

(ii) From (5.2.23) together with singular Gronwall lemma, we get

$$|w(t)| \leq |w(t_0)|e^{-\frac{1}{\varepsilon}t} + \frac{1}{\varepsilon} \int_{t_0}^t e^{-\frac{1}{\varepsilon}(t-r)} \left[G(r)|v(r)| + |\mathcal{F}(T-S)(r) \cdot f| \right] dr \quad (5.2.28)$$

where $G(r) = G(v(r))$. Consequently, for any $\delta > 0$ there exists t_0 such that for any $t \geq t_0$

$$\begin{aligned} & \frac{1}{\varepsilon} \int_{t_0}^t e^{-\frac{1}{\varepsilon}(t-r)} \left[G(v(r))|v(r)| + |\mathcal{F}(T-S)(r) \cdot f| \right] dr \leq \\ & \leq \delta + \limsup_{t \rightarrow \infty} \left[G(v(t))|v(t)| + |\mathcal{F}(T-S)(t) \cdot f| \right] (1 - e^{-\frac{1}{\varepsilon}(t-t_0)}) \end{aligned} \quad (5.2.29)$$

this is

$$\limsup_{t \rightarrow \infty} |w(t)| \leq \limsup_{t \rightarrow \infty} \left[G(v(t))|v(t)| + |\mathcal{F}(T-S)(t) \cdot f| + \delta \right], \quad (5.2.30)$$

for any $\delta > 0$, and using the result (i) we get (5.2.18).

Part (ii) (i) From (5.2.9) together with (5.2.10) we get

$$\|T\|^2 \leq \frac{L_0}{2\nu\pi^2 + l_0} \|T_a\|^2 + \left(\|T_0\|^2 - \frac{L_0}{2\nu\pi^2 + l_0} \|T_a\|^2 \right)_+ e^{-(2\pi^2\nu + l_0)t} \text{ and} \quad (5.2.31)$$

$$\left\| \frac{\partial T}{\partial x} \right\|^2 \leq \frac{L_0}{2\nu\pi^2 + l_0} \left\| \frac{\partial T_a}{\partial x} \right\|^2 + \left(\|T_0\|^2 - \frac{L_0}{2\nu\pi^2 + l_0} \|T_a\|^2 \right)_+ e^{-(2\pi^2\nu + l_0)t} \quad (5.2.32)$$

then we obtain (5.2.19).

(ii) From (5.2.12) together with (5.2.32) we get

$$\frac{d}{dt}\|S\|^2 + c\pi^2\|S\|^2 \leq \frac{b^2}{c} \left(\frac{L_0}{2\nu\pi^2 + l_0} \right) \left\| \frac{\partial T_a}{\partial x} \right\|^2 + N e^{-(2\pi^2\nu + l_0)t} \quad (5.2.33)$$

where $N = \left(\|T_0\|^2 - \frac{L_0}{2\nu\pi^2 + l_0} \|T_a\|^2 \right)_+$. Given $\delta > 0$, there exists $t_0 > 0$ such that

$$\frac{d}{dt}\|S\|^2 + c\pi^2\|S\|^2 \leq \frac{b^2}{c} \left(\frac{L_0}{2\nu\pi^2 + l_0} \right) \left\| \frac{\partial T_a}{\partial x} \right\|^2 + \delta, \forall t \geq t_0 \quad (5.2.34)$$

and from the Gronwall lemma, for every $\delta > 0$, we get

$$\limsup_{t \rightarrow \infty} \|S\|^2 \leq \frac{B_l}{c\pi^2} \left\| \frac{\partial T_a}{\partial x} \right\|^2 + \delta, \forall \delta > 0, \text{ where } B_l = \frac{b^2}{c} \left(\frac{L_0}{2\nu\pi^2 + l_0} \right) > 0 \quad (5.2.35)$$

and thus we obtain (5.2.20). Using Part I, the rest (iii) and (iv) are obvious. Finally,

since the sectorial operator B , as defined in Theorem 5.2.1, has compact resolvent, the

rest follows from [24] [Theorem 4.2.2 and 3.4.8]. \square

Remark 5.2.2 *First, we note that the hypothesis about the function $l(v)$ in the above Theorem 5.2.3, $l(v) \leq L_0$ is satisfied when we consider the Newton's linear cooling law $l(v) = k(T_a - T)$, where k is a positive quantity i.e., $l(v) = k = L_0$ as [33]. Moreover, this condition is also satisfied if we consider $l = l(v)(T_a - T)$ where $l(v)$ is a positive upper bounded function.*

Second, it is important to note that we prove in the next section the existence of the global compact and connected attractor and the inertial manifold for the system (5.1.1), when we consider the general Newton's linear cooling law, without the additional above hypothesis; and for every $\nu \geq 0$.

In order to get this, we consider the Fourier expansions and observe the dynamics of each coefficient of Fourier expansions to improve, in some sense, the asymptotic bounded of temperature. In particular we will prove $\limsup_{t \rightarrow \infty} \|T(t)\| \leq \|T_a\|$ and $\|S(t)\| \leq \frac{b}{c} \|T_a\|$ for every locally Lipschitz and positive function $l(v)$ and for every $\nu \geq 0$.

5.3 Asymptotic behavior: finite-dimensional systems

In this section, the asymptotic behavior of the system (5.2.2) is deduced to study the other finite dimensional systems in some cases. Take a close look at the dynamics of (5.2.2)

by considering the Fourier expansions of all the functions of the system (temperature and solute concentration). First, consider the Fourier expansion for the function associated to the geometry of the loop f , and the ambient temperature T_a , whose coefficients are very important to study the asymptotic behavior of the system. Then, prove the asymptotic behavior of the system (5.2.2), described by suitable Fourier coefficients associated to f and T_a .

Note the Fourier expansion for all $g \in \dot{H}_{per}^m(0, 1)$, $m \geq 0$ is given by the expression $g(x) = \sum_{k \in \mathcal{Z}^*} a_k e^{2\pi k i x}$ with $\mathcal{Z}^* = \mathcal{Z} \setminus \{0\}$ and we have

$$\|g\|_{\dot{H}_{per}^m(0,1)} = (2\pi)^m \left(\sum_{k \in \mathcal{Z}^*} k^{2m} |a_k|^2 \right)^{\frac{1}{2}}. \quad (5.3.36)$$

Assume that $T_a, T \in \dot{H}_{per}^1(0, 1)$ and $f, S \in \dot{L}_{per}^2(0, 1)$ are given by the following Fourier series expansions:

$$T_a(x) = \sum_{k \in \mathcal{Z}^*} b_k e^{2\pi k i x} \text{ and } f(x) = \sum_{k \in \mathcal{Z}^*} c_k e^{2\pi k i x} \text{ with } \mathcal{Z}^* = \mathcal{Z} \setminus \{0\} \quad (5.3.37)$$

$$T(t, x) = \sum_{k \in \mathcal{Z}^*} a_k(t) e^{2\pi k i x} \text{ and } S(t, x) = \sum_{k \in \mathcal{Z}^*} d_k(t) e^{2\pi k i x} \quad (5.3.38)$$

with the initial data $T_0 \in \dot{H}_{per}^1(0, 1)$ is given by $T_0(x) = \sum_{k \in \mathcal{Z}^*} a_{k0} e^{2\pi k i x}$ and $S_0 \in \dot{L}_{per}^2(0, 1)$ is given by $S_0(x) = \sum_{k \in \mathcal{Z}^*} d_{k0} e^{2\pi k i x}$.

Proposition 5.3.1 *Under the above notations and hypothesis of Theorem 5.2.1, consider $T_a \in \dot{H}_{per}^1(0, 1)$ and $f \in \dot{L}_{per}^2(0, 1)$ given by (5.3.37) and the initial data $T_0 \in \dot{H}_{per}^1(0, 1)$ given by $T_0(x) = \sum_{k \in \mathcal{Z}^*} a_{k0} e^{2\pi k i x}$ and $S_0 \in \dot{L}_{per}^2(0, 1)$ given by $S_0(x) = \sum_{k \in \mathcal{Z}^*} d_{k0} e^{2\pi k i x}$. Let (w, v, T, S) be the solution of the system (5.1.1) given by Theorem 5.2.1; then we have:*

(i) *The coefficients $a_k(t)$ and $d_k(t)$ in (5.3.38), verify the equations*

$$\begin{cases} \dot{a}_k(t) + \left(2k\pi v i + 4\nu k^2 \pi^2 + l(v) \right) a_k(t) = l(v) b_k(t), & a_k(0) = a_{k0}, \quad k \in \mathcal{Z}^* \\ \dot{d}_k(t) + \left(2k\pi v i + 4c k^2 \pi^2 \right) d_k(t) = 4b\pi^2 k^2 a_k(t), & d_k(0) = d_{k0}, \quad k \in \mathcal{Z}^*. \end{cases} \quad (5.3.39)$$

(ii) The equation for the velocity is

$$\varepsilon \frac{d^2 v}{dt} + \frac{dv}{dt} + G(v)v = \sum_{k \in \mathcal{Z}^*} a_k(t) \bar{c}_k - \sum_{k \in \mathcal{Z}^*} d_k(t) \bar{c}_k.$$

PROOF. It is sufficient to note that

$$\oint (T - S)f = \sum_{k \in \mathcal{Z}^*} a_k(t) \bar{c}_k - \sum_{k \in \mathcal{Z}^*} d_k(t) \bar{c}_k. \quad (5.3.40)$$

Since all the functions involved are real and periodic, we have for all $k \in \mathcal{Z}^* = \mathcal{Z} \setminus \{0\}$,

$\bar{a}_k = a_{-k}$, $\bar{b}_k = b_{-k}$, $\bar{c}_k = c_{-k}$ and $\bar{d}_k = d_{-k}$. Therefore, the equation for the velocity in

(5.1.1) is:

$$\varepsilon \frac{d^2 v}{dt} + \frac{dv}{dt} + G(v)v = \sum_{k \in \mathcal{Z}^*} a_k(t) c_{-k} - \sum_{k \in \mathcal{Z}^*} d_k(t) c_{-k}, \quad v(0) = v_0, \quad \frac{dv}{dt}(0) = w_0.$$

□

Remark 5.3.1 Note that the system (5.1.1) is equivalent to the system (5.2.2) for acceleration, velocity, temperature and solute concentration and from the above proposition, it is equivalent to the following infinite system of ODEs (5.3.41)

$$\begin{cases} \frac{dw}{dt} + \frac{1}{\varepsilon} w = -\frac{1}{\varepsilon} G(v)v + \frac{1}{\varepsilon} \sum_{k \in \mathcal{Z}^*} a_k(t) c_{-k} - \frac{1}{\varepsilon} \sum_{k \in \mathcal{Z}^*} d_k(t) c_{-k}, & w(0) = w_0 \\ \frac{dv}{dt} = w, & v(0) = v_0 \\ \dot{a}_k(t) + \left(2k\pi v i + 4\nu k^2 \pi^2 + l(v) \right) a_k(t) = l(v) b_k, & a_k(0) = a_{k0}, \quad k \in \mathcal{Z}^* \\ \dot{d}_k(t) + \left(2k\pi v i + 4c k^2 \pi^2 \right) d_k(t) = 4b k^2 \pi^2 a_k(t), & d_k(0) = d_{k0}, \quad k \in \mathcal{Z}^*. \end{cases} \quad (5.3.41)$$

The system of equations (5.3.41) reflects two of the main features: (i) the coupling between the modes enter through the velocity, while the diffusion acts as a linear damping term, (ii) it is important to note that the non linear term, given by the Newton's cooling law in the temperature influences the solute concentration of this model.

In what follows, we will exploit this explicit equation for the temperature and solute concentration modes to analyze the asymptotic behavior of the system and to obtain the

explicit low-dimensional models. A similar explicit construction was given by Bloch and Titi in [6] for a nonlinear beam equation where the nonlinearity occurs only through the appearance of the L^2 norm of the unknown. A related construction was given by Stuart in [54] for a nonlocal reaction-diffusion equation.

In the following section, we obtain the boundedness of these coefficients which improve, in some sense, the boundedness of temperature and solute concentration, in order to prove the existence of the inertial manifold for the system (5.2.2).

5.3.1 Inertial manifold

Consider the general case $\nu > 0$ together with the nonlinear Newton's cooling law introduced by [28, 56], that is $l(v)(T_a - T)$ with $l(v) \geq l_0 > 0$ locally Lipschitz function and use inertial manifold techniques, in the spirit of nondiffusion case of [50], to give an explicit low-dimensional system of ODEs that describes the asymptotic dynamics of (5.2.2). The existence of an inertial manifold does not rely, in this case, on the existence of large gaps in the spectrum of the elliptic operator but on the invariance of certain sets of Fourier modes.

Proposition 5.3.2 *Under the above notations and hypothesis of Theorem 5.2.3, for every solution of the system (5.2.2), (w, v, T, S) , and for every $k \in \mathcal{I}^*$ we have*

(i)

$$\limsup_{t \rightarrow \infty} |a_k(t)| \leq |b_k|, \quad (5.3.42)$$

$$\limsup_{t \rightarrow \infty} |d_k(t)| \leq \frac{b|b_k|}{c}, \quad (5.3.43)$$

$$\limsup_{t \rightarrow \infty} |v(t)| \leq \frac{I_0}{G_0} \left(1 + \frac{b}{c}\right) + H_0, \quad \text{with } I_0 = \sum_{k \in \mathcal{I}^*} |b_k| |c_k| \quad (5.3.44)$$

and G_0 a positive constant such that $G(v) \geq G_0$,

$$\limsup_{t \rightarrow \infty} |w(t)| \leq G_0^* H_0 + \left(1 + \frac{G_0^*}{G_0}\right) \left(1 + \frac{b}{c}\right) I_0, \quad \text{with } G_0^* = \limsup_{t \rightarrow \infty} G(v(t)). \quad (5.3.45)$$

(ii)

$$\limsup_{t \rightarrow \infty} \|T(t)\| \leq \|T_a\| \quad (5.3.46)$$

$$\limsup_{t \rightarrow \infty} \|S(t)\| \leq \frac{b}{c} \|T_a\| \quad (5.3.47)$$

$$\limsup_{t \rightarrow \infty} |v(t)| \leq \frac{\|f\| \|T_a\|}{G_0} \left(1 + \frac{b}{c}\right) + H_0 \quad (5.3.48)$$

$$\limsup_{t \rightarrow \infty} |w(t)| \leq G_0^* H_0 + \left(1 + \frac{G_0^*}{G_0}\right) \left(1 + \frac{b}{c}\right) \|f\| \|T_a\|. \quad (5.3.49)$$

In particular, we have a global compact and connected attractor $\mathcal{A} \subset [-M, M] \times [-N, N] \times \mathcal{C} \times \mathcal{C}$ where M, N are the upper bounds for acceleration and velocity as given in (5.3.49) and (5.3.48) respectively and $T_0, S_0 \in \mathcal{C} = \{R(x) = \sum_{k \in \mathcal{Z}^*} r_k e^{2\pi k i x}, |r_k| \leq d|b_k|\}$, where $d = \max\{1, \frac{b}{c}\}$.

PROOF. (i) From (5.3.39), we have

$$a_k(t) = a_{k0} e^{-4\nu\pi^2 k^2 t} e^{-\int_0^t [2\pi k v i + l(v)]} + b_k \int_0^t e^{-4\nu\pi^2 k^2 (t-s)} l(v(s)) e^{-\int_s^t [2\pi k v i + l(v)]} ds \quad (5.3.50)$$

and taking into account that

$$|e^{-\int_0^t 2\pi k v i}| = |e^{-\int_s^t 2\pi k v i}| = 1, \quad e^{-4\nu\pi^2 k^2 (t-s)} \leq 1, \quad \text{and} \quad \int_0^t l(v(s)) e^{-\int_s^t l(v)} ds = 1 - e^{-\int_0^t l(v)} \quad (5.3.51)$$

we obtain:

$$|a_k(t)| \leq |a_{k0}| e^{-4\nu\pi^2 k^2 t} e^{-\int_0^t l(v)} + |b_k| (1 - e^{-\int_0^t l(v)}) \quad (5.3.52)$$

and we get (5.3.42) i.e., $\limsup_{t \rightarrow \infty} |a_k(t)| \leq |b_k|$.

From (5.3.39), we have

$$d_k(t) = d_{k0} e^{-4c\pi^2 k^2 t} e^{-\int_0^t 2\pi k v i} + 4b\pi^2 k^2 \int_0^t a_k(s) e^{-4c\pi^2 k^2 (t-s)} e^{-\int_s^t 2\pi k v i} ds. \quad (5.3.53)$$

Then substituting (5.3.50) in (5.3.53), we have

$$|d_k(t)| \leq |d_{k0}|e^{-4c\pi^2 k^2 t} + 4b\pi^2 k^2 (|I_1(t)| + |I_2(t)|) \quad (5.3.54)$$

where

$$I_1(t) = \int_0^t a_{k0} e^{-\int_0^s [2\pi k v i + l(v)]} e^{-4c\pi^2 k^2 (t-s)} e^{-\int_s^t 2\pi k v i} e^{-4\nu\pi^2 k^2 s} ds$$

and

$$I_2(t) = b_k \int_0^t \left[e^{-4c\pi^2 k^2 (t-s)} e^{-\int_s^t 2\pi k v i} \left(\int_0^s l(v(r)) e^{-\int_r^s [2\pi k v i + l(v)]} e^{-4\nu\pi^2 k^2 (s-r)} dr \right) \right] ds.$$

Then, using (5.3.51) and $l(v) \geq l_0$ in $I_1(t)$, we get,

$$|I_1(t)| \leq |a_{k0}| e^{-4c\pi^2 k^2 t} \int_0^t e^{(4c\pi^2 k^2 - 4\nu\pi^2 k^2 - l_0)s} ds$$

and since $e^{-l_0 s} \leq 1$, we have

$$|I_1(t)| \leq \frac{|a_{k0}|}{4\pi^2 k^2 |c - \nu|} |e^{-4\pi^2 k^2 \nu t} - e^{-4c\pi^2 k^2 t}|. \quad (5.3.55)$$

Then, working with $I_2(t)$, using again $|e^{-\int_0^t 2\pi k v i}| = |e^{-\int_s^t 2\pi k v i}| = 1$, we have

$$|I_2(t)| \leq |b_k| \int_0^t e^{-4c\pi^2 k^2 (t-s)} \left(\int_0^s l(v(r)) e^{-\int_r^s l(v)} e^{-4\nu\pi^2 k^2 (s-r)} dr \right) ds$$

$$|I_2(t)| \leq |b_k| \int_0^t e^{-4c\pi^2 k^2 (t-s)} \left(\int_0^s l(v(r)) e^{-\int_r^s l(v)} dr \right) ds$$

and using

$$e^{-4\nu\pi^2 k^2 (s-r)} \leq 1, \int_0^s l(v(r)) e^{-\int_r^s l(v)} dr = 1 - e^{-\int_0^s l(v)} \leq 1$$

we get

$$|I_2(t)| \leq \frac{|b_k|}{4c\pi^2 k^2} (1 - e^{-4c\pi^2 k^2 t}). \quad (5.3.56)$$

Then from (5.3.54) together with (5.3.55) and (5.3.56), we have

$$|d_k(t)| \leq |d_{k0}| e^{-4c\pi^2 k^2 t} + \frac{b|a_{k0}|}{|c - \nu|} |e^{-4\pi^2 k^2 \nu t} - e^{-4c\pi^2 k^2 t}| + \frac{b|b_k|}{c} (1 - e^{-4c\pi^2 k^2 t})$$

that is

$$|d_k(t)| \leq \frac{b|b_k|}{c} + (|d_{k0}| - \frac{b|b_k|}{c}) e^{-4c\pi^2 k^2 t} + \frac{b|a_{k0}|}{|c - \nu|} |e^{-4\pi^2 k^2 \nu t} - e^{-4c\pi^2 k^2 t}| \quad (5.3.57)$$

and we get (5.3.43) i.e., $\limsup_{t \rightarrow \infty} |d_k(t)| \leq \frac{b|b_k|}{c}$.

From (5.2.15) in Theorem 5.2.3 together with $\oint(T-S)f = \sum_{k \in \mathcal{Z}^*} a_k(t)c_{-k} - \sum_{k \in \mathcal{Z}^*} d_k(t)c_{-k}$

and using (5.3.42) and (5.3.43), we get

$$\limsup_{t \rightarrow \infty} |\oint(T-S)f| \leq \left(1 + \frac{b}{c}\right) I_0 \text{ where } I_0 = \sum_{k \in \mathcal{Z}^*} |b_k(t)||c_k(t)|. \quad (5.3.58)$$

From this we obtain (5.3.44) i.e.,

$$\limsup_{t \rightarrow \infty} |v(t)| \leq \frac{I_0}{G_0} \left(1 + \frac{b}{c}\right) + H_0$$

and using (5.2.17), we obtain (5.3.45) i.e.,

$$\limsup_{t \rightarrow \infty} |w(t)| \leq G_0^* H_0 + \left(1 + \frac{G_0^*}{G_0}\right) \left(1 + \frac{b}{c}\right) I_0, \text{ with } G_0^* = \limsup_{t \rightarrow \infty} G(v(t)).$$

(ii) Using again Theorem 5.2.3 and taking into account of (5.3.36) together with $I_0 = \sum_{k \in \mathcal{Z}^*} |b_k(t)||c_k(t)| \leq \|T_a\| \|f\|$, we obtain (5.3.46), (5.3.47), (5.3.48) and (5.3.49).

The rest follows from [24] [Theorem 4.2.2 and 3.4.8]. \square

In the following result we will prove that there exists an inertial manifold \mathcal{M} for the semigroup $S^*(t)$ in the phase space $\mathcal{Y} = \mathbb{R}^2 \times \dot{H}_{per}^1(0, 1) \times \dot{L}_{per}^2(0, 1)$, i.e., a submanifold of \mathcal{Y} such that

(i) $S^*(t)\mathcal{M} \subset \mathcal{M}$ for every $t \geq 0$,

(ii) there exists $\delta > 0$ verifying that for every bounded set $B \subset \mathcal{Y}$, there exists $C(B) \geq 0$ such that $dist(S(t), \mathcal{M}) \leq C(B)e^{-\delta t}$, $t \geq 0$ see, for example, [20] and [47].

Assume that $T_a \in \dot{H}_{per}^1(0, 1)$ with

$$T_a = \sum_{k \in K} b_k e^{2\pi k i x}$$

with $b_k \neq 0$ for every $k \in K \subset \mathbb{Z}^*$ with $0 \notin K$, since $\oint T_a = 0$. We denote by V_1 and V_0 the closure of the subspaces of $\dot{H}_{per}^1(0, 1)$ and $\dot{L}_{per}^2(0, 1)$ respectively generated by $\{e^{2\pi k i x}, k \in K\}$.

Theorem 5.3.3 *Assume that $T_a \in \dot{H}_{per}^1(0, 1)$ and $f \in \dot{L}_{per}^2(0, 1)$. Then the set $\mathcal{M} = \mathbb{R}^2 \times V_1 \times V_0$ is an inertial manifold for the flow of $S^*(t)(w_0, v_0, T_0, S_0) = (w(t), v(t), T(t), S(t))$ in the space $\mathcal{Y} = \mathbb{R}^2 \times \dot{H}_{per}^1(0, 1) \times \dot{L}_{per}^2(0, 1)$. Moreover if K is a finite set, the dimension of \mathcal{M} is $2|K| + 2$, where $|K|$ is the number of elements in K .*

PROOF. Step (i) First, we show that \mathcal{M} is invariant. Note that if $k \notin K$, then $b_k = 0$, and therefore if $a_{k0} = 0$, from (5.3.50), we get that $a_k(t) = 0$ for every t , i.e., $T(t, x) = \sum_{k \in K} a_k(t) e^{2\pi k i x}$ and if $d_{k0} = 0$, using $a_k(t) = 0$, from (5.3.53) we get $d_k(t) = 0$ for every t , i.e., $S(t, x) = \sum_{k \in K} d_k(t) e^{2\pi k i x}$. Therefore, if $(w_0, v_0, T_0, S_0) \in \mathcal{M}$, then $(w(t), v(t), T(t), S(t)) \in \mathcal{M}$ for every t , i.e., \mathcal{M} is invariant.

Step (ii) From previous assertions, $\oint (T - S) \cdot f = \sum_{k \in K} a_k(t) \cdot c_{-k} - \sum_{k \in K} d_k(t) \cdot c_{-k}$ and the flow on \mathcal{M} is given by

$$\left\{ \begin{array}{l} \dot{w} + \frac{1}{\varepsilon}w + \frac{1}{\varepsilon}G(v)v = \frac{1}{\varepsilon} \sum_{k \in K} a_k(t) \cdot c_{-k} - \frac{1}{\varepsilon} \sum_{k \in K} d_k(t) \cdot c_{-k} \\ \dot{v} = w \\ \dot{a}_k(t) + \left[2\pi k v i + 4\nu\pi^2 k^2 + l(v) \right] a_k(t) = l(v) b_k, \quad k \in K \\ \dot{d}_k(t) + \left[2\pi k v i + 4c\pi^2 k^2 \right] d_k(t) = 4b\pi^2 k^2 a_k(t), \quad k \in K \\ a_k = d_k = 0, k \notin K \end{array} \right. \quad (5.3.59)$$

Now, we consider the following decomposition in $\dot{H}_{per}^1(0, 1)$, $T = T^1 + T^2$, where T^1 is the projection of T on V_1 and T^2 is the projection of T on the subspace generated by $\{e^{2\pi k i x}, k \in \mathcal{Z}^* \setminus K\}$ i.e., $T^1 = \sum_{k \in K} a_k e^{2\pi k i x}$ and $T^2 = \sum_{k \in \mathcal{Z}^* \setminus K} a_k e^{2\pi k i x} = T - T^1$.

Analogously, we consider the decomposition $S = S^1 + S^2$ in $\dot{L}_{per}^2(0, 1)$ where S^1 is the projection of S on V_0 , i.e., $S^1 = \sum_{k \in K} d_k e^{2\pi k i x}$ and $S^2 = S - S^1$. Then, given $(w_0, v_0, T_0, S_0) \in \mathcal{Y}$ we decompose $T_0 = T_0^1 + T_0^2$, $S_0 = S_0^1 + S_0^2$, and $T(t) = T^1(t) + T^2(t)$, $S(t) = S^1(t) + S^2(t)$ and we consider $(w(t), v(t), T^1(t), S^1(t)) \in \mathcal{M}$ and then

$$(w(t), v(t), T(t), S(t)) - (w(t), v(t), T^1(t), S^1(t)) = (0, 0, T^2(t), S^2(t)).$$

From (5.3.52) taking into account that $b_k = 0$ for $k \in \mathcal{Z}^*$, we have $|a_k(t)| \leq |a_{k0}| e^{-4\nu\pi^2 k^2 t}$ and together with $4\nu\pi^2 k^2 t \geq 4\nu\pi^2 t$ for every $k \in \mathcal{Z}^*$ with (5.3.36), implies that $\|T^2(t)\|_{\dot{H}_{per}^1} \leq \|T_0^2\|_{\dot{H}_{per}^1} e^{-4\nu\pi^2 t}$ i.e., $T^2(t) \rightarrow 0$ in $\dot{H}_{per}^1(0, 1)$ if $t \rightarrow \infty$.

Moreover, we have $S^2(t) = \sum_{k \in \mathcal{Z}^* \setminus K} d_k(t) e^{2\pi k i x}$, therefore

$$\|S^2(t)\|_{\dot{L}_{per}^2(0,1)}^2 = \sum_{k \in \mathcal{Z}^* \setminus K} |d_k(t)|^2.$$

Since $b_k = 0$ for $k \in \mathcal{Z}^* \setminus K$, from (5.3.57) we have

$$|d_k(t)|^2 \leq \left(|d_{k0}| e^{-4c\pi^2 k^2 t} + \frac{b|a_{k0}|}{|c - \nu|} |e^{-4\pi^2 k^2 \nu t} - e^{-4c\pi^2 k^2 t}| \right)^2$$

Then, using $(\alpha + \beta + \gamma)^2 \leq 4(\alpha^2 + \beta^2 + \gamma^2)$, together with $\pi^2 k^2 \delta t \geq \pi^2 \delta t$ for every $k \in \mathcal{Z}^*$ and $\delta = \min\{\nu, c\}$, we get

$$|d_k(t)|^2 \leq 4e^{-8\pi^2 \delta t} \left(|d_{k0}|^2 + 2 \frac{b^2 |a_{k0}|^2}{|c - \nu|^2} \right)$$

From this, we obtain

$$\|S^2(t)\|_{L^2_{per}}^2 \leq 4e^{-8\pi^2 \delta t} \left(\|S_{20}\|_{L^2_{per}}^2 + \frac{2b^2}{|c - \nu|^2} \|T_{20}\|_{L^2_{per}}^2 \right). \quad (5.3.60)$$

Therefore, $\|T^2(t)\|_{\dot{H}^1_{per}}$ and $\|S^2(t)\|_{L^2_{per}} \rightarrow 0$ as $t \rightarrow \infty$ with exponential decay rate $e^{-4\pi^2 \delta t}$.

Thus, \mathcal{M} attracts $(w(t), v(t), T(t), S(t))$ with exponential rate $e^{-4\pi^2 \delta t}$ in $\mathbb{R}^2 \times \dot{H}^1_{per}(0, 1) \times \dot{L}^1_{per}(0, 1)$. \square

Remark 5.3.2 If $T_0, S_0 \in \dot{H}^m_{per}(0, 1)$, from $|a_k(t)| \leq |a_{k0}| e^{-4\delta\pi^2 t}$ and taking into account of (5.3.36), we get $\|T^2(t)\|_{\dot{H}^m_{per}(0,1)} \leq e^{-4\delta\pi^2 t} \|T_0^2\|_{\dot{H}^m_{per}(0,1)}$; and we note from

$$|d_k(t)|^2 \leq 4e^{-8\delta\pi^2 t} \left(|d_{k0}|^2 + 2 \frac{b^2 |a_{k0}|^2}{|c - \nu|^2} \right),$$

we have

$$\|S^2(t)\|_{\dot{H}^m_{per}(0,1)}^2 \leq 4e^{-8\delta\pi^2 t} \left(\|S_{20}\|_{\dot{H}^m_{per}(0,1)}^2 + \frac{2b^2}{|c - \nu|^2} \|T_{20}\|_{\dot{H}^m_{per}(0,1)}^2 \right)$$

and the invariant \mathcal{M} , attracts the solutions $(w(t), v(t), T(t), S(t))$ in $\mathbb{R}^2 \times \dot{H}^m_{per}(0, 1) \times \dot{H}^m_{per}(0, 1)$ with exponential rate $e^{-4\pi^2 \delta t}$.

5.3.2 The reduced subsystem

Under the hypotheses and notations of Theorem 5.3.3, we suppose that

$$f(x) = \sum_{k \in J} c_k e^{2\pi k i x}, \quad (5.3.61)$$

with $c_k \neq 0$ for every $k \in J \subset \mathcal{Z}$ and $c_k = 0$ if $k \notin J$. Since all functions involved are real and periodic, we have $\bar{a}_k = a_{-k}$, $\bar{b}_k = b_{-k}$, $\bar{c}_k = c_{-k}$ and $\bar{d}_k = d_{-k}$, as we consider only the real functions. On the inertial manifold

$$\oint (T - S) \cdot f = \sum_{k \in K} a_k(t) \cdot c_{-k} - \sum_{k \in K} d_k(t) \cdot c_{-k} = \sum_{K \cap J} (a_k(t) - d_k(t)) c_{-k}.$$

So, the evolution of velocity v and acceleration w depend on the coefficients of T and S which belong to the set $K \cap J$. After solving this, we must solve the equations for $k \notin K \cap J$ which are linear autonomous equations. We note that $0 \notin K \cap J$ and since $K = -K$ and $J = -J$ then the set $K \cap J$ has an even number of elements, that we denote by $2n_0$. Therefore, the number of positive elements of $K \cap J$, $(K \cap J)_+$, is n_0 .

Corollary 5.3.4 *Under the notations and hypotheses of the Theorem 5.3.3, we suppose that the set $K \cap J$ is finite and then $|K \cap J| = 2n_0$. Then the asymptotic behavior of the system (5.2.2), is described by a system of $N = 4n_0 + 2$ coupled equations in \mathbb{R}^N , which determines (w, v, a_k, d_k) , $k \in K \cap J$, and a family of $|K \setminus (K \cap J)|$ linear non-autonomous equations. In particular, if $K \cap J = \emptyset$, $l(v) = l_0$ and $G(v) = G_0$ then for every $(w_0, v_0, T_0, S_0) \in \mathbb{R}^2 \times \dot{H}_{per}^1(0, 1) \times \dot{L}_{per}^2(0, 1)$ we have that the associated solution verifies that $v(t) \rightarrow 0$ and $T(t) \rightarrow \theta_\infty$ in $\dot{H}_{per}^1(0, 1)$ and $S(t) \rightarrow \frac{b}{c} \theta_\infty$ in $\dot{L}_{per}^2(0, 1)$ where $\theta_\infty(x)$ is the unique solution in $\dot{H}_{per}^2(0, 1)$ of the equation*

$$-\nu \frac{\partial^2 \theta_\infty}{\partial x^2} + l_0 \theta_\infty = l_0 T_a(x). \quad (5.3.62)$$

PROOF. On the inertial manifold $\oint (T - S)f = \sum_{k \in K} (a_k - d_k)(t) c_{-k} = \sum_{k \in K \cap J} a_k(t) c_{-k} - \sum_{k \in K \cap J} d_k(t) \cdot c_{-k}$. Therefore, the dynamics of the system depends on the coefficients in

$K \cap J$. Moreover the equations for a_{-k} and d_{-k} are conjugates of the equations for a_k and d_k , and therefore we have $\sum_{k \in K \cap J} a_k(t)c_{-k} = 2Re \left(\sum_{k \in (K \cap J)_+} a_k(t)c_{-k} \right)$ and $\sum_{k \in K \cap J} d_k(t)c_{-k} = 2Re \left(\sum_{k \in (K \cap J)_+} d_k(t)c_{-k} \right)$. From this, taking real and imaginary parts of $a_k, (a_1^k, a_2^k)$ and $d_k, (d_1^k, d_2^k), k \in (K \cap J)_+$ in (5.3.41) with $n_0 = |(K \cap J)_+|$, we conclude.

Finally, if $K \cap J = \emptyset, l(v) = l_0$ and $G(v) = G_0$ then on the inertial manifold we get a homogeneous linear equation for the velocity with positive coefficients, that is:

$$\varepsilon \frac{d^2 v}{dt^2} + \frac{dv}{dt} + G_0 v = 0$$

and therefore we have $v(t) \rightarrow 0$ when $t \rightarrow \infty$.

Moreover from the equation for the temperature in (5.2.2) we have that the function $\theta = T - \theta_\infty$ satisfies the equation:

$$\frac{\partial \theta}{\partial t} + v \frac{\partial \theta}{\partial x} = -v \frac{\partial \theta_\infty}{\partial x} + \nu \frac{\partial^2 \theta}{\partial x^2} - l_0 \theta. \quad (5.3.63)$$

We can multiply by θ in $\dot{L}_{per}^2(0, 1)$ and taking into account that $\oint \frac{\partial \theta}{\partial x} \theta = \frac{1}{2} \oint \frac{\partial(\theta^2)}{\partial x} = 0$, since θ is periodic, we have

$$\frac{1}{2} \frac{d}{dt} \|\theta\|^2 + \nu \left\| \frac{\partial \theta}{\partial x} \right\|^2 = -v \oint \frac{\partial(\theta_\infty)}{\partial x} \theta - \oint l_0 \theta^2 \quad (5.3.64)$$

and using Cauchy-Schwarz and Young inequality with $\delta, C_\delta = \frac{1}{4\delta}$ and then the Poincaré inequality, since $\oint \theta = 0$, we have

$$\frac{1}{2} \frac{d}{dt} \|\theta\|^2 + (\nu\pi^2 + l_0) \|\theta\|^2 \leq |v| (C_\delta \left\| \frac{\partial \theta_\infty}{\partial x} \right\|^2 + \delta \|\theta\|^2). \quad (5.3.65)$$

Using $v(t) \rightarrow 0$, together with Gronwall lemma, we prove that $\theta(t) \rightarrow 0$ in $\dot{L}_{per}^2(0, 1)$.

We note that $S - \frac{b}{c}\theta_\infty$ verifies the equation

$$\frac{\partial(S - \frac{b}{c}\theta_\infty)}{\partial t} - c \frac{\partial^2(S - \frac{b}{c}\theta_\infty)}{\partial x^2} = -v \frac{\partial S}{\partial x} - b \frac{\partial^2(\theta)}{\partial x^2} \quad (5.3.66)$$

multiplying this equation by $S - \frac{b}{c}\theta$ integrating by parts and taking into account, the periodicity of S , we obtain $\oint \frac{\partial S}{\partial x} S = 0$, and applying the Young and Poincaré inequality, we get the inequality $\dot{u} + c^*u \leq \frac{\epsilon}{2}$ for every $t \geq t_0$, large enough, with $u = \|S - \frac{b}{c}\theta_\infty\|^2$, and $c^* > 0$. Finally, from singular Gronwall lemma we have

$$u(t) \leq u(t_0)e^{-c^*(t-t_0)} + \frac{\epsilon}{2}(1 - e^{-c^*(t-t_0)})$$

and thus $\limsup_{t \rightarrow \infty} u(t) \leq \frac{\epsilon}{2}$ for every $\epsilon > 0$. \square

Remark 5.3.3 *Taking real and imaginary parts of the coefficients of temperature $a_k(t)$, heat flux at the wall of the loop b_k , geometry of the circuit c_k and solute concentration $d_k(t)$, $k \in (K \cap J)_+$, in*

$$a_k(t) = a_1^k(t) + ia_2^k(t), b_k = b_1^k + ib_2^k, c_k = c_1^k + ic_2^k, d_k(t) = d_1^k(t) + id_2^k(t)$$

the asymptotic behavior of the system (5.2.2) is given by a reduced explicit system in \mathbb{R}^N , where $N = 4n_0 + 2$, given by

$$\left\{ \begin{array}{l} \frac{dw}{dt} + \frac{1}{\epsilon}w + \frac{1}{\epsilon}G(v)v(t) = \frac{1}{\epsilon}2 \sum_{k \in (k \cap J)_+} [a_2^k(t)c_2^k - a_1^k(t)c_1^k] - \frac{1}{\epsilon}2 \sum_{k \in (k \cap J)_+} [d_2^k(t)c_2^k - d_1^k(t)c_1^k] \\ \frac{dv}{dt} = w \\ \dot{a}_1^k(t) + [l(v) + 4\pi^2k^2\nu a_1^k(t) - 2\pi kv(t)a_2^k(t)] = l(v)b_1^k, \quad k \in (K \cap J)_+ \\ \dot{a}_2^k(t) + [l(v) + 2\pi kv(t)a_1^k(t) + 4\pi^2k^2\nu a_2^k(t)] = l(v)b_2^k, \quad k \in (K \cap J)_+ \\ \dot{d}_1^k(t) + [4c\pi^2k^2d_1^k(t) - 2\pi kv(t)d_2^k(t)] = 4b\pi^2k^2a_1^k(t), \quad k \in (K \cap J)_+ \\ \dot{d}_2^k(t) + [4c\pi^2k^2d_2^k(t) + 2\pi kv(t)d_1^k(t)] = 4b\pi^2k^2a_2^k(t), \quad k \in (K \cap J)_+ \end{array} \right. \quad (5.3.67)$$

Thus, we reduce the asymptotic behavior of the initial system (5.2.2) to the dynamics of the reduced explicit system (5.3.67). We observe that from the above analysis,

it is possible to design the geometry of circuit and/or the external heating, by properly choosing the functions f and/or the ambient temperature, T_a , so that the resulting system has an arbitrary number of equations of the form $N = 4n + 2$.

Note that K and J may be infinite sets, but their intersection is finite. Also, for a circular circuit we have $f(x) \sim a\sin(x) + b\cos(x)$, i.e., $J = \{\pm 1\}$ and then $K \cap J$ is either $\{\pm 1\}$ or the empty set.

5.4 Numerical experiments

In this section, the process of numerical approximation is described for the results of the numerical experiments obtained using the MATHEMATICA package [61] for the resolution of the differential equations, using the fourth-order explicit Runge-Kutta method for stiffness equations [23, 27]. Solve the system of ordinary differential equations which are the projection of the partial differential equations (5.2.2) on the inertial manifold. Numerical approximations are done for the resolution of the nonlinear system of differential equations (5.3.59) which includes acceleration, velocity, temperature and the solute concentration. To study the asymptotic behavior of the system of equations, we consider the coefficients of temperature $a_k(t)$ and the coefficients of solute concentration $d_k(t)$ with $k \in K \cap J$, the *relevant modes*. Then, we have the finite system of differential equations:

$$\left\{ \begin{array}{l} \dot{w} = \frac{2\text{Re}(\sum_{k \in (K \cap J)_+} a_k(t)c_{-k})}{\varepsilon} - \frac{2\text{Re}(\sum_{k \in (K \cap J)_+} d_k(t)c_{-k})}{\varepsilon} - \frac{G(v)v}{\varepsilon} - \frac{w}{\varepsilon}, \\ \dot{v} = w, \\ \dot{a}_k(t) = l(v)b_k - l(v)a_k(t) - 4\nu\pi^2 k^2 a_k(t) - 2\pi k v a_k(t)i, \\ \dot{d}_k(t) = -4c\pi^2 k^2 d_k(t) + 4b\pi^2 a_k(t) - 2\pi k v d_k(t)i. \end{array} \right. \quad (5.4.68)$$

Since we deal with the circular geometry, we have $J = \{\pm 1\}$ and $K \cap J = \{\pm 1\}$.

Also we take $k = 1$ and omit the equation for $-k$, the conjugate of k . Therefore, we have the following transformed set of equations:

$$\left\{ \begin{array}{l} \dot{w} = \frac{2\text{Re}(a_1(t)c_{-1})}{\varepsilon} - \frac{2\text{Re}(d_1(t)c_{-1})}{\varepsilon} - \frac{G(v)v}{\varepsilon} - \frac{w}{\varepsilon}, \\ \dot{v} = w, \\ \dot{a}_1(t) = l(v)b_1 - l(v)a_1(t) - 4\nu\pi^2 a_1(t) - 2\pi v a_1(t)i, \\ \dot{d}_1(t) = -4c\pi^2 d_1(t) + 4b\pi^2 a_1(t) - 2\pi v d_1(t)i \end{array} \right. \quad (5.4.69)$$

where the unknowns are $w(t)$, the acceleration of the fluid, $v(t)$, the velocity of the fluid, $a_1(t)$, the Fourier mode of the temperature and $d_1(t)$, the Fourier mode that determines the solute concentration.

To reduce the number of free parameters, we make the following change of variables $a_1 c_{-1} \rightarrow a_1$ and $d_1 c_{-1} \rightarrow d_1$ and we define the real and imaginary parts of the equations in the following way:

$$a_1(t) = a^1(t) + ia^2(t),$$

$$d_1(t) = d^1(t) + id^2(t)$$

$$b_1 = A + iB$$

with $A \in \mathbb{R}, B \in \mathbb{R}$. We obtain the following system of equations to solve for this model:

$$\left\{ \begin{array}{l} \dot{w} = \frac{2a^1 - 2d^1 - G(v)v - w}{\varepsilon}, \\ \dot{v} = w, \\ \dot{a}^1 = l(v)A - l(v)a^1 - 4\nu\pi^2 a^1 + 2v\pi a^2 \\ \dot{a}^2 = l(v)B - l(v)a^2 - 4\nu\pi^2 a^2 - 2v\pi a^1 \\ \dot{d}^1 = -4c\pi^2 d^1 + 4b\pi^2 a^1 + 2v\pi d^2 \\ \dot{d}^2 = -4c\pi^2 d^2 + 4b\pi^2 a^2 - 2v\pi d^1 \end{array} \right. \quad (5.4.70)$$

This forms a system of six differential equations with six unknowns where we need to make explicit choices for the constitutive laws of both the fluid-mechanical and thermal properties. The function $G(v)$ has a clear physical meaning; it interpolates between a low Reynolds number friction law (in which the overall friction, $G(v)v$ is non-linear (Stokes friction law) and high Reynolds number (in which the friction is a quadratic law). For the friction law $G(v)$ and heat flux $h(x, v, T) = l(v)(T_a - T)$, we will take the ones used in the references [23, 27]. For the numerical experiments, which are of a similar model of thermosyphon for a fluid with one component, they use the functions $G(v) = (|v| + 10^{-4})$ and $l(v) = (10^{-2}|v| + 1)$.

Numerical analysis has been carried out keeping ε the viscoelastic coefficient as the tuning parameter ranging from 10^{-5} (almost Newtonian) to 10^1 a highly viscoelastic value. The impact of ε on the system has been keenly observed for the intervals of time t , as short as 100 time units and as long as 1000 time units. All the variables and equations

that we deal with are non-dimensional.

For the Soret effect diffusion coefficients (b and c), we will assume the values calculated by Hart in [26] that consider a thermosyphon of circular geometry of radius R_0 (for the loop) and R_p (for the pipe). Hart takes the values for a mixture of alcohol and water, borrowed from Hurle and Jakeman [26]. This reference settles down that $c = \frac{D_s}{VR_0}$ is the number of Lewis, where D_s is the diffusivity of the solute that has a value for such a mixture of $10^{-5}cm^2s^{-1}$ and V is the scale of velocity, with a value of $0.01cms^{-1}$ for a circular thermosyphon whose loop to pipe radius ratio is 10. Therefore we will take $c = 0.001$. Also, as Hart indicates in [26], b (Soret diffusion coefficient) is a multisigned parameter that determines the qualitative behaviour of the variables. Therefore, in the numerical experiments we treat the value of b the Soret coefficient as another tuning parameter ranging from 10^{-5} to 10^1 .

We plot the *relevant modes* of temperature and solute concentration as they are the ones to have influence on the acceleration $w(t)$ and velocity $v(t)$. The real and imaginary parts of the temperature and solute concentration give two plots each, one corresponding to the real part and the other corresponding to the imaginary part. As the system is multi-dimensional, we present the results in temporal graphs (a given variable versus time) and phase-space graphs (two physical variables plot against each other). We will show that, in analogy with the classical Lorenz system, as ε varies, the dynamics of the model undergoes various transformations including steady asymptotic behavior, meta-stable chaos, i.e., transient irregular behavior followed by convergence to equilibria, periodic behaviors

and chaotic progressions.

We analyze and discuss the behavior of the system for various parameters of the viscoelastic coefficients with various Soret coefficients. At the outset, we define and fix the various parameters that are employed in this model. A and B refer to the position-dependant (x) given ambient temperature inside the loop. Without loss of generality, we will assume $A = 0$, while B is fixed to be 30, in order to simplify in analogy with Lorenz's model, as it is shown in references [23, 27] (changing A and B simultaneously only results in a change in the *phase* of initial temperature profile). The heat diffusion coefficient is fixed to $\nu = 0.002$, namely, temperature diffusion is present but not dominant. The initial conditions are fixed as $w(0) = 0, v(0) = 0, a_1(0) = 1, a_2(0) = 1, d_1(0) = 0.01$, and $d_2(0) = 1$.

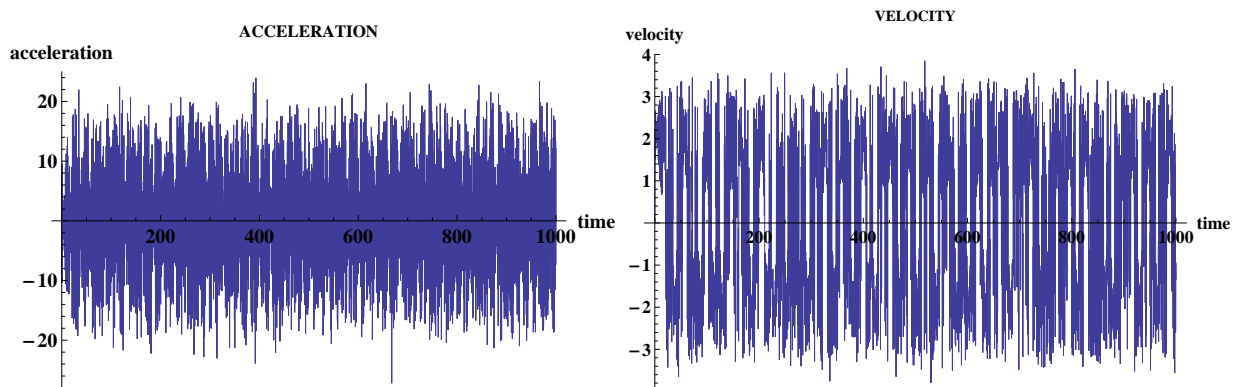


Figure 5.1: The chaotic behavior of acceleration and velocity for $\varepsilon=0.00001$, $A=0$, $B=30$, $b=0.00001$, $\nu = 0.002$, $G(v) = (|v| + 10^{-4})$ and $l(v) = (10^{-2}|v| + 1)$.

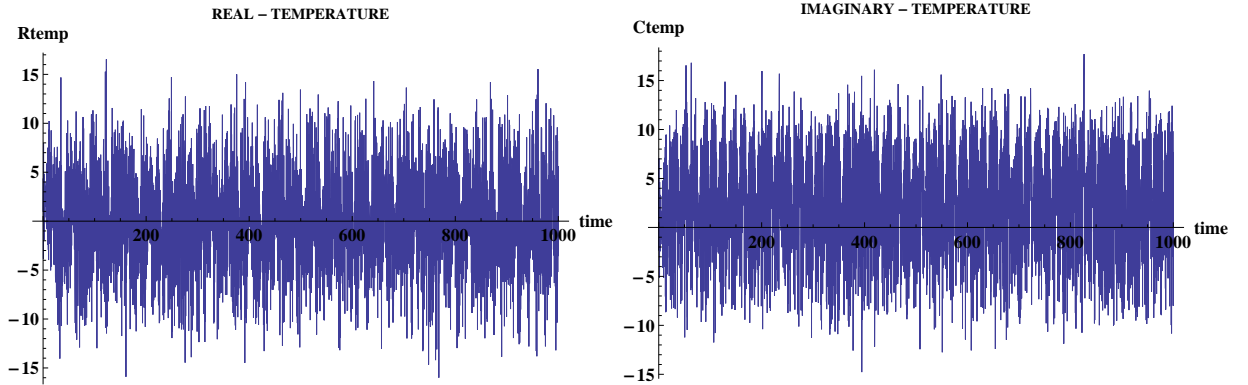


Figure 5.2: The chaotic behavior of the real and imaginary parts of temperature for $\varepsilon=0.00001$, $A=0$, $B=30$, $b=0.00001$, $\nu = 0.002$, $G(v) = (|v| + 10^{-4})$ and $l(v) = (10^{-2}|v| + 1)$.

5.4.1 Experiment I: Soret coefficient $b = 0.00001$

In this very first numerical experiment, keeping the Soret coefficient b as low as 0.00001, we observe the impact of ε the viscoelastic coefficient on the system. Numerical experiments were carried out for different viscoelastic coefficients ε ranging from 0.00001 to 10 as tuning parameters. In Figs. 5.1, 5.2 and 5.3 we show the behavior of the system for a particular case of numerical experiments for the values of $\varepsilon=0.00001$ and Soret gradient 0.00001, plotting acceleration, velocity, temperature and the solute concentration versus time.

Clearly, the chaotic behavior of the system is observed for these range of parameters. The plots in Fig. 5.1 of acceleration and velocity portray the chaotic nature of the behavior of the system. The acceleration ranges from -20 to 20 while the velocity ranges from -3 to 3. As velocity is the time derivative of acceleration, the deviation in the time series plot of velocity is reduced to -3 to 3. But both the plots exhibit chaotic progresses for the entire

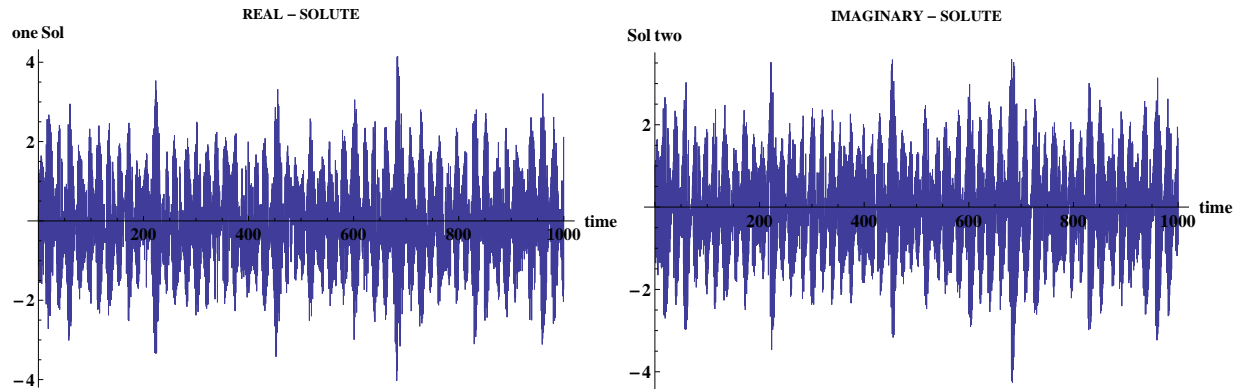


Figure 5.3: The chaotic behavior of the real and imaginary parts of solute concentration for $\varepsilon=0.00001$, $A=0$, $B=30$, $b=0.00001$, $\nu = 0.002$, $G(v) = (|v| + 10^{-4})$ and $l(v) = (10^{-2}|v| + 1)$.

range of 1000 time units. When the viscoelastic coefficient as well as the Soret coefficient is small enough (~ 0.00001) the system has, apparently, chaotic behaviors.

The real and imaginary parts of the temperature are plotted in Fig. 5.2, giving two time series plots for 1000 time units, the first part corresponding to the real part of the temperature and the second part corresponding to the imaginary part of the temperature. Both the plots exhibit complex and chaotic progress till the end of the entire 1000 time units, though the imaginary part of the temperature plot looking apparently more chaotic than the real part of the temperature. As in the case of acceleration and velocity, the temperature too has chaotic progress, when both the viscoelastic and Soret effect coefficients are as low as 0.00001, reaffirming the chaotic onset. This is a consequence of the coupling between the variables.

The real and imaginary parts of solute concentration are given in Fig. 5.3 for 1000 time units, the first part corresponding to the real part of the solute concentration and

the second part corresponding to the imaginary part of the solute concentration. Both the plots have a similar pattern of chaotic behavior. Unlike the deviation of acceleration, velocity and temperature, the deviation in solute concentration is very minimum, varying from -3 to 3. Comparing the plots of temperature with solute concentration, we find that the deviation in temperature is very well distributed throughout the progression, whereas the deviation in the solute concentration is found to be more concentrated at the centre.

To sum up this first numerical experiment, we find that when the value of viscoelastic component and Soret coefficient are both 0.00001, the system is chaotic. Similar type of chaotic behaviors are found for all the values of the viscoelastic components ε ranging from 0.00001 to 10, when the value of Soret coefficient is 0.00001. From the above observations, we can qualitatively state that when the Soret coefficient b is 0.00001, the system has chaotic behaviors. In Sec. 5.4.4 we will extend these results quantitatively by means of standard Lyapunov exponent analysis.

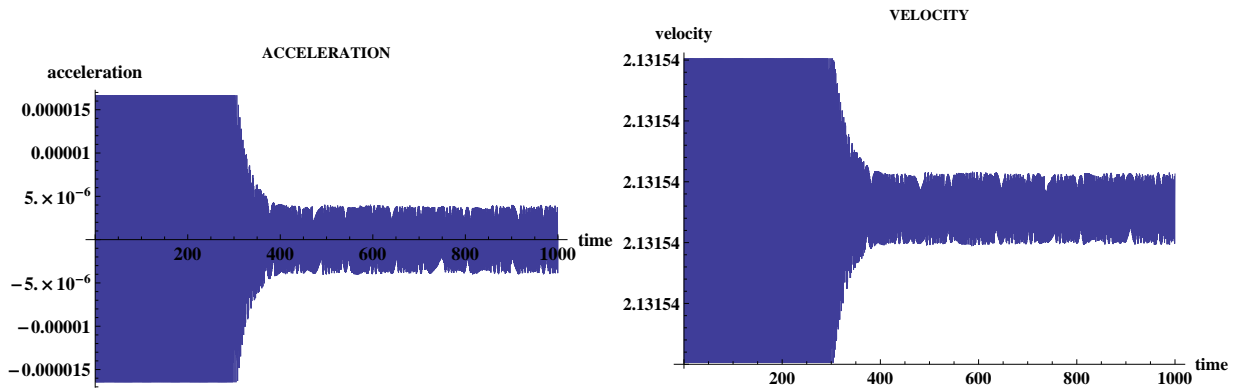


Figure 5.4: The chaotic transition of the fluid acceleration and velocity for $\varepsilon=0.1$, $A=0$, $B=30$, $b=0.001$, $\nu = 0.002$, $G(v) = (|v| + 10^{-4})$ and $l(v) = (10^{-2}|v| + 1)$.

5.4.2 Experiment II: Soret coefficient $b = 0.001$

In the second numerical experiment, keeping the Soret coefficient b to be 0.001, we determine the impact of ε the viscoelastic coefficient on the system. Numerical experiments were carried out for different viscoelastic coefficients ranging from 0.00001 to 10 as tuning parameters and setting the Soret coefficient b to 0.001. We show three cases of different kinds of behaviors for different parameters of the viscoelastic coefficient.

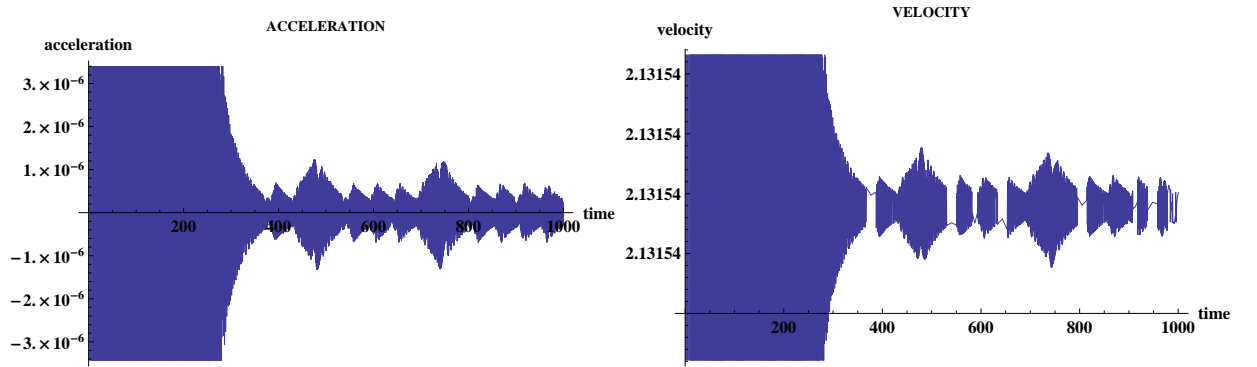


Figure 5.5: The transition from chaotic to quasi-periodic behavior of the fluid acceleration and velocity for $\varepsilon=1$, $A=0$, $B=30$, $b=0.001$, $\nu = 0.002$, $G(v) = (|v| + 10^{-4})$, $l(v) = (10^{-2}|v| + 1)$.

Case I: Transition from chaotic behavior for $\varepsilon=0.1$

Numerical experiments were carried out for the viscoelastic coefficients 0.00001, 0.0001, 0.001, 0.01, and 0.1, keeping the Soret coefficient b fixed to be 0.001. Until the value of $\varepsilon=0.1$, the system has chaotic behavior. But at $\varepsilon=0.1$, the system begins to change from fully chaotic behavior to periodic or stable behavior. To avoid redundancy, we will show hereafter, only the plots for the acceleration and velocity.

The time series plots of acceleration and velocity in Fig. 5.4, portray the transition that takes place in the nature of the behavior of the system, though it still is chaotic apparently. The plot exhibits a chaotic progress up to the range of 400 time units. But after reaching 400 time units, the system begins to change its behavior to conserve. This change of behavior is present also in the time series plots of temperature and solute concentration which help us to make note of the changing phenomena for these particular parameters.

Case II: The quasi-periodic behavior for $\varepsilon=1$

Continuing from the previous numerical experiment, when ε is increased to 1, a relatively greater value from the previous experiment, we find a significant change from chaotic behavior to quasi-periodic behavior taking place in the system. The time series plots of acceleration and velocity in Fig. 5.5 has a very chaotic beginning but as time progressed it begins to have quasi-periodic behaviors after the time unit 400. Once crossing the 400 time unit all the plots have quasi-periodic behaviors till the end of 1000 time units. This gives us a broad understanding that when the viscoelastic coefficient is changed from 0.1 to 1, a transition takes place from chaotic to quasi-periodic behavior. A transition from chaotic to quasi-periodic behaviors of the system are observed also in the time series plots of the real and imaginary parts of the temperature and solute concentration as in the case of acceleration and velocity plots in Fig. 5.5.

To sum up, we have found that when the viscoelastic coefficient is 1 and the Soret

coefficient is 0.001, the system has the transition from chaotic behavior to a quasi-periodic behavior. It also shows that the system is slowly transforming towards a state of stable behavior.

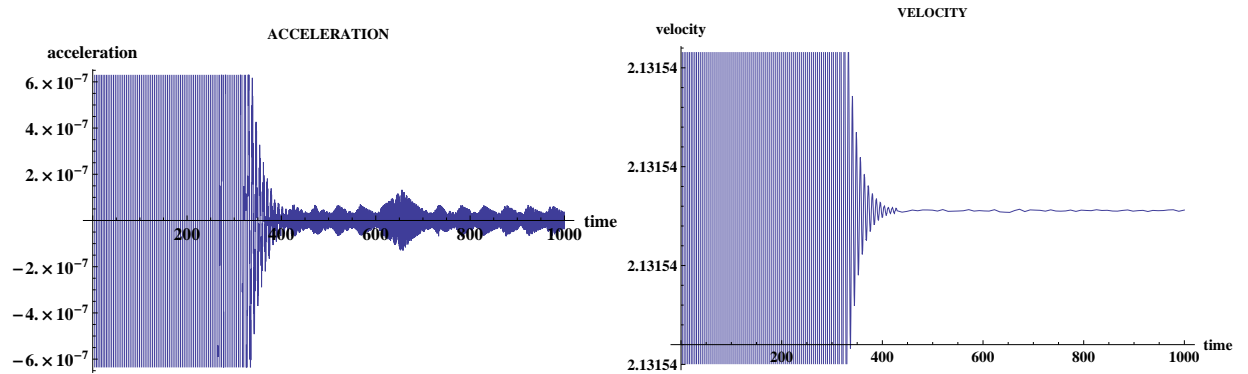


Figure 5.6: The transition from chaotic to stable behavior of the fluid acceleration and velocity for $\varepsilon=10$, $A=0$, $B=30$, $b=0.001$, $\nu = 0.002$, $G(v) = (|v| + 10^{-4})$, $l(v) = (10^{-2}|v| + 1)$.

Case III: The stable behavior for $\varepsilon=10$

Numerical experiments were carried out for the viscoelastic coefficient $\varepsilon=10$, keeping the Soret coefficient fixed to be 0.001. For $\varepsilon=10$, a relatively large value, the time series plots of acceleration and velocity in Fig. 5.6 show a chaotic beginning but as time progressed they begin to stabilize around the time unit 400. Once crossing the 400 time mark the plots have stable progresses till the end of 1000 time units. A transition from chaotic to stable behaviors of the system are observed also in the time series plots of the real and imaginary parts of the temperature and solute concentration as in the case of the acceleration and velocity plot in Fig. 5.6. The velocity is stable around 2.13. The real part

of the temperature is stable at 2.27, while the complex part of the temperature is stable at 0.186. The real part of the solute concentration is stable at 0.0005 while the imaginary part of the solute concentration is stable at -0.0066. This gives us a broad understanding that when the viscoelastic coefficient is high i.e., $\varepsilon=10$, the system tends to stabilize as the time progresses. To sum up, we find that when the value of viscoelastic component is 10 and the Soret coefficient is 0.001, the system has a transformation from chaos to stability. From the above observation, we can state that when the value of viscoelastic component is 10, the system has stabilizing effects.

To sum up the numerical experiment II, we find that when the Soret coefficient is 0.001, the system has different kinds of behaviors depending on the range of ε the viscoelastic coefficient. When ε is relatively small, i.e., $\varepsilon=0.00001, 0.0001, 0.001, 0.01$ and 0.1 the system has chaotic effect. But when $\varepsilon=1$, the system has quasi-periodic effect and at $\varepsilon=10$, it begins to stabilize. From these results, we can state that when the Soret coefficient is 0.001, the system has different kinds of behaviors depending on the values of ε the viscoelastic coefficient.

5.4.3 Experiment III: Soret coefficient $b = 1$

In the third experiment, numerical analysis were carried out, keeping the Soret coefficient b fixed to be 1, while the viscoelastic coefficient ε ranging from 0.00001 to 10 as tuning parameter. A significant change in the behavior of the system is observed for the viscoelastic coefficient $\varepsilon=1$. That is, when the viscoelastic coefficient and the Soret

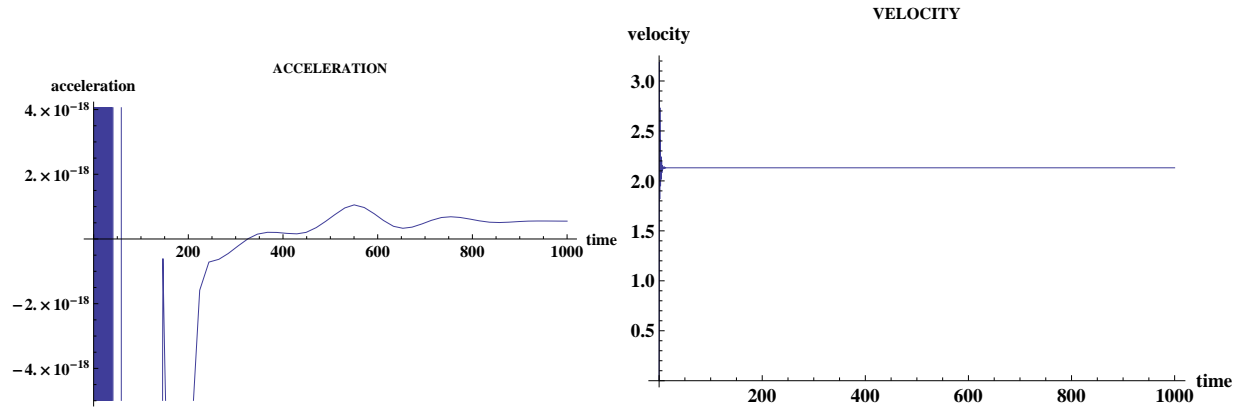


Figure 5.7: Stable progress of the fluid acceleration and velocity for $\varepsilon=1$, $A=0$, $B=30$, $b=1$, $\nu = 0.002$, $G(v) = (|v| + 10^{-4})$, $l(v) = (10^{-2}|v| + 1)$.

coefficient are equal to 1, the system has a stable behavior.

The time series plots of acceleration and velocity in Fig. 5.7 show that for the given parameter of viscoelastic coefficient $\varepsilon=1$ and Soret coefficient $b = 1$, the system has a stable progress. The acceleration, velocity, temperature and the solute concentration all attain a stable and steady flow all through the 1000 time units. The velocity is stable around 2.13. The real part of the temperature is stable at 2.13, while the complex part of the temperature is stable at 0.187. The real part of the solute concentration is stable at 0.0022 while the imaginary part of the solute concentration is stable at -0.0053. And same type of stable behavior is obtained for $\varepsilon=0.1$. In all the other cases, the usual chaotic behavior is observed.

To sum up, we find that when the Soret coefficient value is 1, the system attains stable behavior for the values of $\varepsilon=1$ and 0.1 while all the other values of ε induce chaos on the system.

ε/b	10^{-5}	10^{-4}	10^{-3}	10^{-2}	10^{-1}	10^0	10^1
10^1	C	C	S	S	S	S	S
10^0	C	C	QP	S	S	S	S
10^{-1}	C	C	C	S	S	S	S
10^{-2}	C	C	C	C	C	C	C
10^{-3}	C	C	C	C	C	C	C
10^{-4}	C	C	C	C	C	C	C
10^{-5}	C	C	C	C	C	C	C

Table 5.1: Qualitative summary of the overall behavior of the system for different values of the viscoelastic characteristic time, ε (columns) and the Soret coefficient b (rows). We introduce the following notation to account for the obtained numerical results: ‘S’ a stable behavior, ‘C’ denotes a fully chaotic behavior, and ‘QP’ a transitional behavior from chaotic to quasi-periodic.

Concluding all the three numerical experiments, we want to emphasize that the overall impact of the viscoelastic coefficient on the system for the entire range of parameters ranging from 10^{-5} to 10^1 for both viscoelastic and Soret gradients. We observe that when the viscoelastic coefficient is small, i.e., $\varepsilon=0.00001$, 0.0001 , 0.001 and 0.01 the system has chaotic behaviors irrespective of the Soret gradient. But when $\varepsilon=0.1$, 1 and 10 the system has three different kinds of behaviors depending on the Soret gradients. At first, when the Soret coefficient is 0.00001 and 0.0001 , the system has chaotic behavior for all the values of viscoelastic coefficients. In the second place, when the Soret gradient is 0.001 , the system has chaotic, quasi-periodic and stable behavior when $\varepsilon=0.1$, 1 and 10 respectively. And in the third place, when the values of viscoelastic coefficient and the Soret gradient are 0.1 , 1 and 10 , the system has stable behavior. The table 5.1 gives the qualitative details of the behavior of the system for various parameters, where we have introduced the following notation to account for the obtained numerical results: ‘S’

a stable behavior, ‘C’ denoting a fully chaotic behavior, and ‘QP’ a transitional behavior from chaotic to quasi-periodic behavior.

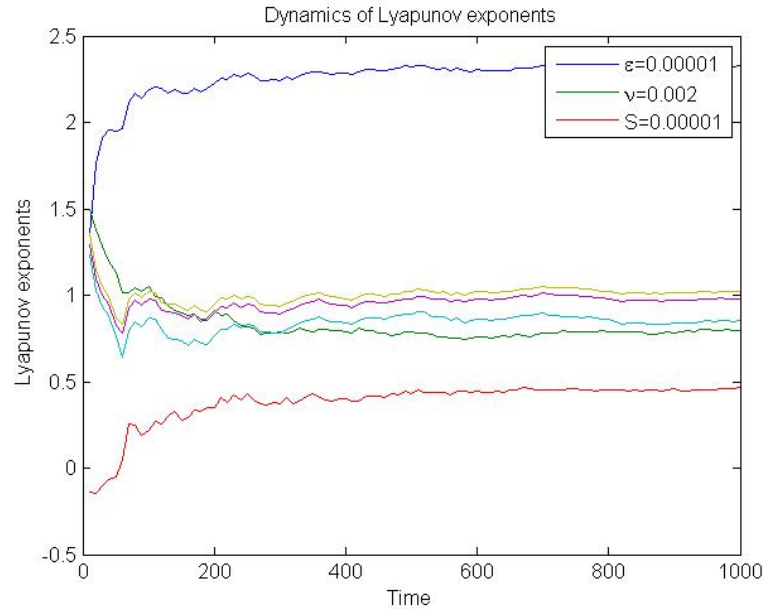


Figure 5.8: The chaotic behavior of the system determined by the Lyapunov exponents for $\varepsilon=0.00001$, $A=0$, $B=30$, $b=0.00001$, $\nu = 0.002$, $G(v) = (|v| + 10^{-4})$ and $l(v) = (10^{-2}|v| + 1)$.

5.4.4 Analysis of the behavior of the system using Lyapunov exponents

The behavior of physical systems has been a matter of primary importance to scientists, engineers and mathematicians in order to determine and characterize the dynamical behavior of the system. In this aspect, the behavior of the system that we are working with has to be ascertained as it has non-linear dynamics with many variables. To ascertain the dynamical behavior of any system, Russian mathematician Alexandr Lyapunov

ε/b	10^{-5}	10^{-4}	10^{-3}	10^{-2}	10^{-1}	10^0	10^1
10^1	0.39	0.39	-0.03	-0.39	-0.52	-0.52	-0.52
10^0	0.45	0.45	0.07	-0.39	-0.49	-1.10	-1.11
10^{-1}	0.42	0.42	0.40	-0.01	-0.24	-0.46	-0.46
10^{-2}	2.61	2.61	1.25	1.36	1.36	1.36	0.87
10^{-3}	2.22	2.22	2.22	2.22	2.22	2.22	2.22
10^{-4}	2.24	2.24	2.24	2.24	2.24	2.24	2.24
10^{-5}	2.29	2.29	2.34	2.29	2.29	2.29	2.29

Table 5.2: The maximum Lyapunov exponent of the system for different values of the viscoelastic characteristic time, ε (columns) and the Soret coefficient b (rows). We can assume that maximum Lyapunov exponents close to 0 ± 0.1 correspond to quasi-periodic behavior (as simple inspection of the time series plots confirm).

gave the definition and criteria for chaotic, periodic, quasi-periodic and stable behavior by introducing the linearization of the equations of motion to determine the behavior of any system, known as Lyapunov exponents. The signs and the values of the Lyapunov exponents allow us to determine the qualitative and quantitative patterns of behavior of any system [60].

The Lyapunov exponents have been proved useful for determining and distinguishing the various types of orbits and behaviors of our system. In the first case, when the viscoelastic coefficients ε are 0.00001, 0.0001, 0.001, and 0.01, relatively lesser gradients, the system has positive Lyapunov exponents, which is a clear indicator for chaotic or strange behavior of the system. In the second case, when the viscoelastic coefficients ε are 0.1, 1 and 10, relatively higher gradients, the system has positive, negative and around the zero point Lyapunov exponents which imply different kinds of behaviors. In this case, depending on the value of Soret gradients the system exhibits chaotic, quasi-periodic, periodic and stable behaviors. As the viscoelastic and Soret gradients increased, the sys-

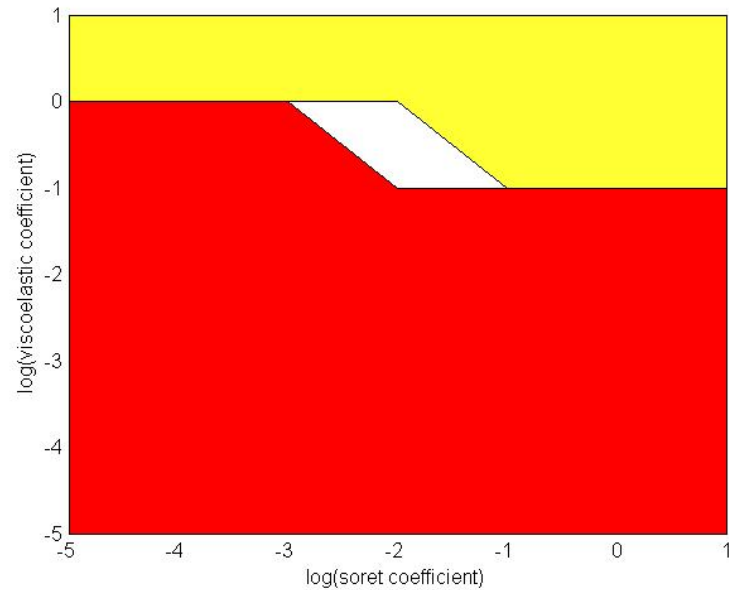


Figure 5.9: The overall behavior of the system for different values of viscoelastic and Soret coefficients (the dark area indicates chaos, shaded area indicates the stable behavior and the white area indicates the quasi-periodic behavior).

tem has more negative Lyapunov exponents which confirm to greater stable behaviors. In a particular case, when the viscoelastic gradient is 1 and the Soret gradient is 0.001, the system has the Lyapunov exponent in and around zero, which is an indication for a quasi-periodic behavior. Along with the Lyapunov exponent values, an example of the plot for the Lyapunov exponents is given in Fig. 5.8 with positive Lyapunov exponents for the chaotic behavior of the system.

The table 5.2 gives the summary of the overall pattern of behavior of the system for the different values of viscoelastic coefficients and Soret coefficients. It gives a broad outlook of the behavior of the entire system. As the table 5.2 shows, we can observe

that for a major part of the experiment, chaos is the common feature of the behavior of the system, apart from a few stable and quasi-periodic behavior of the system where the viscoelastic as well as the Soret gradients are high. The Fig. 5.9 gives the overall behavior of the system, where the dark area indicates the chaos, the shaded area indicates the stable behavior and the white area indicates the quasi-periodic behavior of the system.

5.5 Conclusions

In this chapter we have derived the system of equations that governs the motion of a viscoelastic material with Soret effect inside a closed-loop thermosyphon. Our results suggest that when the value of the viscoelastic coefficient ε is less, it drives the dynamics to a chaotic behavior for all the physical observable (acceleration, velocity, temperature and solute concentration). As the value of ε gradually increases, the system has a transition from chaotic to quasi-periodic or stable behavior depending on the Soret gradient. From these numerical experiments, we observe that the viscoelastic material with Soret gradients drives the system chaotically when the viscoelastic coefficient ε is small and stabilizes the system when the viscoelastic coefficient ε is higher.

Physically, this means that when the viscoelastic effects are large (namely, the time scale ε^{-1} is comparable with the characteristic time scale of variation due to thermodiffusion and Soret effect, the *memory* smoothening arising from equation (2.2.3) drives the system towards a stable fixed point. This might explain why chaotic behaviors are more commonly observed in fluids than in solids in which (sustained) elastic oscillations are

periodic or damped out with time due to dissipation.

Chapter 6

Conclusions and future works

6.1 Summary of conclusions

In this work, we have studied the evolution of linear viscoelastic fluids confined in a closed loop thermosyphon subject to different external (temperature gradients) or internal drives (due to the Soret effect).

From the results of this research, the following conclusions can be drawn:

1. In the first model, where we considered one component viscoelastic fluids with Newton's linear cooling law (Chapter 3), the results suggest that, when the value of $\varepsilon = 10$ is large, it drives the dynamics of the system to chaotic behaviors for all the physical observable (acceleration, velocity and temperature). As the value of ε gradually decreases, the system is no longer chaotic but stable or periodic. Physically, this induction of chaotic behaviors might be related to the memory effects inherent to viscoelastic models. Thus, in the same way as delayed equations are known to produce chaos, even in the simplest situations, viscoelasticity produces the same kind of transition (see, for instance [41]). Other interesting results are related to the

effect of heat diffusion. It is found that as the heat diffusion increases, the system tends to stabilize either to a fixed equilibrium point or to a (ν -dependent periodicity) periodic orbit. Naturally, in a generic case, the balance between destabilizing viscoelastic effects and stabilizing thermal diffusion rules the overall behavior of the fluid.

2. In the second model where we considered one component viscoelastic fluids with a prescribed heat flux (Chapter 4), it is observed that when the value of ε is large the system has also chaotic effects. As the value of ε decreases the system becomes stable and periodic. The interpretation of the role of viscoelasticity remains the same. But one special observation in this case is that the ranges of parameters where periodic behavior arises are broader.
3. In the third model, where we considered binary viscoelastic fluids (Chapter 5), the system of equations that governs the motion of a binary viscoelastic material with Soret effect inside a closed-loop thermosyphon is derived. Our results suggest that when the value of the viscoelastic coefficient $\varepsilon = 0.00001$ (very small), viscoelasticity drives the dynamics to chaotic behaviors for all the physical observables (acceleration, velocity, temperature and solute concentration). As the value of ε gradually increases, the system has a transition from chaotic to quasi-periodic or stable behavior depending on the Soret gradient. From the numerical experiments, it is observed that the viscoelastic fluid with Soret gradients sets the system in chaos when the

viscoelastic coefficient ε is small and stabilizes the system when the viscoelastic coefficient ε is higher. This result is unexpected as the role of ε is the opposite as in the case without the Soret effect. In this case, memory effects, presumably, smoothen out rapid variations inside the fluid. Physically, this means that when the viscoelastic effects are large (namely, the time scale ε^{-1} is comparable with the characteristic time scale of variation due to thermodiffusion), the *memory* smoothening arising from the equation (2.2.3) drives the system towards a stable fixed point. This might explain why chaotic behaviors are more commonly observed in fluids than in solids in which (sustained) elastic oscillations are periodic or damped out with time due to dissipation. However, a simple clear-cut explanation of the role of viscoelasticity cannot be presented. This emphasizes the need for detailed mathematical calculations of the model equations (as the ones presented in this work) to avoid misinterpretations or simple hand-waving expectations of the model outcome.

6.2 Future works

In this work we have worked with a specific Maxwell constitutive equation for the viscoelastic fluid. Although this could be too restricted, Maxwell model of viscoelasticity has been proved accurate in many physical systems. However, this assumption can be relaxed in many different ways from changing the constitutive equation (from Maxwellian to other more complex situations) or to include shear-thinning effects [46] common to many non-Newtonian materials. Shear-thinning is the manifestation of a shear-rate dependent

viscosity. Thus, it is commonly observed that many fluids reduce their resistance to flow for large enough imposed stresses (in our case, temperature gradients), for instance tooth paste, paint or lava.

Heat diffusion is a major factor that has great impact on the behavior of viscoelastic fluids in a thermosyphon. Another interesting feature of this research could be to study the effect of heat diffusion on this system which could be one of the many possible future researches. As shown in Ref. [53], diffusion can also damp out chaotic oscillations so the system could undergo reentrant transitions from states dominated by either Soret effects, viscoelasticity or thermal diffusion.

Finally, and more importantly, all the work presented here concerns linear viscoelasticity. Although this approximation has been proved valid in many contexts, there are some interesting systems in which this assumption cannot be stressed consistently (one case is blood). In those cases, more sophisticated descriptions are mandatory in order to provide physically relevant answers to specific problems.

Chapter 7

Conclusiones y trabajos futuros

7.1 Resumen de las conclusiones

En esta tesis se ha estudiado la evolución de un fluido viscoelástico lineal confinado en un termosifón de bucle cerrado sujeto a diferentes fuerzas externas (gradientes de temperatura, gravedad) o internas (debido al efecto Soret).

De los resultados de esta investigación, las conclusiones que pueden extraerse son las siguientes:

1. En el primer modelo, en el que se considera un líquido de un componente viscoelástico con la ley de enfriamiento lineal de Newton (captulo 3), los resultados sugieren que, cuando el valor de ε es grande, la dinámica es caótica para todos los observables físicos (aceleración, velocidad y temperatura). Cuando el valor de ε disminuye gradualmente, el sistema ya no es caótico sino estable o periódico. Físicamente, esta inducción de comportamientos caóticos podría estar relacionado con los efectos de memoria inherentes a los modelos viscoelásticos. Así, de la misma

forma que las ecuaciones con retraso son conocidas por producir caos (véase, por ejemplo [41]), incluso en las situaciones más sencillas, la viscoelasticidad podría inducir el mismo tipo de transición. Otros resultados interesantes están relacionados con el efecto de la difusión del calor. Se ha encontrado que, a medida que aumenta la difusión del calor, el sistema tiende a estabilizarse ya sea a un punto de equilibrio fijo o a una órbita periódica. Naturalmente, en un caso genérico, el equilibrio entre los efectos desestabilizadores viscoelásticos y la difusión gobernarán el comportamiento global del fluido.

2. En el segundo modelo, donde se considera un fluido mono-componente viscoelástico con un flujo térmico prescrito (capítulo 4) se observa que, cuando el valor de ε es grande, tiene un efecto caótico en el sistema. A medida que el valor de ε disminuye el sistema se vuelve estable o periódico en función de otros parámetros. La interpretación de la función de viscoelasticidad sigue siendo la misma, pero, en este caso, los rangos de parámetros donde surge un comportamiento periódico son más amplios.
3. En el tercer modelo, donde se considera un sistema binario de fluido viscoelástico con solutos —con lo que aparece el efecto Soret—, (capítulo 5), el sistema de ecuaciones que rigen el movimiento de un material viscoelástico binario en el interior de un termosifón de bucle cerrado es derivado explícitamente. Nuestros resultados sugieren que, cuando el valor del coeficiente de viscoelástico ε es pequeño, la dinámica es

caótica para todos los observables físicos (aceleración, velocidad, temperatura y concentración de soluto). A medida que el valor de ε aumenta poco a poco, el sistema tiene una transición de comportamiento caótico a quasi-periódico o estable en función del coeficiente de gradiente Soret. Este resultado es inesperado, pues el papel de ε es el contrario que en el caso sin efecto Soret. En este caso, los efectos de memoria, presumiblemente, suavizan las variaciones rápidas en el interior del fluido. Físicamente, esto significa que, cuando los efectos viscoelásticos son grandes (es decir, la escala de tiempo ε^{-1} es comparable con la escala de tiempo característica de variación debido a termodifusión), la *memoria* suaviza las soluciones y el sistema converge hacia un punto fijo estable. Esto podría explicar por qué comportamientos caóticos son más comúnmente observados en los fluidos que en los sólidos en los que las oscilaciones elásticas son periódicas o amortiguadas con el tiempo debido a la disipación. Sin embargo, una simple explicación de la función de viscoelasticidad no puede ser presentada a la luz de nuestros resultados. Esto pone de relieve la necesidad de detallados cálculos matemáticos de las ecuaciones del modelo (como las que se presentan en este trabajo), para evitar interpretaciones erróneas o demasiado simplistas.

7.2 Trabajos futuros

En esta tesis se ha trabajado con una ecuación constitutiva específica para el fluido viscoelástico. Aunque esto pudiera parecer demasiado restringido, el modelo de Maxwell se ha demostrado preciso en muchos sistemas físicos. Sin embargo, esta suposición puede relajarse en muchas formas diferentes, desde cambiar la ecuación constitutiva (de Maxwell a otras situaciones más complejas) o incluyendo los efectos de *shear-thinning* [46] común a muchos materiales no newtonianos. El efecto de *shear-thinning* es la manifestación de una viscosidad dependiente de los esfuerzos cortantes aplicados sobre el fluido. Así, se observa comúnmente que muchos fluidos reducen su resistencia al flujo para grandes tensiones (en nuestro caso, los gradientes de temperatura) como, por ejemplo, la pasta de dientes, la pintura o la lava.

La difusión de calor es un factor importante que tiene gran impacto en el comportamiento de los fluidos viscoelásticos en un termosifón. Otra característica interesante para generalizar esta investigación podría ser estudiar en mayor detalle el efecto de la difusión del calor en este sistema. Como se muestra en Ref. [53], la difusión también puede amortiguar las oscilaciones caóticas por lo que el sistema puede experimentar transiciones de estados reentrantes dominados por el efecto Soret, la viscoelasticidad o la propia difusión térmica.

Por último, y lo más importante, todo el trabajo que aquí se presenta se refiere viscoelasticidad lineal. Aunque esta aproximación se ha demostrado válida en muchos

contextos, hay algunos sistemas interesantes en los que este supuesto no se puede asumir en general (el caso de la sangre). En esos casos, descripciones más sofisticadas son obligatorias para poder dar respuestas pertinentes a problemas físicos específicos.

Appendix A

Appendix

A.1 Boundary layer theory

The system of equations (2.2.5) can be seen as a singular perturbation problem provided that when $\varepsilon = 0$, the order of the differential equation reduces to one. In order to provide some insight about the solutions of those equations a standard boundary layer theory is customary (see, for instance, Ref. [57]).

In particular, one splits the problem into two parts: the inner problem and the outer problem. The inner problem is defined as the dynamics of the system for times up to $1/\varepsilon$ in which the term $\varepsilon d^2v/dt^2$ is dominant. This regime is strongly dominated by transient impulsive changes in the physical variables. Following Ref. [57], we define a new time scale $\tau = t/\varepsilon$. So, the first equation in (2.2.5), up to order ε , is given by

$$\frac{d^2v}{d\tau^2} + \frac{dv}{d\tau} = O(\varepsilon), \quad (1.1.1)$$

whose solution is

$$v(\tau) = v(0) + \beta(e^{-\tau} - 1), \quad (1.1.2)$$

with β a constant that can be determined by *matching* with the outer solution. For instance, if one assumes the velocity has initial condition $v(0)$ and the matching time is $\tau = O(1) \simeq 1$, then it is straightforward to see that the velocity at a *matching* time $\tau = 1$, converges exponentially to $v_{\text{matching}} = v(0) + \beta(e^{-1} - 1)$.

Besides, the outer problem is defined as the naive approximation $\varepsilon \rightarrow 0$. Thus, the system of equations (2.2.5) reduces to that in Ref. [52] with an effective initial condition given by v_{matching} . So one would expect the same qualitative behaviors as in that work.

For instance, if the parameter $B = 10$, the model in Ref. [52] predicts a stable behavior. However, as shown in Table 2 (second row), increasing the value of ε induces a chaotic behavior. Naturally, different values of the parameters (including B) would provide different values of ε for which the trivial case $\varepsilon \rightarrow 0$ cannot account for the observed dynamics (even for small enough values of ε).

This simple analysis shows the intrinsic complexity of the physical problem when viscoelasticity is considered and more importantly, the need to study every parameter set in detail to provide an accurate description of the type of dynamics in which the system evolves.

A.2 Sectorial Operators

A.2.1 Definition of sectorial operator

We call a linear operator A in a Banach space X a **Sectorial operator** if it has a densely closed operator such that for some ϕ in $(0, \frac{\pi}{2})$, for some constant $M \geq 1$ and a

real number a , such that the sector

$$S_{a,\phi} = \{\lambda \in \mathbb{C}, \quad \phi \leq |\arg(\lambda - a)| \leq \pi, \lambda \neq a\}$$

is contained in the resolvent of A and it has

$$\|(\lambda - A)^{-1}\| \leq \frac{M}{|\lambda - a|} \text{ for all } \lambda \in S_{a,\phi}. [27]$$

A.2.2 The interpolation scale of spaces

Let us look at the definition of the potential fractional powers of the sectorial operator and the spaces of interpolation associated to the sectorial operator as in [27].

Definition A.2.1 Suppose A is a sectorial operator in a Banach space X with $\operatorname{Re}\sigma(A) > 0$, then for any $\alpha > 0$ we define

$$A^{-\alpha} = \frac{1}{\Gamma(\alpha)} \int_0^\infty t^{\alpha-1} e^{-At} dt.$$

$A^\alpha = (A^{-\alpha})^{-1}$ is the inverse operator of $A^{-\alpha}$, with $D(A^\alpha) = R(A^{-\alpha})$, $A^0 \equiv$ the identity in X .

Definition A.2.2 Suppose A is a sectorial operator in a Banach space X with $\operatorname{Re}\sigma(A) > 0$, then for any $\alpha \geq 0$, we define $X^\alpha = D(A_a^\alpha)$ with the property of the norm, then

$$\|x\|_\alpha = \|A_a^\alpha x\|, x \in X^\alpha, \text{ where } A_a = A + aI \text{ with } a \geq 0 \text{ such that } \sigma(A_a) > 0. \quad (1.2.3)$$

The family $\{X^\alpha\}_{\alpha \geq 0}$ denotes the chain of spaces of the potential fractional powers of the sectorial operator A .

Proposition A.2.1 Suppose A is a sectorial operator in a Banach space X , then it has:

i) For every $\alpha \geq 0$, the norm as defined in (1.2.3) is independent of the choice of a . Moreover X^α is a Banach space with the said norm.

ii) The space $X^0 = X$, for $\alpha \geq \beta \geq 0$, X^α is a dense subspace of X^β with continued inclusion. Moreover, if $\alpha, \beta \in \mathbb{R}^+$ and $\theta \in [0, 1]$, then for all $x \in X^\gamma$ with $\gamma = \max\{\alpha, \beta\}$, there exists a constant $C > 0$ that depends on α, β and θ , the denominator constant of interpolation, such that:

$$\|x\|_{\theta\alpha + (1-\theta)\beta} \leq C \|x\|_\alpha^\theta \|x\|_\beta^{1-\theta}.$$

iii) If A has a compact resolvent, the inclusion $X^\alpha \subset X^\beta$ is always compact for $\alpha > \beta \geq 0$.

iv) The operator A is a sectorial operator in X^α for all $\alpha \geq 0$.

Lemma A.2.2 *Suppose A is a sectorial operator in a Banach space X with $\operatorname{Re}(\sigma(A)) > \delta > 0$, then for any $\alpha \geq 0$, there exists $c_\alpha > 0$ such that:*

$$\|A^\alpha e^{-At}\| \leq c_\alpha t^{-\alpha} e^{-\delta t} \text{ for all } t > 0.$$

If, $0 < \alpha \leq 1$ and $w \in D(A^\alpha)$, then

$$\|(e^{-At} - I)w\| \leq \frac{1}{\alpha} c_{1-\alpha} t^\alpha \|A^\alpha w\|$$

Moreover c_α is bounded if α moves in the compact interval of $(0, \infty)$, beside ever closed if $\alpha \mapsto 0^+$, where e^{-At} represents the analytic semigroup whose infinitesimal generator is A [2, 3, 27, 49].

The proofs of the above proposition and lemma are given in [27]. The next result is based on the interpolation inequality types of Gagliardo-Nirenberg [45].

Lemma A.2.3 *Given k a positive number, $p \geq 1, r \leq \infty$ and $j = 0, \dots, k$. We define*

$$\frac{1}{q} = \frac{j}{k} \left(\frac{1}{p} - \frac{1}{r} \right) + \frac{1}{r}.$$

Let $\Omega \subset \mathbb{R}^N$ be an open bounded and regular domain, if $u \in W^{k,p}(\Omega) \cap L^r(\Omega)$, then for all multi-index σ , such that $|\sigma| = j$, $D^\sigma u \in L^q(\Omega)$, and

$$\|D^\sigma u\|_{L^q} \leq C \sum_{|\mu|=k} \|D^\mu u\|_{L^p}^{\frac{j}{k}} \|u\|_{L^r}^{1-\frac{j}{k}},$$

with $C > 0$ independent of u .

We have some results about the potential spaces associated to the sectorial operator $-\Delta_P$, where the subindex P of Laplacian represents the periodic boundary condition.

Proposition A.2.4 *If $1 \leq p < \infty$, the operator $-\Delta_P$ in $X^0 = L^p_{\text{per}}$ with domain $X^1 = W^{2,p}_{\text{per}}$ is a compact resolvent sectorial operator. Moreover, if we consider $\mu > 0$ such that $\sigma(-\Delta_P + \mu I) > 0$, the fractional potential spaces $X^\alpha_P = W^{2\alpha,p}_{\text{per}} = D[(-\Delta_P + \mu I)^\alpha]$, provided with the norm of the graph that we shall denote by $\|\cdot\|_{W^{2\alpha,p}_{\text{per}}}$, (or simply $\|\cdot\|_\alpha$), for $\alpha > 0$ and $\|\cdot\|_{L^p_{\text{per}}}$ (or $\|\cdot\|$), are well defined and verify that*

$$W^{2\alpha,p}_{\text{per}} \subset W^{2\alpha,p}(\Omega) \tag{1.2.4}$$

with continued inclusion for all $\alpha \in [0, 1]$, where $W^{2\alpha,p}$ is a Sobolev space [2].

Remark A.2.1 In this work, we denote $L_{per}^p = L_{per}^p(\Omega)$ and consider $\Omega = (0, 1)$. Moreover, we consider that all the functions are with zero average. That is:

$$\dot{L}_{per}^p(\Omega) = \dot{L}_{per}^p(0, 1) = \{u \in L_{loc}^p(\mathbb{R}), u(x+1) = u(x) \text{ a.e.}, \oint u = 0\}.$$

By this reason, $-\Delta_P$ is positive.

Remark A.2.2 For the particular case $p = 2$, we have that $-\Delta_P$ is a sectorial operator about L_{per}^2 that is a Hilbert space and as a consequence, we have a spectral representation of the form:

$$\|x\|_\alpha = \left(\sum_{n=1}^{\infty} |\lambda_n|^{2\alpha} |x_n|^2 \right)^{\frac{1}{2}} = \|(-\Delta_P + I)^\alpha x\|_0$$

define a Hilbertian norm in X^α being a spectral decomposition of x :

$$x = \sum_{n=1}^{\infty} x_n e_n,$$

with e_n a normalized Hilbertian base of L_{per}^2 formed by proper functions of $-\Delta_P$. Therefore we have the operator

$$-\Delta_P^\alpha : D(-\Delta_P^\alpha) = H_{per}^\alpha \longmapsto L_{per}^2$$

defined by:

$$-\Delta_P^\alpha x = \sum_{n=1}^{\infty} \lambda_n^\alpha x_n e_n.$$

In this form, we have the scale of the extended interpolation space for all $\alpha \in \mathbb{R}$, and the Proposition A.2.1 follows for all $\alpha \in \mathbb{R}$ with constant interpolation $C = 1$ in the division. Moreover, the negative exponents of the spaces obtained by the duality of the form that if $p = 2$ we shall denote by $H_{per}^{-2\alpha} = (H_{per}^{2\alpha})'$, $\alpha \geq 0$, to the dual space $H_{per}^{2\alpha, p}$, and we have the following result.

Proposition A.2.5 We suppose $p = 2$, then we have: $H_{per}^m(\Omega)$, $m \in \mathbb{N}$, $H_{per}^{-1} = (H_{per}^1(\Omega))'$, $H_{per}^{-2} = (H_{per}^2(\Omega))'$ and $W_{per}^{-2\alpha, p} = (W_{per}^{2\alpha, p}(\Omega))'$, $0 \leq \alpha \leq 1$ where $1 < p < \infty$ and $p' = \frac{p}{p-1}$.

Remark A.2.3 $H_{per}^m(\Omega)$ is the dual space of $W_{per}^{2\alpha, p'}$ with respect to the duality product of $L^{p'}(\Omega) \times L^p(\Omega)$. In particular $W_{per}^{-1, p} = (W_{per}^{1, p'}(\Omega))'$. In this case all the results are true on $\dot{W}_{per}^{2\alpha, p'}$ or \dot{H}_{per}^m if $p = 2$.

A.3 Semilinear equations: existence and uniqueness

We have some results for the existence and uniqueness of solutions of the evolution of equations that describe a **sectorial operator**. In the first place, we enunciate a few lemmas whose proofs are given in [49, 51] which we shall use frequently in this work.

Lemma A.3.1 Given the equation:

$$\begin{cases} \frac{dw}{dt} + Aw = f(t), t \geq t_0 \\ w(t_0) = w_0 \in X^\beta. \end{cases} \quad (1.3.5)$$

where A is a sectorial operator in the Banach space X and $X^\alpha = D(A_a^\alpha)$ with $A_a = A + aI, \alpha \geq 0$, the spaces of the fractional powers associated to the operator A and $f : [t_0, T) \mapsto X^\beta$.

i) Suppose that $f \in L^1(0, T; X^\beta)$, then there exists a solution of (1.3.5), a weak denominated solution that comes from 'the formula of variation of constants'. That is:

$$w(t) = e^{-A(t-t_0)}w_0 + \int_{t_0}^t e^{-A(t-s)}f(s)ds \quad (1.3.6)$$

verifying such that $w \in C([0, T); X^\alpha)$ for all $\gamma < \beta + 1$.

ii) Suppose that f is locally Hölder continuous in t of exponent θ and there exists $\rho > 0$ such that $\int_0^\rho \|f(t)\|_{X^\beta} dt < \infty$, then the solution given by the formula of variation of constants verifies the equation (1.3.5), as an equality of the space X^β and almost everywhere $w_t \in X^\beta, w(t) \in X^{\beta+1}, t \in (0, T)$, verifying:

$$w \in C([0, T); X^\beta) \cap w \in C^1((0, T); X^\beta) \text{ and } w \in C([0, T); X^{\beta+\theta}). \quad (1.3.7)$$

Next, we show some results about the existence, uniqueness and regularity of a semilinear equation whose proofs are given in [27, 49].

Theorem A.3.2 We consider the non-linear equation

$$\begin{cases} \frac{dw}{dt} + Aw = f(t, w), t \geq t_0 \\ w(t_0) = w_0, w_0 \in X^\alpha. \end{cases} \quad (1.3.8)$$

where A is a sectorial operator in the Banach space X and $X^\alpha = D(A_a^\alpha)$ with $A_a = A + aI, \alpha \geq 0$, the spaces of the fractional powers associated to the operator A . We suppose that f has an open set U in $\mathbb{R} \times X^\alpha$ in X^β , for some $0 \leq \alpha - \beta < 1$, of the form f that is locally Hölder continuous in t and locally Lipschitz in w .

Then for all $(t_0, w_0) \in U$, there exists $t_1 = t_1(t_0, w_0) > 0$ of the form of Cauchy problem given in (1.3.8), that has a unique solution w in (t_0, t_1) that comes from the formula of variation of constants. That is:

$$w(t) = e^{-A(t-t_0)}w_0 + \int_{t_0}^t e^{-A(t-s)}f(s, w(s))ds \quad (1.3.9)$$

such that $w : [t_0, t_1) \mapsto X$ is a continuous function with $w(t_0) = w_0$, $w(t) \in D(A)$, there exists $\frac{dw}{dt}$, and the function $t \mapsto f(t, w(t))$ is locally Hölder continuous with values in X^β . Moreover, it verifies that

$$w \in C((t_0, t_1); X^\alpha) \cap C((t_0 - t_1); X^{\beta+\theta}). \quad (1.3.10)$$

and it has $w_t : (t_0, t_1) \mapsto X^\beta$ which is a Hölder continuous function.

Theorem A.3.3 Under the hypothesis and the notations of the previous Theorem A.3.2, if $f : U \subset \mathbb{R} \times X^\alpha \mapsto X$ with $0 \leq \alpha < 1$ is locally Lipschitz, then if $\gamma < 1$, the application $t \mapsto \frac{dw}{dt} \in X^\gamma$ is a locally Hölder continuous function for $t_0 \leq t \leq t_1$, with

$$\left\| \frac{dw}{dt} \right\|_\gamma \leq C(t - t_0)^{\alpha - \gamma - 1}. \quad (1.3.11)$$

Proposition A.3.4 Under the hypothesis and the notations of the previous Theorem A.3.2, if we suppose that f maps bounded sets of U in to bounded sets of X such that $U \subset \mathbb{R} \times X^\alpha \mapsto X$. Then if (t_0, t_1) is the maximal interval in w given by the previous theorem, then it has that $t_1 = \infty$, is to say that the solution is global or the norm of the solution that explodes in finite time, i.e., to say that there exists a succession of time $t_n \mapsto t_1$, such that $\|w(t_n)\|_\alpha \mapsto \infty$ [27, 49].

A.4 Dissipative semigroups

We have some definitions of dissipative semigroups from [24]:

1. Given $S^*(t), t \geq 0$ a semigroup in the Banach space X . We say that a set $\mathcal{A} \subset X$ is a **maximal or global attractor** for the semigroup $S^*(t)$, if it is the maximal compact set and invariant $S^*(t)(\mathcal{A}) = \mathcal{A}$, $t \geq 0$, that attracts to the bounded set X i.e., $\text{dist}(S^*(t)B, \mathcal{A}) \mapsto 0$ if $t \mapsto \infty$ for all B bounded in X , where we have:

$$\text{dist}(x, A) = \inf\{d(x, a), a \in A\} \text{ with } x \in X, A \subset X.$$

$$\text{dist}(A, B) = \sup\{\text{dist}(a, B), a \in A\} \text{ with } A, B \subset X.$$

2. Given $S^*(t), t \geq 0$ a semigroup in the Banach space X with maximal attractor \mathcal{A} . We say that \mathcal{M} is an **inertial manifold** of class C^k and dimension N for $S^*(t)$, if \mathcal{M} is a topological manifold of dimension N and class k , submanifold for X (i.e., the topology of \mathcal{M} is induced by X) such that:

i) $S^*(t)\mathcal{M} \subset \mathcal{M}$ for all $t \geq 0$.

ii) \mathcal{M} contains the maximal attractor \mathcal{A} of $S^*(t)$.

iii) There exists $\delta > 0$ verifying that for all $B \subset X$ bounded, there exists $C(B) \geq 0$ such that:

$$\text{dist}(S^*(t), \mathcal{M}) \leq C(B)e^{-\delta t}, t \geq 0.$$

We observe that if \mathcal{M} is closed in X , then the third condition implies the second condition. This definition, together with some more properties of the inertial manifold can be seen in [47, 48].

The theorem 4.2.2. of [24] states that:

Theorem A.4.1 If \mathcal{A} and f satisfy the following conditions: 1) $\dot{u} + Au = f(u), t > 0, u(0) = u_0$, 2) \mathcal{A} is a sectorial operator on X and there is an $\alpha \in [0, 1)$ such that $f : X^\alpha \mapsto X$ is locally Lipschitz continuous, i.e., f is continuous and for any bounded set U in X^α there is a constant k_U such that $|f(u) - f(v)| \leq k_U|u - v|_\alpha$ for $u, v \in U$ and in addition, the resolvent of \mathcal{A} is compact and $S^*(t)$ takes bounded sets into bounded sets for each $t > 0$, then $S^*(t)$ is compact on X^α for $t > 0$.

The proof of this theorem is given in [24] on page 73.

The Theorem 3.4.8. of [24] states that:

Theorem A.4.2 If there is a $t_1 \geq 0$ such that the C_-^r semigroup $S^*(t) : X \mapsto X, t \geq 0$ is completely continuous for $t \geq t_1$ and point dissipative, then there is a global attractor \mathcal{A} . If X is a Banach space, then \mathcal{A} is connected and, if $t_1 = 0$, there is an equilibrium point of $S^*(t)$. If, in addition, $S^*(t)$ is one-to-one on \mathcal{A} , then $S^*(t)|_{\mathcal{A}}$ is a C_-^r group.

The proof of this theorem is given in [24] on page 40.

A.5 L'Hopital rule

The generalization of L'Hopital rule for limit superior whose proof is given in [52].

Lemma A.5.1 Let F_1 and F_2 be real and differential functions in $(a, b), b \leq \infty$, such that $F_2'(t) \neq 0$ in (a, b) and $\limsup_{t \rightarrow b} F_2(t) = \infty$ (respectively $\liminf_{t \rightarrow b} F_2(t) = \infty$). Then, if

$$\limsup_{t \rightarrow b} \frac{F_1'(t)}{F_2'(t)} = L, \text{ we have } \limsup_{t \rightarrow b} \frac{F_1(t)}{F_2(t)} \leq L.$$

and respectively, if

$$\liminf_{t \rightarrow b} \frac{F_1'(t)}{F_2'(t)} = L, \text{ we have } \liminf_{t \rightarrow b} \frac{F_1(t)}{F_2(t)} \leq L.$$

A.6 Inequalities

A.6.1 Young Inequality

If a and b are non-negative real numbers and p and q are positive real numbers such that $\frac{1}{p} + \frac{1}{q} = 1$, then

$$ab \leq \frac{a^p}{p} + \frac{b^q}{q}$$

A.6.2 Hölder's Inequality

Suppose that f and g are two non negative real valued functions defined on a measure space (X, Ω) . For $1 < p, q < \infty$ and $f \in L^p(\Omega)$, $g \in L^q(\Omega)$ and $\frac{1}{p} + \frac{1}{q} = 1$, then $fg \in L^1(\Omega)$ and $\|fg\|_{L^1} \leq \|f\|_{L^p} \|g\|_{L^q}$. Hölder's inequality becomes an equality if and only if $\|f\|_p$ and $\|g\|_q$ are linearly dependent in $L^1(\Omega)$. The numbers p and q are said to be Hölder conjugates of each other. The special case $p = q = 2$ gives a form of Cauchy-Schwarz inequality.

A.7 Singular Gronwall lemma

Let $a, b \geq 0, 0 \leq \alpha, \beta < 1$ and $u : [0, T] \mapsto \mathbb{R}$ an integrable function such that for $t \in [0, T]$,

$$0 \leq u(t) \leq at^{-\alpha} + b \int_0^t (t-s)^{-\beta} u(s) ds$$

Then there exists $K = K(b, \beta, T)$ such that

$$u(t) \leq \frac{K}{1-\alpha} at^{-\alpha}, t \in [0, T]$$

A.8 Lyapunov exponent

The Lyapunov exponent or Lyapunov characteristic exponent of a dynamical system is a quantity that characterizes the behavior of the system. The signs of the Lyapunov exponents provide the qualitative behaviors of the dynamics of the system. Any system containing at least one positive Lyapunov exponent is defined to be chaotic [60], if all the Lyapunov exponents are negative then the system is said to be stable and around the values of zero, it is said to be periodic.

The Lyapunov exponent is defined in [60] as:

$$\lambda_i = \lim_{t \rightarrow \infty} \frac{1}{t} \log \frac{p_i(t)}{p_i(0)}$$

where λ_i is the Lyapunov exponent and $p_i(t)$ is the length of the ellipsoidal principal axis.

Bibliography

- [1] A. Abbasi, “Theoretical investigation of thermodiffusion (Soret effect) in multicomponent mixtures”, *Doctoral thesis, University of Toronto*, (2010).
- [2] H. Amann, “Parabolic evolution equations and nonlinear boundary conditions”, *J. of Diff. Equ.*, 72, 201-269, (1988).
- [3] H. Amann, “Nonhomogeneous linear and quasilinear elliptic and parabolic boundary value problems”, in *Function Spaces, Diff. Operation and nonlinear analysis*, H. Schneisser and H. Triebel Eds., *Teubner-Texte Zur Math*, 133, 9-126, (1993).
- [4] H.A. Barnes, *A handbook of elementary rheology*, *Institute of Non-Newtonian Fluid Mechanics, University of Wales UK*, 2000.
- [5] S. Bhattacharyya, D.N. Basu and P.K. Das, “Two-Phase Natural Circulation Loops: A Review of the Recent Advances”, *Heat Transfer Engineering*, 33, 4-5, 461-482, (2012).
- [6] A.M. Bloch and E.S. Titi, “On the dynamics of rotating elastic beams”, in *New Trends in System Theory, Prog. Systems Control Theory 7*, Birkhäuser, Boston, MA, 128-135, (1991).
- [7] M.E. Bravo-Gutiérrez, M. Castro, A. Hernandez-Machado and E. Corvera Poiré, “Controlling Viscoelastic Flow in Microchannels with Slip”, *Langmuir, ACS Publications*, 27-6, 2075-2079, (2011).
- [8] H. Brézis, “Análisis funcional”, *Alianza Editorial*, (1984).
- [9] D. Brochet and D. Hilhorst, “Universal Attractor and Inertial sets for the Phase Field Model”, *Appl. Math. Lett.*, 4, 6, 59-62, (1991).
- [10] D. Brochet, X. Chen and D. Hilhorst, “Finite dimensional exponential attractor for the phase field model”, *Applied Analysis*, 49, 3-4, 197, (1993).
- [11] G. Caginalp, “An Analysis of a Phase Field Model of a Free Boundary”, *Arch. Rat. Mech. Analysis*, 92, 205-245, (1986).

- [12] *S. Cano-Casanova et al.*, Spectral theory and nonlinear analysis with applications to spacial ecology, *World Scientific Publishing Company, Singapore, 2005.*
- [13] *N. Chafee and E.F. Infante*, “A bifurcation problem for a nonlinear partial differential equation of parabolic type”, *Applied Analysis*, 4, 17-37, (1977).
- [14] *K. Chen*, “On the oscillatory instability of closed loop thermosyphon”, *Trans. of the ASME*, 107, 826-977, (1985).
- [15] *M.C. Cross and H. Greenside*, “Pattern formation and dynamics in nonequilibrium systems”, *Cambridge University Press, New York, 2009.*
- [16] *F. Debbasch and J.P. Rivet*, “The Ludwig-Soret effect and stochastic processes”, *J. of Chem. Thermodynamics*, 43, 3, 300-306, (2010).
- [17] *R.T. Dobson and J.C. Ruppertsberg*, “Flow and heat transfer in a closed loop thermosyphon”, *J. of Energy in Southern Africa*, 18, 3, 32-40, (2007).
- [18] *W.N. Findley et al.*, Creep and relaxation of nonlinear viscoelastic materials, *Dover Publications Inc., New York, 1989.*
- [19] *A.M. Fink*, “Almost Periodic Differential Equations”, *Lecture Notes in Mathematics, Springer-Verlag, New York, 1989.*
- [20] *C. Foias, G.R. Sell and R. Temam*, “Inertial Manifolds for Nonlinear Evolution Equations”, *J. of Diff. Equ.*, 73, 309-353, (1988).
- [21] *G. Fusco and J.K. Hale*, “Slow-Motion Manifolds, Dormant Instability and Singular Perturbations”, *J. of Dynamics and Diff. Equ.*, 1,1, (1989).
- [22] *D. Gilbard and N.S. Trudinger*, “Elliptic partial differential equations of second order”, *Springer-Verlag, New York, 1977.*
- [23] *R. Greif, Y. Zvirin and A. Mertol*, “The transient and stability behavior of a natural convection loop”, *J. of Heat Transfer*, 107, 684-688, (1987).
- [24] *J.K. Hale*, “Asymptotic Behavior of Dissipative Systems”, *AMS, Providence, RI, (1988).*
- [25] *J.E. Hart*, “Observations of Complex oscillations in a closed loop thermosyphon”, *J. of Heat Transfer*, 107, 833-839, (1985).
- [26] *J.E. Hart*, “A Model of Flow in a Closed-Loop Thermosyphon including the Soret Effect”, *J. of Heat Transfer*, 107, 840-849, (1985).

- [27] D. Henry, “Geometric Theory of Semilinear Parabolic Equations”, *Lectures Notes in Mathematics* 840, Springer-Verlag, Berlin, New York, 1981.
- [28] M.A. Herrero and J.J-L. Velazquez, “Stability analysis of a closed thermosyphon”, *European J. of Appl. Math.*, 1, 1-24, 1990.
- [29] C.J. Ho, S.Y. Chiu and J.F. Lin, “Heat transfer characteristics of a rectangular natural circulation loop containing solid-liquid phase-change material suspensions”, *International Journal of Numerical Methods for Heat and Fluid Flow*, 15, 5, 441-461, (2005).
- [30] St. Hollinger and M. Lucke, “Influence of the Soret effect on convection of binary fluids”, *Phys. Review, E* 57, 4238-4248, (1998).
- [31] J.P. Holman, “Termodinámica”, MacGraw Hill, Mexico (1977).
- [32] D.T.J. Hurle and E. Jakerman, “Soret-driven thermosolutal convection”, *J. of Fluid Mech.*, 47, 667-687, (1971).
- [33] F.P. Incropera, T.L. Bergman, A.S. Lavine and D.P. DeWitt, “Fundamentals of heat and mass transfer”, Wiley, 2011.
- [34] A. Jiménez-Casas, and A. Rodríguez-Bernal, “Finite-dimensional asymptotic behavior in a thermosyphon including the Soret effect”, *Math. Meth. in the Appl. Sci.*, 22, 117-137, (1999).
- [35] A. Jiménez-Casas, “A coupled ODE/PDE system governing a thermosyphon model”, *Nonlin. Analysis*, 47, 687-692, (2001).
- [36] A. Jiménez-Casas and A.M-L. Ovejero, “Numerical analysis of a closed-loop thermosyphon including the Soret effect”, *Applied Math. Comput.*, 124, 289-318, (2001).
- [37] A. Jiménez Casas and A. Rodríguez-Bernal, *Dinámica no lineal: modelos de campo de fase y un termosifón cerrado*, Editorial Académica Española, LAP LAMBERT Academic Publishing GmbH and Co., KG, 2012.
- [38] A. Jiménez-Casas, M. Castro and J. Yasappan, “Finite-dimensional behavior in a thermosyphon with a viscoelastic fluid”, (submitted)
- [39] J.B. Keller, “Periodic oscillations in a model of thermal convection”, *J. of Fluid Mech.*, 26, 3, 599-606, (1966).
- [40] J. Kirk Storey, “Modeling the transient response of a thermosyphon”, *PhD Thesis*, Brigham Young University, UK, (2003).

- [41] Y. Kuang, "Delay differential equations: with applications to population dynamics", Academic Press, CA, 1993.
- [42] P.A. Lakshminarayana, P.V.S.N Murthy and Rama Subba Reddy Gorla, "Soret-driven thermosolutal convection induced by inclined thermal and solutal gradients in a shallow horizontal layer of a porous medium", *J. of Fluid Mech.*, 612, 1-19, (2008).
- [43] Y. Lee and S.H. Rhi, "Lumped and sectoral flow pattern methods for computer simulation of two-phase loop thermosyphons", *Proc.6th IHPS, Chang Mai, 2000*.
- [44] A. Liñan, "Analytical description of chaotic oscillations in a toroidal thermosyphon", in *Fluid Physics, Lecture Notes of Summer Schools*, (M.G. Velarde and C.I. Christor Eds.,) 507-523, World Scientific, River Edge, NJ, (1994).
- [45] K. McLeod and A. Milani, "On some global well posedness and asymptotic results for quasilinear parabolic equation", *NoDEA*, 3, 79-114, (1996).
- [46] F. Morrison, *Understanding rheology*, Oxford University Press, USA, 2001.
- [47] A. Rodríguez-Bernal, "Inertial manifolds for dissipative semiflows in Banach spaces", *Applied Analysis*, 37, 95-141, (1989).
- [48] A. Rodríguez-Bernal, "Sistemas dinámicos infinito dimensionales: aplicaciones a la ecuación de Kuramoto-Velarde", *Tesis doctoral, U.C.M.*, (1990).
- [49] A. Rodríguez-Bernal, "Sistemas dinámicos en dimensión infinita", *Notes of the doctoral course given in U.C.M.*, (1992-1996).
- [50] A. Rodríguez-Bernal, "Attractor and Inertial Manifolds for the Dynamics of a Closed Thermosyphon", *Journal of Mathematical Analysis and Applications*, 193, 942-965, (1995).
- [51] A. Rodríguez-Bernal and E. Zuazua, "Parabolic singular limit of a wave equation with localized boundary damping", *Disc. and Cont. Dyn. System*, 1, 3, 303-346, (1995).
- [52] A. Rodríguez-Bernal and E.S. Van Vleck, "Complex oscillations in a closed thermosyphon", *Intern. J. of Bif. Chaos*, 8, 1, 41-56, (1998).
- [53] A. Rodríguez-Bernal and E.S. Van Vleck, "Diffusion Induced Chaos in a Closed Loop Thermosyphon", *SIAM J. of Appl. Math.*, 58, 4, 1072-1093, (1998).
- [54] A.M. Stuart, "Perturbation theory of infinite-dimensional dynamical systems", *Theory and Numerics of Ordinary and Partial differential Equations*, (M. Ainsworth, J. Levesley, W.A. Light and M. Marletta, Eds.) Oxford University Press, UK, 1994.

- [55] R. Temam, “*Infinite Dimensional Dynamical Systems in Mechanics and Physics*”, *Appl. Math. Sci.*, 68, Springer-Verlag, New York, (1988).
- [56] J.J-L. Velázquez, “On the dynamics of a closed thermosyphon”, *SIAM J. of Appl. Math.*, 54, 6, 1561-1593, (1994).
- [57] F. Verhulst, “*Methods and applications of singular perturbations*”, Springer-Verlag, New York, 2005.
- [58] C.J. Vincent and J.B.W. Kok, “Investigation of the over-all transient performance of the industrial two-phase closed loop thermosyphon”, *Intern. J. of Heat Mass Transfer*, 35, 6, 1419-1426, (1992).
- [59] P. Welander, “On the oscillatory instability of a differentially heated fluid loop,” *J. of Fluid Mech.*, 29, 1, 17-30, (1967).
- [60] A. Wolf et al., “Determining Lyapunov exponents from a time series”, *Physica*, 285-317, (1985).
- [61] S. Wolfram, *The mathematica book*, Cambridge University Press, 1999.
- [62] J. Yasappan, A. Jiménez-Casas and M. Castro, “Chaotic behavior of the closed loop thermosyphon model with memory effects”, *Chaotic Modeling and Simulation*, 2, 281-288, (2013).
- [63] J. Yasappan, A. Jiménez-Casas and M. Castro, “Asymptotic behavior of a viscoelastic fluid in a closed loop thermosyphon: physical derivation, asymptotic analysis and numerical experiments”, *Abstract and Applied Analysis*, 2013, 748683, 1-20, (2013).
- [64] J. Yasappan, A. Jiménez-Casas and M. Castro, “Chaotic behavior of viscoelastic fluid with Soret effect in a closed loop thermosyphon”, (submitted).